# IV. Influence of details on structural preformance

# SEMINAR

# IV

# Influence of Details on Structural Performance

# Influence des détails de construction sur le comportement des structures

# Einfluss von Konstruktionsdetails auf das Tragwerkverhalten

Chairman: R. Maquoi, Belgium

Technical Adviser: J. C. Badoux

Leere Seite
Blank page
Page vide

# Structural Performance of Steel Frames with Semi-Rigid Connections

Comportement de cadres métalliques avec des assemblages semi-rigides

Verhalten von Stahlrahmen mit teilweise steifen Verbindungen

**David A. NETHERCOT**
Reader in Civil & Struct. Eng.
University of Sheffield
Sheffield, UK

**Patrick A. KIRBY**
Lecturer in Civil & Struct. Eng.
University of Sheffield
Sheffield, UK

**J. Buick DAVISON**
Lecturer in Civil & Struct. Eng.
University of Sheffield
Sheffield, UK

David Nethercot has 20 years experience of teaching, research and specialist advisory work, principally in the field of structural steelwork, since graduating from University College Cardiff. He has contributed to national and international standards, is a member of several technical committees and the author of some 100 publications.

Patrick Kirby obtained his degrees from the University of Liverpool where he began his teaching career; moving to the University of Sheffield in 1971. Throughout this period he has been active in the field of structural response in particular in the behaviour of steel structures, has published many papers and participated in numerous short courses for practising engineers.

Buick Davison graduated from Sheffield University in 1980. He worked for a Consultant for four years before returning to the University as a Research Assistant. He was awarded a PhD in 1987 for his work on the performance of beam-columns in flexibly connected steel frames and is now a lecturer at Sheffield University.

## SUMMARY
The results of a programme of research into the effects of semirigid joint action on the performance of non-sway steel frames are drawn together to explain behaviour up to collapse. Full-scale testing and numerical analyses of the frames, supported by detailed studies of components and subassemblies, are used. Actual behavior is contrasted with that normally assumed for design purposes.

## RÉSUMÉ
Les résultats d'un programme de recherche des effets de l'action d'assemblages semi-rigides sur le comportement de cadres métalliques soint présentés afin d'expliquer leur comportement jusqu'à la rupture. Des essais en vraie grandeur et des analyses numériques de cadres ainsi que des études détaillées d'éléments et d'assemblages ont été réalisés. Le comportement réel contraste avec les prédictions obtenues lors des calculs.

## ZUSAMMENFASSUNG
Die Resultate eines Forschungsprogrammes zum Einfluss von teilweise steifen Rahmenknoten auf das Verhalten von seitlich gehaltenen Stahlrahmen werden zusammengefasst, um das Verhalten bis zum Einsturz zu erklären. Versuche in voller Grösse und Rahmenberechnungen, unterstützt durch detaillierte Studien von Komponenten werden dazuverwendet. Das wirkliche Verhalten wird den üblichen Berechnungsannahmen gegenübergestellt.

## 1. INTRODUCTION

Traditional approaches to the design of steel framed structures assume that the connections either function as pins or provide full continuity. The reality is, of course, that all practical types of steelwork joint operate somewhere between these two idealised extremes. A more realistic approach therefore requires the semi-rigid nature of connection behaviour to be properly recognised. This paper draws together results from a co-ordinated programme of research aimed at providing a full understanding of the influence of connection details on the performance of steel frames. It does this by contrasting the actual response, as observed in full-scale tests and through numerical analyses, with the simplified approach normally taken in design. Only non-sway frames in which out of plane deformations were prevented by bracing are considered.

## 2. TEST FRAMES

The type of frame under consideration is illustrated in Fig. 1. Beam to column joints were formed using flange cleats one with the beams framed into the column flanges, in which bay ABCD was not present, and a second with the beams framed into the column web. On the assumption that lateral forces will be resisted elsewhere in the structure e.g. by bracing, shear walls etc, it is customary to employ "simple" connections between beams and columns i.e to design them to transmit beam reactions in shear. The design basis is therefore to assume that the beams act as if simply supported, with only nominal moments transferred into the columns [1,2].

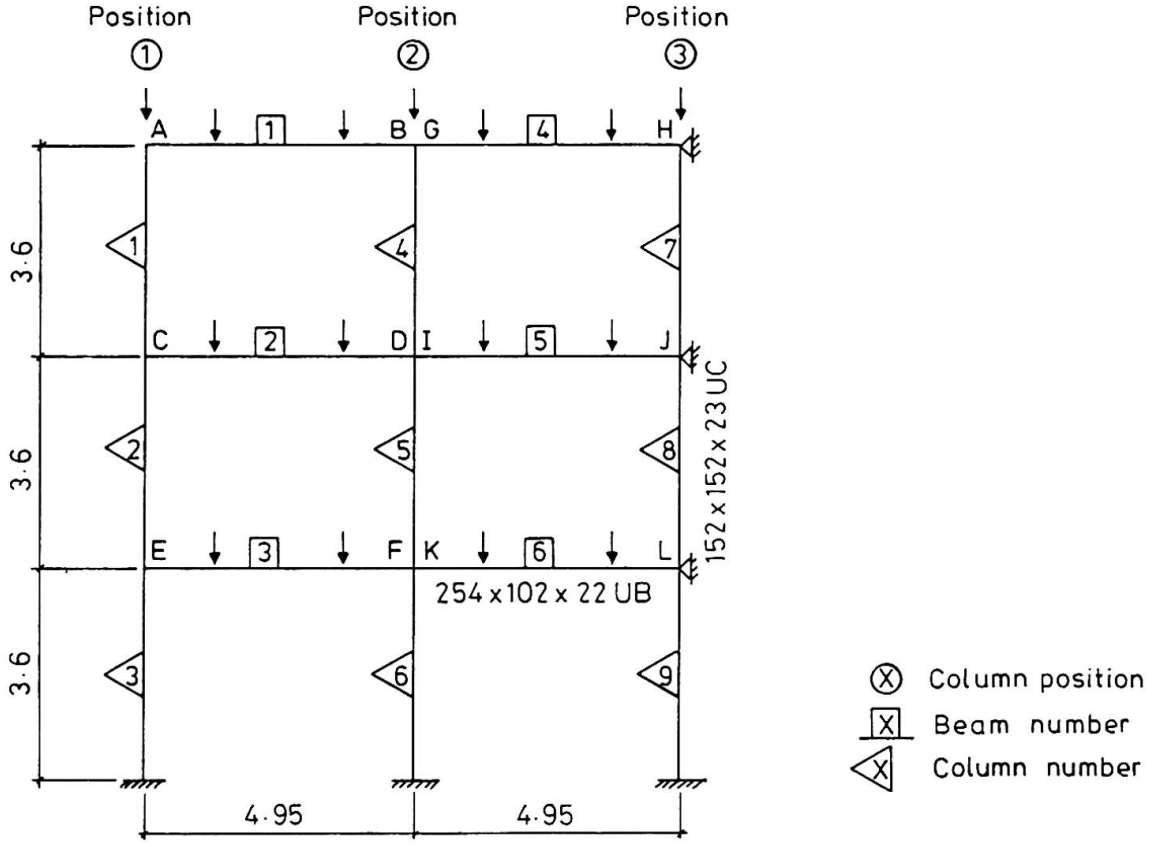


Fig. 1 Details of Frame Considered

Two frames of the type shown in Fig. 1 were tested [3] to collapse under a combination of beam loads and direct column loads and a full record of beam and column deflections, strains at key locations and joint rotations, amounting to some 600 channels of data, taken. Detailed analyses of the frames' behaviour were also undertaken using the SERVAR program developed at the Politechnico di Milano [4]. This program allows for spread of plastic zones, semi-rigid joint action and geometrically non linear effects. Full measured frame properties, including initial geometry, were used in the analyses. Fig. 2 compares bending moment diagrams at an advanced stage of the test for the first frame in which column 1 and beam 1 were absent.

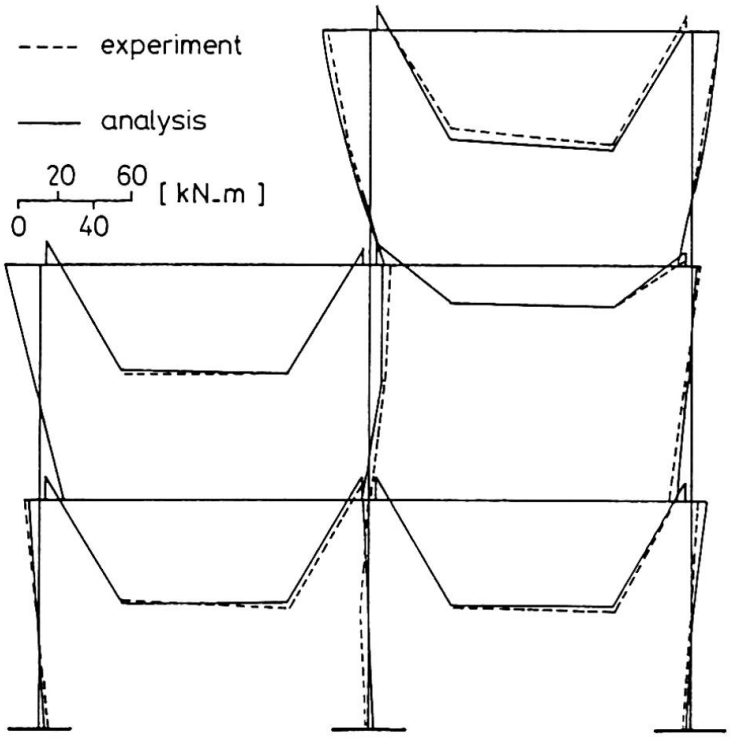


Fig. 2 Comparison of Measured Bending Moments and SERVAR Predictions Under Beam and Column Loading

## 3. FRAME BEHAVIOUR

### 3.1 Joints

The joint moment-rotation (M-Φ) characteristics used in the analyses were obtained from a separate series of connection tests [5]. However, a check on the performance of the connections in the frame was also made and Fig. 3 compares M-Φ curves, including that obtained from a further series of tests on column subassemblages [6]. All joints were nominally identical but were, of course, subject to some variability due to inevitable differences in fit-up. The effect of this level of variability on the performance of beams, columns and frames has been assessed through sample calculations, which show only very small differences in the resulting load-deflection behaviour. It therefore seems probable that variations in joint M-Φ characteristics due to "normal" variations in fabrication, location in a frame etc will have negligible effects on the performance of the frame as a whole.

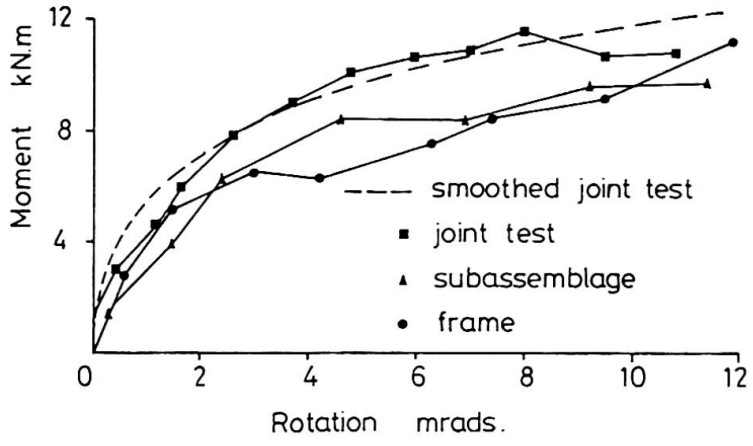


Fig. 3 Comparison of Joint Moment Rotation Characteristics

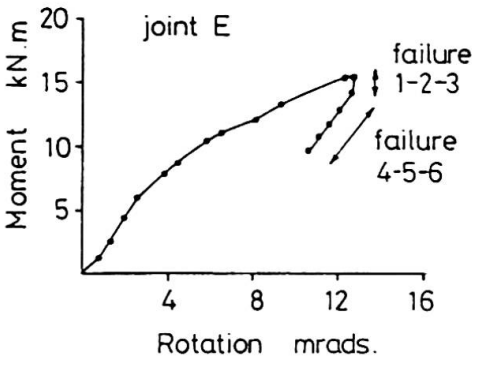


Fig. 4 Behaviour of Joint E Showing Unloading Phase

On the other hand, larger variations of the type produced for example in web cleats or flange cleats by using oversize holes - as might be required in cases of misalignment that were rectified on site - may well have a significant effect. Lack of fit is less important, however, for end plate connections for which quite large plate distortions - as might occur when welding the plate to the beam - have little influence on M-Φ behaviour [7].

One particularly important feature of joint behaviour in frames is their unloading. Fig. 4 shows how, for frame 2, the rotations of a joint to an external column during the three phases of frame loading; beam loads, column 1-2-3 additional direct load to failure, column 4-5-6 additional direct load to failure, reverse as column failure is initiated. Since the operative joint stiffness is then effectively its initial value [5], this is clearly beneficial in terms of stabilising the column. This feature has been explained in more detail both theoretically [8] and in full-scale tests [7] on column subassemblages, where it was found that greatly enhanced column loads were obtained as compared with those given by current design methods.

### 3.2 Beams

Clearly for beams the presence of end restraint provided by the semi-rigid connections will tend to reduce span deflections and moments as compared with the design assumptions. This is illustrated quantitatively for one beam in the test frame in Fig. 5, where the measured response is compared with that predicted by both the normal design approach and by the analysis in which end restraint has been included.

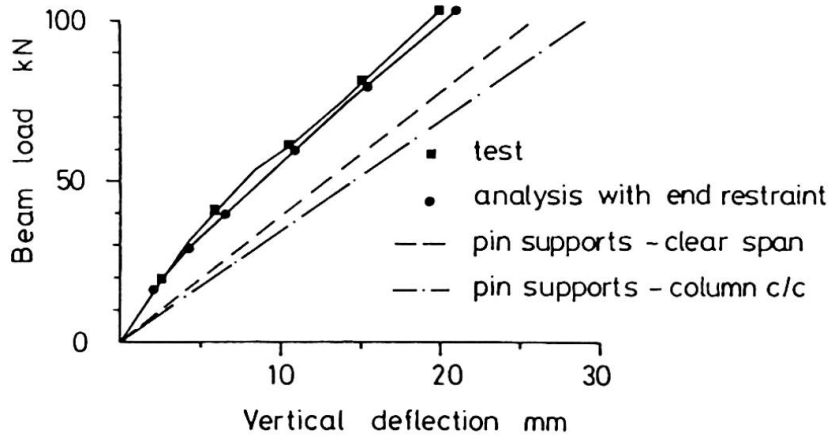


**Fig. 5 Load Deflection Response of a Beam in Frame 1**

### 3.3 Columns

The real behaviour of the columns is actually the most complex feature of the frame response. Whilst deflections are reduced as compared with those that would be expected of equivalent pin-ended members, the actual loads in the columns - especially the end moments transferred by the beams - require very careful assessment as collapse is approached. Fig. 6 shows the variation of moment at the column head at each level for column 1-2-3 of frame 2 as loads are increased to produce failure in the column. For both columns 1 and 2 two distinct phases can be observed; an initial linear phase corresponding to the application of beam loads followed by a non linear phase as column load is increased. For column 3, however, this second phase includes a reversal of moment. Similar behaviour has been observed in both tests and analyses of single column subassemblages [6, 8].

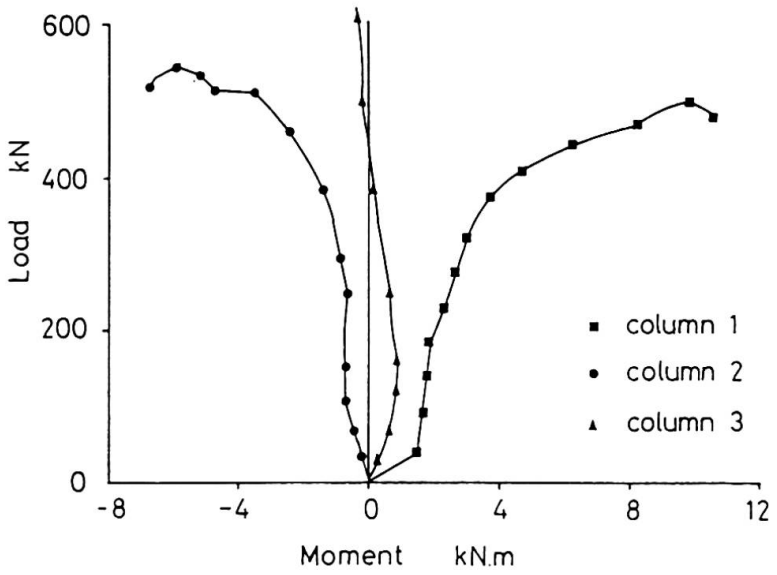


Fig. 6 Development of Column Moments

It is therefore not sufficient merely to regard the effect of the semi-rigid end connections on the column as simply providing some restraint against end rotation. Moments must be transferred from the beam through the connections and the exact form of these moments depends on the balance of stiffness. As frame loading is increased beam stiffnesses will be reduced by plasticity, connection stiffnesses reduce with increasing rotations according to their M-Φ curve unless a reversal in direction of rotation causes them to provide a higher unloading stiffness, whilst column stiffnesses will be reduced - very rapidly as collapse is approached - by the combination of plasticity and destabilising effects.

## 4. DESIGN IMPLICATIONS

The principal effect of semi-rigid joint action is to cause the frame to respond as a complete structure rather than as a set of isolated members as is assumed in the simple design approach. If the frame contains beams which are stiff and strong compared with the column clearly the beams will, via the connections, provide support to the columns thus improving their load carrying capacity. If on the other hand the columns are stiff and strong compared with the beams then restraint offered by the column will reduce both the beam midspan moments and also the deflections. These situations represent extreme limits to the real situation in which collapse will be initiated by the weaker components which will nevertheless receive assistance from the remainder of the frame. To convert the knowledge of such behaviour into a design procedure it is necessary to determine the extent to which such interactions occur and to

devise rules which exploit the effect at both the ultimate and the serviceability limit states yet are sufficiently simple to be practical.

## 5. CONCLUSIONS

Connection details have been shown to have a significant influence on the structural performance of steel frames. Using the results of full scale tests and numerical analyses the exact nature of this influence has been described. Although the main features have been identified, it remains for these to be represented by simple design rules.

## 6. ACKNOWLEDGEMENTS

The work reported herein was supported by a grant from the Science and Engineering Research Council, supplemented by contributions and assistance from the Building Research Establishment, Construction Industry Research and Information Association and Constrado (whose activities have now been subsumed into the Steel Construction Institute) and has benefited from collaboration with the Politechnico di Milano.

## 7. REFERENCES

1. British Standards Institution, BS 5950 : Part 1 : 1985, Structural Use of Steelwork in Building. BSI, London, 1985.

2. Eurocode 3, Common Unified Rules for Steel Structures. Directorate-General for Internal Market and Industrial Affairs", Commission of the European Communities, 1984.

3. KIRBY, P.A., DAVISON, J.B. and NETHERCOT, D.A., Large Scale Tests on Column Subassemblages and Frames. State-of-the-Art Workshop on Connections, Strength and Design of Steel Structures, Cachan, France, May 1987.

4. POGGI, C., and ZANDONINI, R., Behaviour and Strength of Steel Frames with Semi Rigid Connections, in Connection Flexibility and Steel Frames, ed. W.F. Chen, ASCE, New York, 1985, pp. 57-76.

5. DAVISON, J.B., KIRBY, P.A. and NETHERCOT, D.A., Rotational Stiffness Characteristics of Some Steel Beam to Column Connections. Journal of Constructional Steel Research, Vol. 8, 1987, pp. 17-54.

6. NETHERCOT, D.A., KIRBY, P.A. and DAVISON, J.B., Column Behaviour in PR Construction - Experimental Behaviour. Journal of Structural Engineering, ASCE, Vol. 113, No. 9, September 1987, pp. 2032-2050.

7. DAVISON, J.B., KIRBY, P.A. and NETHERCOT, D.A., Effect of Lack of Fit on Connection Restraint. Journal of Constructional Steel Research, Vol. 8, 1987, pp. 55-69.

8. NETHERCOT, D.A., KIRBY, P.A. and RIFAI, A.M., Column Behaviour in PR Construction - Theoretical Behaviour. Canadian Journal of Civil Engineering (in press).

# Nachgiebige Rahmenknoten in Stahlrahmen

Yielding Joints in Steel Frames

Assemblages non rigides de cadres métalliques

**Ferdinand TSCHEMMERNEGG**
Univ.Prof.Dipl.-Ing.Dr.tech.
Universität Innsbruck
Innsbruck, Öesterreich

Ferdinand Tschemmernegg, geboren 1939, promovierte 1968 als Bauingenieur an der Technischen Universität Graz. Er arbeitete in der deutschen Industrie und in Südamerika im Großbrückenbau. Seit 1980 ist Ferdinand Tschemmernegg Vorstand des Institutes für Stahlbau und Holzbau an der Universität Innsbruck.

**ZUSAMMENFASSUNG**
In dieser Veröffentlichung wird über ein Forschungsprojekt berichtet, das am Institut für Stahlbau und Holzbau der Universität Innsbruck durchgeführt wurde. Das Forschungsprojekt befaßte sich mit der Ermittlung der Nachgiebigkeit von Rahmenknoten und den Auswirkungen dieser Nachgiebigkeit bei der Systemberechnung von unverschieblichen und verschieblichen Stahlrahmen.

**SUMMARY**
This paper reports on a research project with the aim of analyzing the load-deformation behaviour of joints and the implications thereof for the design of braced and unbraced frames.

**RÉSUMÉ**
Cet article résume les résultats d'une étude du comportement des assemblages poutres-colonnes. Le but de ce projet était de définir la rigidité et la capacité portante des noeuds sans raidisseurs et l'influence des assemblages sur le comportement des cadres avec ou sans contreventements.

## 1. RAHMENKNOTENMODELL

Um das M-$\vartheta$ Verhalten zu beschreiben, wurde ein allgemeingültiges Rahmenknotenmodell gefunden, das das nichtlineare Verhalten eines Rahmenknotens mechanisch zutreffend erfaßt. In der Fig. 1 ist dieses Knotenmodell dargestellt. Es besteht aus einer elastisch-plastischen Krafteinleitungsfeder (E), Querkraftfeder (Q) und einer Anschlußfeder (A), die hintereinander geschaltet sind.

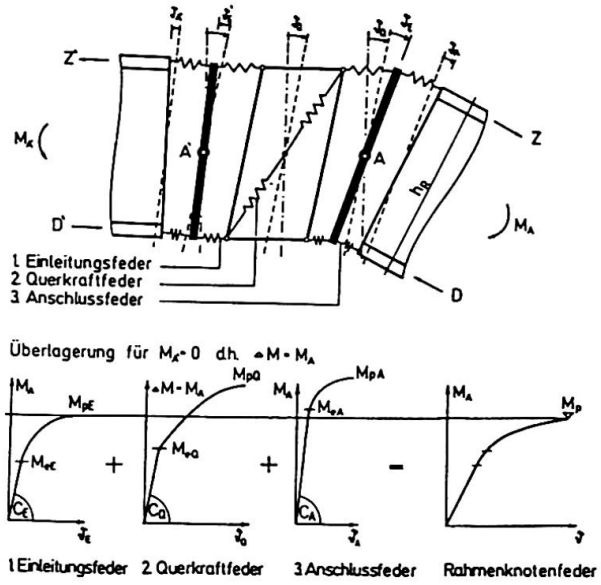


Fig. 1: Allgemeingültiges Rahmenknotenmodell

Die Krafteinleitungs- und Anschlußfeder reagieren hintereinander geschaltet auf die jeweilig angreifenden Momente $M_A$ bzw. $M_A'$, während die Querkraftfeder auf die Momentendifferenz $\Delta M = M_A - M_A$ reagieren. Die Verformungsanteile $\vartheta$ aus den einzelnen Federn addieren sich, während die Gesamttragfähigkeit des Knotens $M_p$ durch die Tragfähigkeit der schwächsten Feder bestimmt wird.
Es wurden die Federkennwerte aller dieser Einzelfedern versuchstechnisch getrennt ermittelt, und zwar des elastischen Grenzmomentes $M_e$, des plastischen Grenzmomentes $M_p$, der elastischen Grenzrotation $\vartheta_e$, der plastischen Grenzrotation $\vartheta_p$. Die Ergebnisse wurden in [1] und [2] veröffentlicht.
Mit Hilfe von Tabellen nach [1] kann das Momentenrotationsverhalten für Rahmenknoten bei beliebigen Kombinationen von Riegeln und Stützen aus europäischen Walzprofilen ermittelt werden.

Fig. 2 zeigt solche Momentenrotationslinien für einen geschweißten Rahmenknoten bei Stützen HEB 180 und Riegel IPE 270 aus St 360.

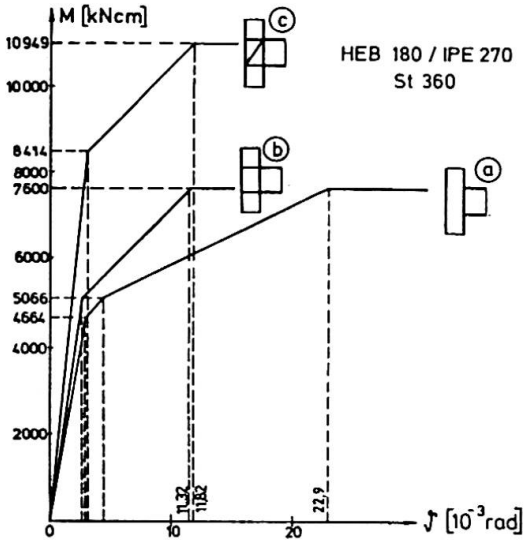


Fig. 2: M-ϑ Kurven für den geschweißten Knoten HEB 180, IPE 270, St 360;

Bei geschweißten Rahmenknoten kann die Anschlußverdrehung $\vartheta_A \simeq 0$ vernachlässigt werden und die Momentenrotationskurven ergeben sich aus der Überlagerung aus Krafteinleitungs- und Querkraftfeder, wobei in diesem Beispiel die Querkraftfeder die geringere Tragfähigkeit hat und somit die Tragfähigkeit des Knotens bestimmt.

Fig 2a zeigt die Momentenrotationskurven für den steifenlosen Rahmenknoten. Bisher wurde das plastische Grenzmoment $M_{pQ}$ eine solchen Rahmenknotens mit Hilfe der plastischen Querkrafttragfähigkeit $Q_{pS}$ der Stütze aus $M_{pQ} = Q_{pS} \times h_R =$ 5.066 kNcm errechnet. Dies ist für den Knoten das elastische Grenzmoment $M_{eQ}$. Das tatsächliche plastische Grenzmoment $M_{pQ}$ für den Rahmenknoten liegt aber bei 7.600 kNcm.
Fig. 2b zeigt einen Rahmenknoten mit Krafteinleitungssteifen versehen. Sie erhöhen nicht die Tragfähigkeit des Rahmenknotens, sondern reduzieren nur etwas die Rotation.

Erst durch eine Diagonalaussteifung bzw. Beilagebleche kann die Rahmenknotentragfähigkeit angehoben werden , Fig.2c.

Es hat sich aber gezeigt, daß steifenlose Knoten doch eine erhebliche Trag fähigkeit besitzen und somit durch die Vermeidung von Aus steifungen erhebliche Kosten im Detail eingespart werden können.

## 2. UNVERSCHIEBLICHE RAHMEN MIT STEIFENLOSEN KNOTEN

### 2.1 Tragfähigkeitsnachweis

Berechnet man die Riegeltragfähigkeit von unverschieblichen Rahmen mit steifenlosen Knoten, so können zwei Fälle unterschieden werden, Fig. 3a und Fig. 3b. Entweder die volle Fließgelenkkette kann sich bei reduzierten plastischen Momenten im Knotenbereich ausbilden, oder die Ausbildung der vollen Fließgelenkkette ist nicht möglich, da der Knoten eine beschränkte Rotationskapazität hat. Diese Beschränkung der Rotationskapazität ergibt sich daraus, daß sich bei symmetrischer Momentenbelastung des Knotens nach Erreichen der plastischen Grenzmomentes $M_{pE}$ im Druckbereich des Stützensteges eine plastische Beule bildet und hierauf die Tragfähigkeit des Knotens abnimmt.

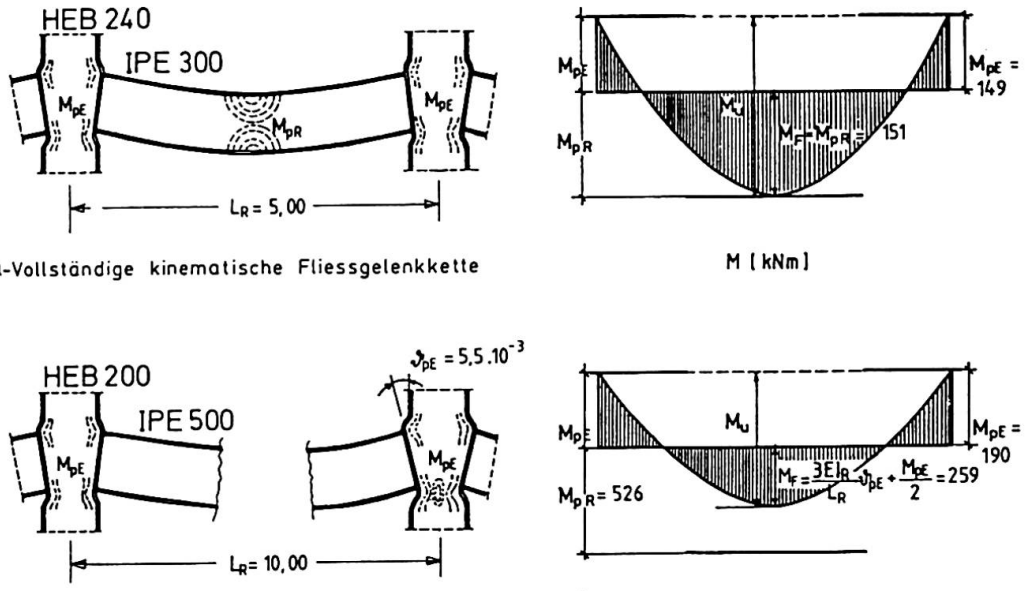


Fig. 3: Unverschiebliche Rahmen mit steifenlosen Knoten

Da die Grenzrotation $\vartheta_{pE} = 5 \times 510^{-3}$ rad gemessen wurde, kann sehr schnell festgestellt werden, ob die Rotationsfähigkeit maßgebend wird. Ist der Wert $3EI_R \cdot \vartheta_{pE}/L_R + M_{pE}/2$ kleiner als das plastische Moment $M_{pR}$ des Riegels, dann ist die Rotationskapazität maßgebend.

## 2.2 Gebrauchstauglichkeitsnachweis

Es hat sich gezeigt, daß die Knotennachgiebigkeit im elastischen Bereich zweckmäßig dadurch berechnet werden kann, daß die Nachgiebigkeit des Knotens durch die Krafteinleitung durch Reduktion der Riegelsteifigkeit im Knotenbereich erfaßt wird, während die Nachgiebigkeit durch die Querkraftbeanspruchung unter Reduktion der Steifigkeit der Stützen im Knotenbereich berücksichtigt wird. Da die Steifigkeiten $C_E$ und $C_Q$ aus Messungen bekannt sind, können die reduzierten Steifigkeiten sehr einfach ermittelt werden und dann mit konventionellen EDV-Programmen die Deformation berechnet werden, Fig. 4.

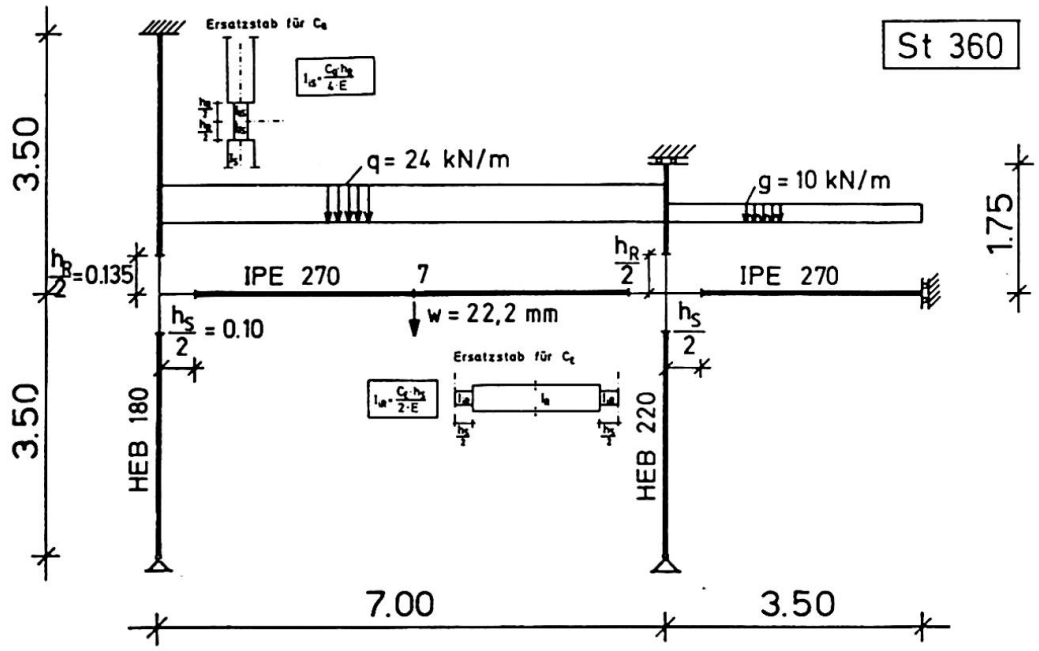


Fig. 4: Gebrauchstauglichkeitsnachweis

## 3. VERSCHIEBLICHE RAHMEN MIT STEIFENLOSEN KNOTEN

Verschiebliche Rahmen mit steifenlosen Knoten werden zweckmäßigerweise mit Stabwerksprogrammen, die das nichtlinere Knotenverhalten berücksichtigen, berechnet.Es wurde ein Programm entwickelt, das bei vorgegebenen Riegeln und Stützen aus europäischen Walzprofilen zunächst die Momentenrotationskurven der Knoten werden und hierauf das Gesamtsystem unter Berücksichtigung der

Knotennachgiebigkeit berechnet wird. Fig. 5 zeigt einen solchen Rahmen und die Ergebnisse für steifenlose und ausgesteifte Knoten. Da die gesamte Lastverformungskurve berechnet wird, kann nicht nur der Einfluß der Rahmenknoten auf die Tragfähigkeit, sondern auch auf die Verformungen aus den Berechnungen entnommen werden.

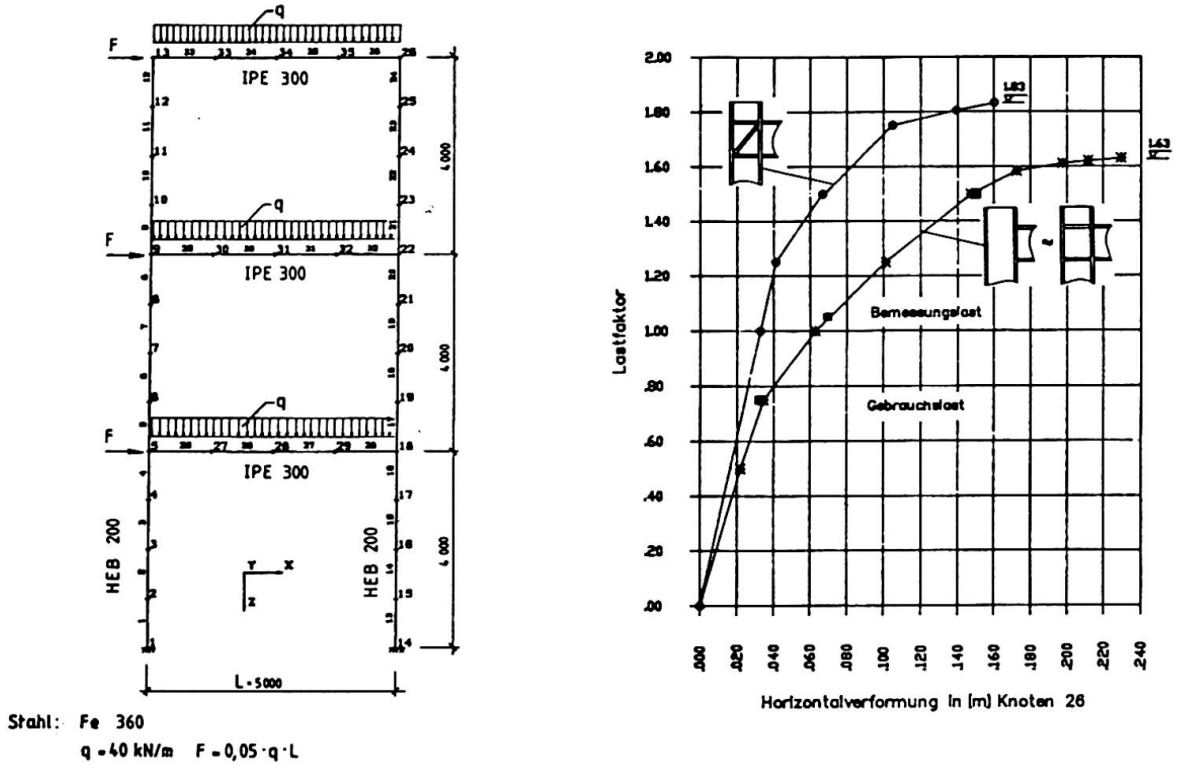


Fig. 5: Lastverformungskurve für einen verschieblichen Rahmen

## 5. LITERATUR

[1] Rahmentragwerke in Stahl unter besonderer Berücksichtigung der steifenlosen Bauweise. Theoretische Grundlagen - Beispiele - Bemessungstabellen. Herausgeber: österreichischer Stahlbauverband (OESTV), 1130 Wien, Larochegasse 28, und Schweizerische Zentralstelle für Stahlbau (SZS), 8034 Zürich, Postfach. 1987.

[2] TSCHEMMERNEGG, F., TAUTSCHNIG, A., KLEIN, H., BRAUN, CH., HUMER, CH.: Zur Nachgiebigkeit von Rahmenknoten. Teil 1.Stahlbau 10/1987 - Seiten 299 bis 306.

# Strength and Deformability of Wide Flange Beams Connected to RHS Column

Résistance et déformation de poutres à larges ailes fixées à des colonnes RHS

Festigkeit und Verformbarkeit von Breitflanschträgern verbunden mit RHS-Stützen

**Kazuo INOUE**
Assistant
Osaka Univ.
Osaka, Japan

**Kozo WAKIYAMA**
Assoc, Prof.
Osaka Univ.
Osaka, Japan

**Eiji TATEYAMA**
Lecturer
Kinki Univ.
Osaka, Japan

**Hiromichi MATSUMURA**
Maneger
NKK Building Techn. Lab.
Kawasaki, Japan

**SUMMARY**
This paper deals with the flexural strength and deformability of beams at the rigid frame connection with diaphragms. An improved detail of the connection is proposed without scallops (rat holes) which are conventionally provided at the beam end. From test and analytical results, it has been confirmed that the non-scallop type of connection has advantages over the scallop type with regard to strength, deformability and fabrication costs.

**RÉSUMÉ**
Ce rapport traite de résistance à la flexion et des déformations de poutres en acier à larges ailes, fixées rigidement à une colonne RHS. La technique de raccordement décrite dans ce rapport, dans laquelle on ne fait pas appel à des pièces de recouvrement, permet d'accroître la résistance à la flexion et de diminuer la déformation tout en réduisant les coûts de fabrication.

**ZUSAMMENFASSUNG**
Dieser Beitrag berichtet über die Ergebnisse, die bei Experimenten und Analysen an mit RHS-Stützen fest verbundenen Breitflanschträgern hinsichtlich der Biegefestigkeit und der Verformbarkeit an den Verbindungsstellen gewonnen wurden. In dieser Schrift wird der vollflächige Anschluss empfohlen, bei dem im Gegensatz zu konventionellen Verfahren mit Ausklinkungen im Steg an den Trägerenden die Biegefestigkeit und die Verformbarkeit der Träger nicht abnimmnt und Konstruktionskosten eingespart werden können.

## 1. INTRODUCTION

In Japan, the rigid frame connections consisting of RHS columns and wide flange beams are generally constructed as shown in Fig.1. For this type of connection, it is technically difficult to construct the web continuation within the RHS column. Therefore, the beam web is practically semi-rigidly connected. Thus the bending strength transferred by the web is smaller than the full plastic moment of web section due to the external deformation of the column tube wall.

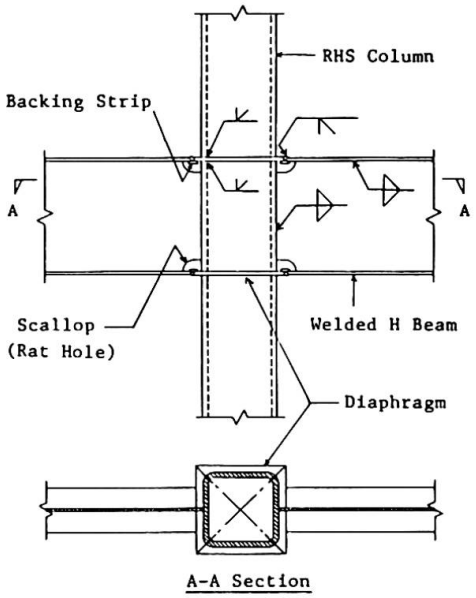


Fig.1 Wide flange beam-to-RHS column connection

For the connections shown in Fig.1, the scallops (rat holes) are usually cut at the end of the beam web to avoid weld lines from intersection and to install the backing strip. The most effective part of the beam web which carries both moment and shear is lost by these scallops. Besides, the strain of the tensile flange concentrates on the scalloped part; the beam fails to tear the tensile flange [1,2]. This type of fracture has also been seen in the present research.

To improve the weak points of the conventional scalloped connection mentioned above, a nonscallop detail is designed. The flexural strength and deformability of beams connected without scallops examined through two types of specimens : one is a simple beam type, and the other is a cruciform subassemblage. Test results are compared with those of the tests on the scalloped specimens. The results of calculation on the flexural strength of beams based on the yield line theory of limit analysis is also presented.

## 2. TEST SPECIMENS AND DETAIL OF BEAM-TO-COLUMN CONNECTION

### 2.1 Test Specimens

Two types of specimens are shown in Fig.2 and Fig.3, respectively. Loading conditions are also shown in Figs.2 and 3. The cruciform subassemblages are subjected to repeated load which corresponds to the earthquake type of loading. During the loading, the joint and the application points of forces on both beam ends are so controlled as to stay in one straight line as shown in Fig.4.

Each specimen is summarized in Table 1. The nine specimens from No.1 through No.9 are the simple beam type and the specimens No.10 and No.11 are the cruciform subassemblage. The specimens of each kind include both scallop and

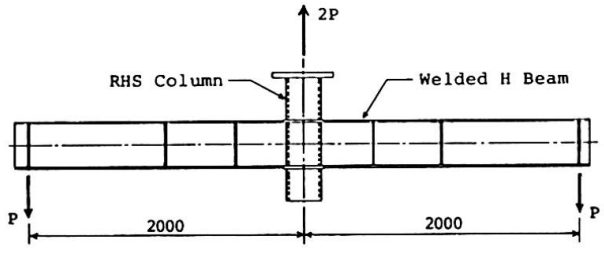


Fig.2 Simple beam specimen

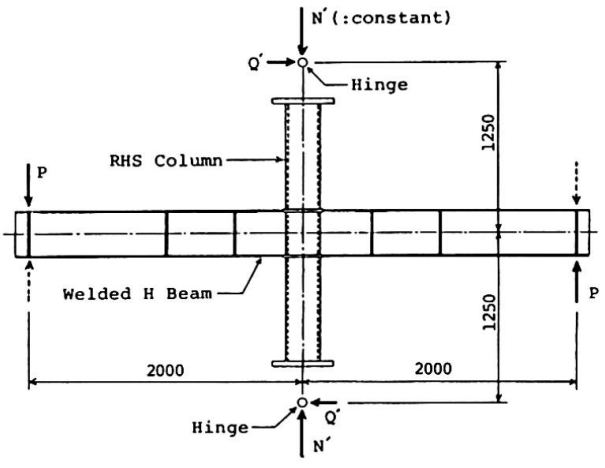


Fig.3 Cruciform subassemblage

| No. | Designation | Beam | Column | Note |
|---|---|---|---|---|
| 1 | SB6-S-2A | Welded H section with two axes of symmetry | □-250²x6 | with scallop |
| 2 | SB9-S-2A | | □-250²x9 | |
| 3 | SB12-S-2A | | □-250²x12 | |
| 4 | SB6-N-2A | | □-250²x6 | non-scallop |
| 5 | SB9-N-2A | | □-250²x9 | |
| 6 | SB12-N-2A | | □-250²x12 | |
| 7 | SB6-S-1A | with a single axis of symmetry | □-250²x6 | with scallop |
| 8 | SB6-N-1A | | □-250²x6 | non-scallop |
| 9 | SB12-N-1A | | □-250²x12 | |
| 10 | CS12-S-2A | with two axes of symmetry | □-250²x12 | with scallop |
| 11 | CS12-N-2A | | □-250²x12 | non-scallop |

Table 1 Summary of test specimens

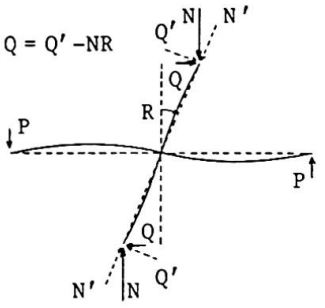


Fig.4

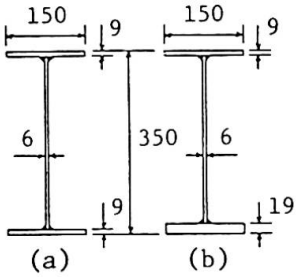


Fig.5 Beam section

nonscallop type of connections. All columns are cold-formed RHS tubes. Beams are welded wide flange steel beams; some having the section with two axes of symmetry and the others having the section with a single axis of symmetry as shown in Fig.5 (a) and (b). In the case of the composite beam subjected to positive bending, the plastic neutral axis lies inside or outside but near the upper flange of steel beam. The specimens No.7 through No.9 with a single axis of symmetry are prepared for examining the flexural strength and deformability of steel beam in the composite beam. Both of the two cruciform specimens are composed of beams with two axes of symmetry shown in Fig.5 (a). Specimen No.10 has scallops and Specimen No.11 is of the nonscallop type.

## 2.2 Detail of Nonscallop Connection

The detail of the scalloped connection is shown in Fig.6. The welding process of the nonscalloped connection is shown in Fig.7(a)-(c). This process is applicable only to the welded wide flange beams and is summarized as follows:

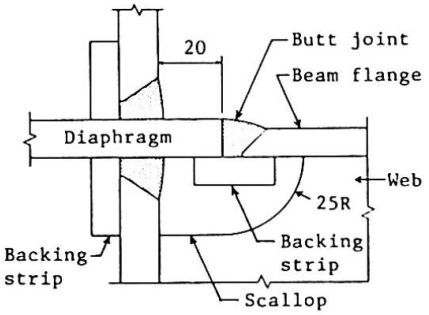


Fig.6 Detail of scalloped connection

(1)The fillet welding of the flange and the web into a wide flange beam is suspended at point A as shown by Fig.7 (a) to install the backing strips. Next, the end corner of beam web is cut in such a shape as to fit the reinforcement of the butt joint of the diaphragm and the RHS column.

(2)Two backing strips are installed, on both side of the web as shown in Fig.7 (b) and (c). They are fillet welded to the diaphragm and to the beam flange. Next, the diaphragm and beam flange are butt welded.

(3)As shown in Fig.7 (b), the fillet welding is started from Point A to connect the beam web and the RHS column.

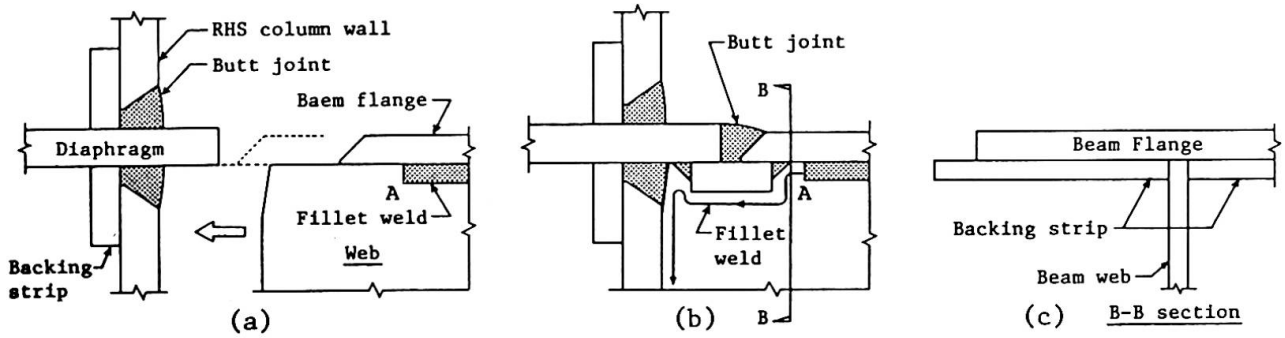


**Fig.7 Welding process of nonscalloped connection**

## 3. TEST RESULTS

### 3.1 Results of Simple Beam Specimens

The relations between the load (P) and the beam rotation (θ) of the simple beam specimens are shown in Fig.8 and Fig.9. The dotted lines in these figures show the results of the bending tests performed to confirm the full plastic moment of the beam member. Fig.10 shows the relations between the beam rotation and the axial strain of the tensile flange in the vicinity of the joint.

In the case of the beams with two axes of symmetry shown in Fig.8, the elastic stiffness and the maximum strength of each specimen do not differ much from those of another. On the other hand, the smaller the thickness of column wall is, the smaller the strength is as the elastic region develops into the plastic region; the strength of the scalloped specimen is apparently smaller than that of the nonscalloped specimen. The drop in the load after the maximum strength is due to the local buckling in the flange and the web.

The same can be said about the results of the specimens with a single axis of symmetry shown in Fig.9 as far as elastic stiffness is concerned. This time, the plastic neutral axis is in the compressive flange, and as seen in Fig.10, the strain of tensile flange is considerably larger than in the case of two axes of symmetry. Further, the strain of the scalloped specimen is larger than that of the nonscalloped specimen. As a result, the scalloped specimen SB6-S-1A caused a ductile fracture in the tensile flange where it is scalloped as shown in Fig.11. On the contrary, not a crack was observed in the the nonscalloped specimens throughout the test.

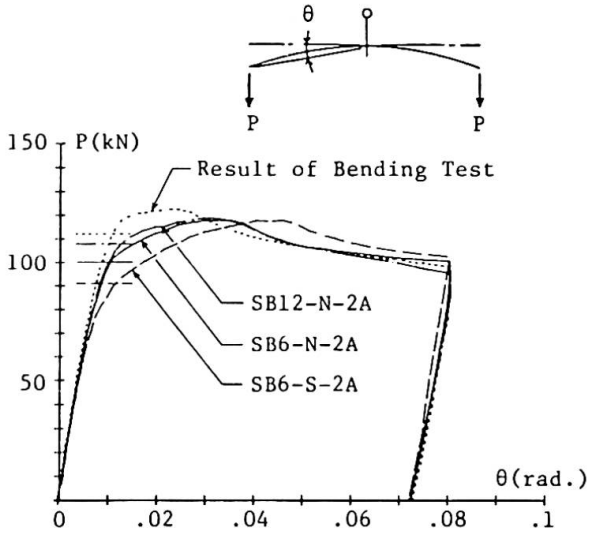


Fig.8 Simple beam with two axes of symmetry

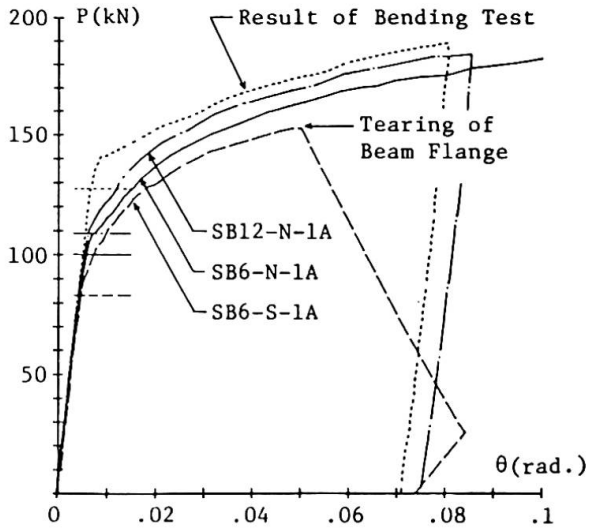


Fig.9 Simple beam with a single axis of symmetry

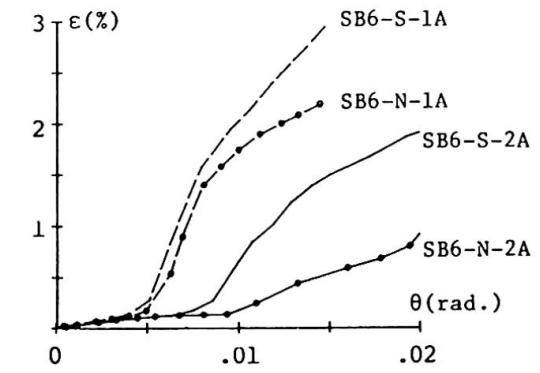


Fig.10 Axial strain of tensile flange

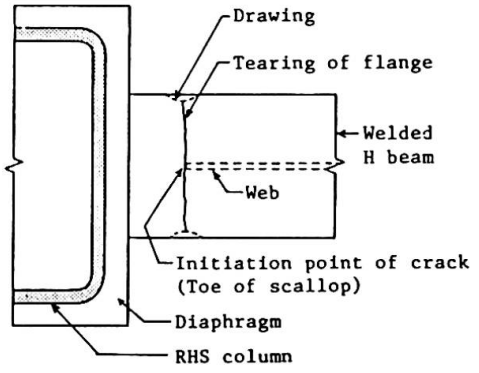


Fig.11 Tearing of tensile flange

### 3.2 Results of Cruciform Subassemblages

The relations between the column shear force (Q) and the column rotation (R) as in Fig.4 are shown in Fig. 12 and Fig. 13. In the case of scalloped specimen No.10, the crack that was initiated at the toe of the scallop the first loading cycle widened outward the second cycle to cause a fracture. On the other hand, as apparent from Fig.13, the nonscalloped specimen No.11 showed a sufficient deformability without any cracks under the repeated loading, the strength of which however decreased due to local bucklings.

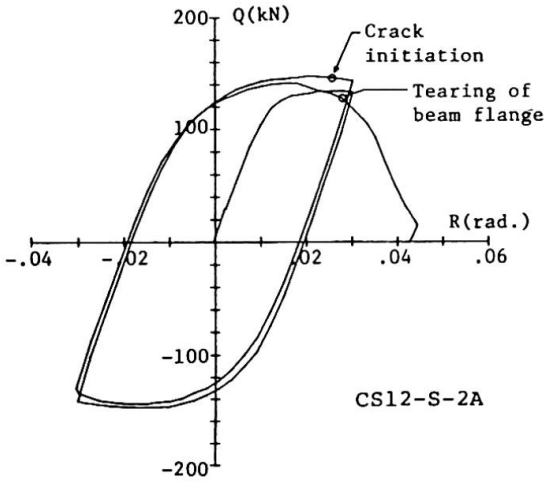


Fig.12 Q-R relation of cruciform subassemblage (with scallop)

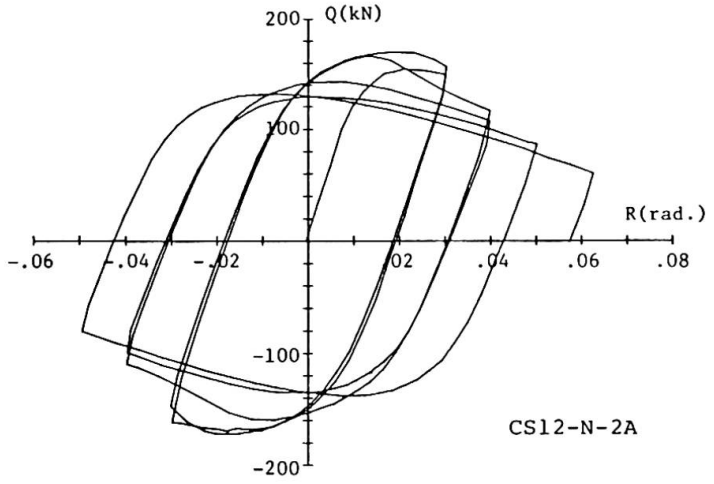


Fig.13 Q-R relation of cruciform subassemblage (without scallop)

### 4. COMPARISON OF THE TEST RESULTS WITH CALCULATED RESULTS

As shown in Fig.8 and Fig.9, the flexural strength of the beams connected to an RHS column is smaller than in the bending test. This is due to the external deformation of the column tube wall to which the beam web is connected. As an example, the distribution of web strain in the simple beam specimen (No.8) at $\theta$ =0.02rad. and the surface contour map of a deformed column wall after testing are shown in Fig.14.

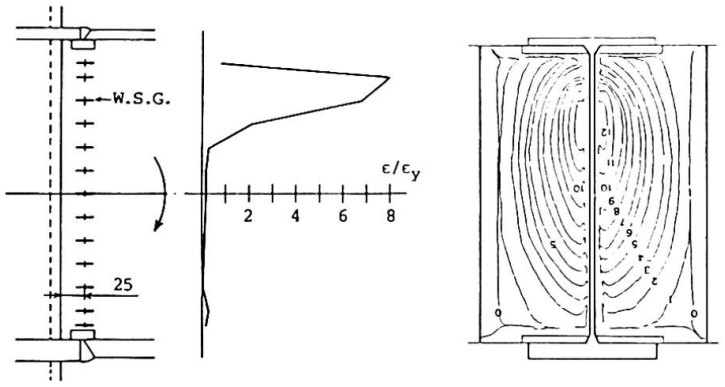


Fig.14 Strain distribution and surface contour map of column tube wall

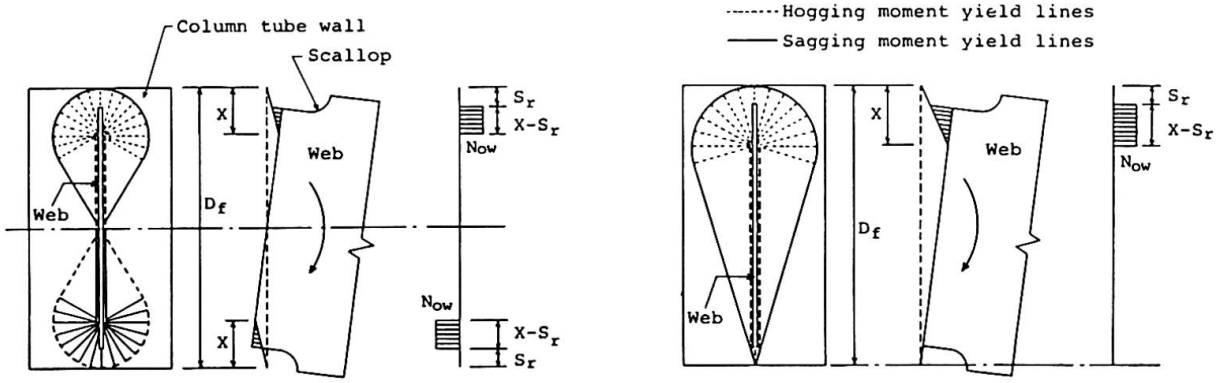


Beam with two axes of symmetry Beam with a single axis of symmetry

Fig.15 Mechanism of column tube wall and assumed stress distribution of beam web

The collapse mechanisms of column tube wall are assumed as shown in Fig.15. The moment transmitted through the beam web can be calculated by using the yield line theory [3,4]. The detailed derivative processes of the equations are omitted here. The length (X) of the plastic region of the web as in Fig.15 can be given approximately by the following equations:

Section with two axes of symmetry: $$X = \sqrt{\frac{4D_f M_{ot}}{N_{ow}}} \quad (1)$$

Section with a single axis of symmetry: $$X = \sqrt{\frac{8D_f M_{ot}}{N_{ow}}} \quad (2)$$

where $M_{ot}$ is the full plastic moment per unit width of the column tube wall and $N_{ow}$ is the yield axial force per unit width of the beam web or the punching shear strength of tube wall. If it is assumed that the yield stress acts only on the area of the web hatched in Fig.15 and the stress of the remaining area of the web is nil, the collapse moment of the beam at the joint can be calculated using the value of X obtained from the above equations. In Fig.15, $S_r$ is the depth of the scallop, and in case of nonscallop, $S_r = 0$.

The horizontal lines in Fig.8 and Fig.9 show the collapse load levels of individual test specimens calculated by the above method. The calculated collapse load of each specimen is close to the corresponding load level at which the gradient of P-θ relations greatly decreases.

## 6. CONCLUSION

From the test results, it has been confirmed that the nonscallop detail shown in Fig.7 has the following advantages over the conventional scalloped connections.
(1)The deformability of the beam is greatly improved.
(2)The flexural strength of the beam as the elastic region advances into the plastic region increases approximately by 10%.
(3)It can save the cost of fabricating the connections by not using scallops.

We may also mention here that the flexural strength of wide flange steel beams connected to RHS columns becomes smaller than their full plastic moment as a result of the external deformation of the column tube wall. The flexural strength can be predicted by the present method based on the yield line theory.

## ACKNOWLEDGMENTS

The authors would like to acknowledge the continuing guidance and encouragement of Professor Sadayoshi Igarashi of Osaka University.

## REFERENCES

1. FUJIMOTO M. et al, Experimental Study on the Brittle Fracture of Beam-to-Column Welded connections in Heavy Members Steel Structures, Part 1. J. of Structural and Construction Eng., Trans. of AIJ, No.349, pp.81-90, 1985.
2. KANATANI H. et al, Rigidity and Strength of Joint Panel of Centrifugally Cast Steel Tubular Column, Trans. of Annual Meeting of AIJ ,pp.921-922, 1985.
3. MANSFIELD E. H., Studies in Collapse Analysis of Rigid-Plastic Plates with Square Yield Diagram. Proc. of the Royal Society London, 241, Series A, pp.311-338, Aug., 1957.
4. DAVIES G. and PACKER J. A., Predicting the strength of branch plate-RHS connections for punching shear. Can. J. Civ. Eng., Vol.9, No.3, pp.458-467,1982.

# Behavior and Design of Semi-Rigid Composite Frames

Comportement et dimensionnement de cadres mixtes semi-rigides

Verhalten und Bemessung von Verbund-Rahmen mit teilweise steifen Verbindungen

**Roberto T. LEON**
Assist. Professor
University of Minnesota
Minneapolis MN, USA

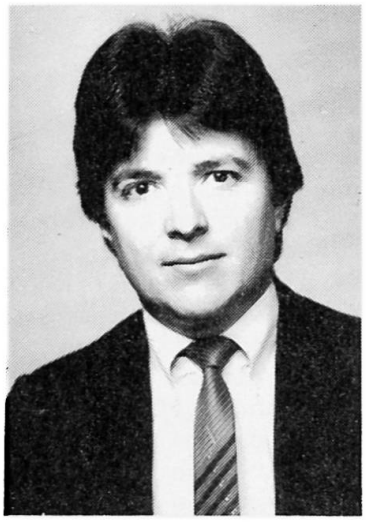

Roberto Leon received his Ph.D. from the University of Texas at Austin in 1983. He is currently engaged in research on connections for composite structures and on seismic design of concrete and steel structures.

**SUMMARY**
The use of composite construction can lead to substantial gains in stiffness and strength in semi-rigid connections. The strength and continuity provided by the reinforcing bars in the floor slab and the additional stiffness provided by the floor diaphragm make semi-rigid composite construction an ideal structural system for braced and unbraced frames up to nine stories. The results of an experimental series, design guidelines, and a sample design for this type of structure are discussed in this paper.

**RÉSUMÉ**
L'emploi d'une construction mixte peut permettre des gains substantiels en rigidité et en résistance dans les liaisons semi-rigides. La résistance et la continuité procurées par des barres d'armature dans une dalle et la rigidité supplémentaire procurée par le diaphragme du plancher font de la construction mixte semi-rigide un système de construction idéal pour des constructions en treillis ou non, allant jusqu'à neuf étages. Les résultats de ces expériences, directives de projet et un exemple d'avant-projet pour ce type de structure sont exposés.

**ZUSAMMENFASSUNG**
Die Verbund-Konstruktion mit teilweise steifen Verbindungen kann die Traglast und die Rahmensteifigkeit erheblich vergrössern. Die Tragfähigkeit und die durchlaufende Betonarmierung in der Deckenplatte, und die zusätzliche Steifigkeit der durchlaufenden Deckenplatte, machen eine solche Bauweise besonders geeignet für bis zu neunstöckige Rahmen. Dieser Artikel beschreibt die Ergebnisse eines Versuchsprogrammes. Entwurfs-Vorschläge und Entwurfs-Beispiele werden ebenfalls gegeben.

## I. INTRODUCTION

The use of semi-rigid construction has been hampered in the past by lack of simple analytical techniques and design guidelines [1]. Connections in steel structures have been idealized as either perfectly rigid or free to rotate for ease of calculation and simplicity in design. It has long been recognized that even the connections that are assumed to be free to rotate actually possess a limited moment capacity and initial stiffness, but these are seldom utilized in design [2]. A new type of structural system, labelled semi-rigid composite construction, is under development to increase and better utilize this strength and stiffness.

## 2. SEMI-RIGID COMPOSITE CONSTRUCTION

The idea behind semi-rigid composite construction is to improve the performance of a relatively weak steel connection, such as the top and seat angle (Fig. 1a), by replacing the top angle with a composite slab (Fig. 1b). The non-composite connection is relatively weak because the top angle will yield under a combination of flexural and tensile forces at a load considerably lower than the tensile capacity of either angle leg. The composite system replaces the weak element (top angle) with a fully composite slab incorporating small diameter bars continuous across the column lines. Under gravity loading the system offers increased moment capacity and stiffness primarily because the steel will yield in almost pure tension, and can be considered to be fully effective if the reinforcing bars are placed close to the column lines. Additional capacity is available also because the moment arm is increased and the yield strength of the reinforcing bars is greater than that of the structural steel.

Three recent events have made the use of this additional capacity attractive to designers in the U.S. The first is the issuance of ultimate strength design code [3] which divides connections into fully restrained (FR Type) or partially restrained (PR Type), implicitly recognizing the "semi-rigid" behavior of even the weakest connections. The second is the advent of the microcomputer into the designer's office and the availability of a large amount of design software and finite element analysis packages. This has made possible, with a moderate effort, the calculation of the forces and deformations for frames with connections idealized as linear or non-linear springs. The third is the increased use of composite floor systems for buildings in the five to twenty-storey range. These systems provide savings in materials and dead loads, permitting the increase of clear spans and the reduction of floor heights.

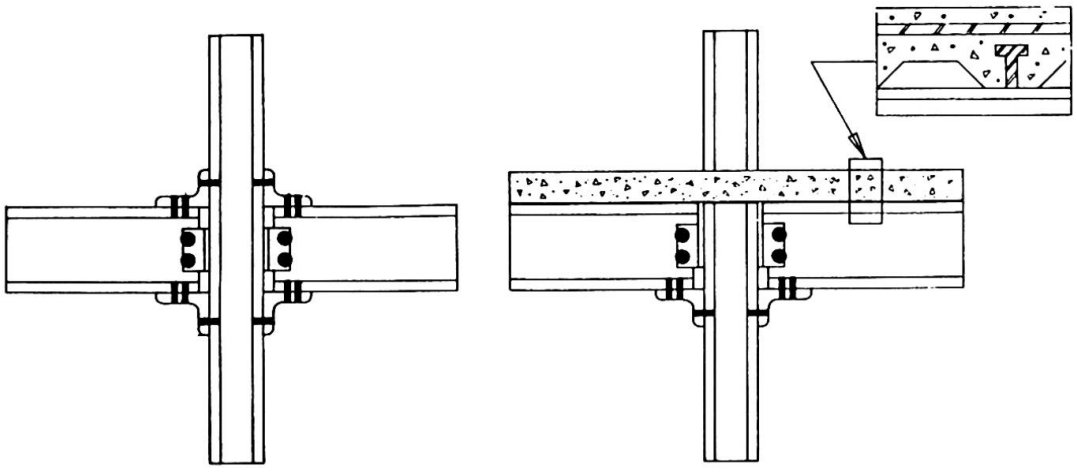

**(a) Non-composite connection** **(b) Composite connection**

Figure 1. Typical non-composite and composite connections

## 3. CONNECTION BEHAVIOR

A typical comparison between a composite and non-composite connection is presented in Fig. 2, which shows a large increase in initial stiffness and ultimate strength. An important advantage of the system is that the non-linear moment-rotation curve can be easily represented by a bi-linear model. This results in considerable savings in computation time, as well as in a simplified design procedure for checking strength under ultimate loads and deflections and drifts under service loads.

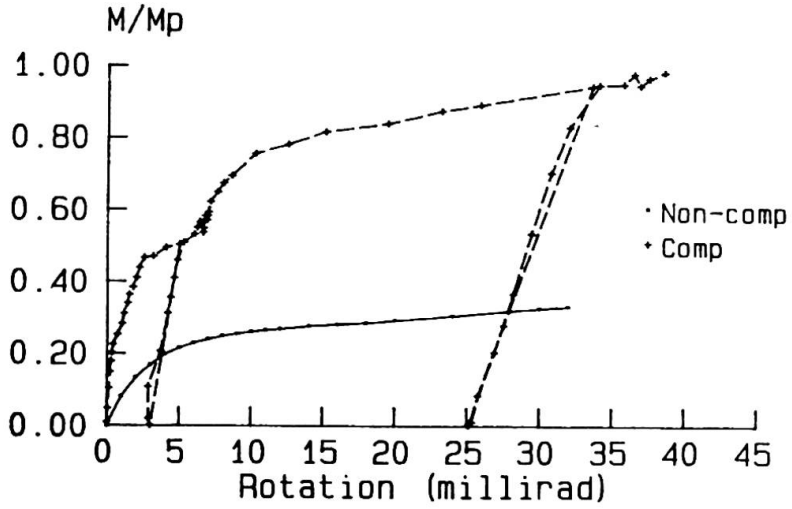


**Figure 2 - Typical moment-rotation curves.**

If the connection is subjected to lateral loads such as those arising from wind or earthquakes, an interior connection is still able to transfer large moments and provide adequate drift control (Fig. 3). In this case, the connection on one side of the column will be loading along the monotonic curve, while the other side is unloading along a branch parallel to the initial curve. While the stiffness of the left connection is decreasing, that of the right connection becomes equal to the initial stiffness due to the unloading. If the load reversals occur before the curve becomes highly non-linear the structure will be perfectly capable of carrying the loads without excessive drifts. Similar behavior can be obtained from exterior connections provided the slab is extended beyond the column line and adequate anchorage for the slab reinforcement is present.

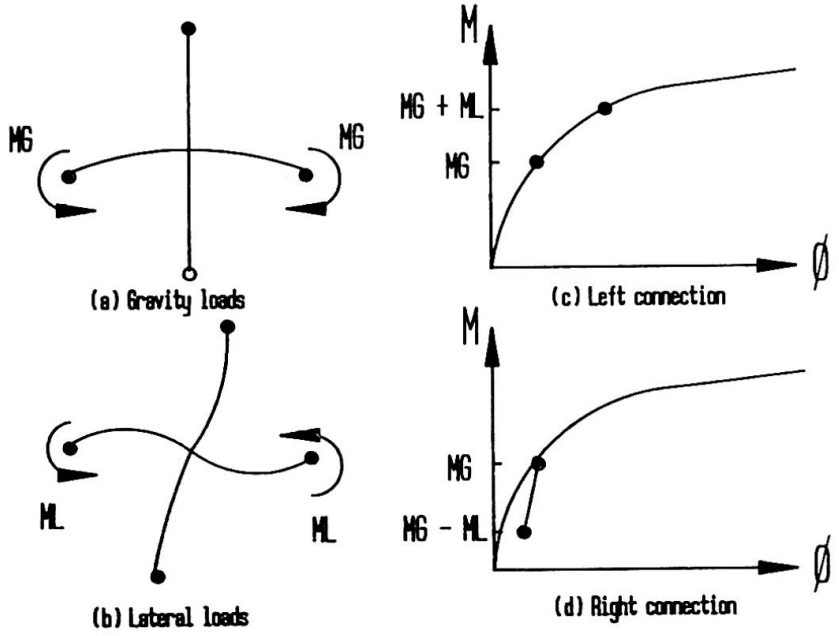


**Figure 3 - Behavior of semi-rigid connection under gravity and lateral loads.**

The additional cost of the system comes from the slab steel and the shear connectors necessary to insure full composite action. Since shear connectors are already being used in most floor systems and slab steel is commonly utilized to control cracking across column lines, the additional cost for this system is relatively minor compared to the gains in strength and stiffness.

Thus, semi-rigid composite construction can be used in areas where wind loads govern lateral load design and where seismic loads are low to moderate. It could also be used as a backup structural system in areas of large seismic exposure such as the western U.S. and some areas of southern Europe. The thrust of the project described herein deals with the effects of lateral loads on semi-rigid composite construction.

## 4. EXPERIMENTAL PROGRAM

Over the past three years a large-scale experimental research program has been carried out at the University of Minnesota to investigate the behavior of semi-rigid composite structures. The program included tests of three cruciform specimens simulating interior connections under monotonic and cyclic loading as well as the testing of a full-scale one-storey, two-bay frame subassemblage. The details for these tests are given in Refs. 4-5. Only some of the results for one test will be used here to illustrate the behavior of an interior connection. The details of one of the specimens along with a moment-rotation curve are shown in Fig. 4. The total specimen size was about 4 m by 6 m.

The specimen was loaded with a cyclic displacement at the bottom of the column equal to 0.1, 0.25, 0.5, 0.75, 1.0, 1.5, 2.0 and 3.0 percent storey drift. The behavior was elastic up to 0.75% storey drift, and the cracks in the slab were small until the 1.0% drift level was reached. Very little deterioration with cycling is observable until the 3.0% level was reached in the negative direction. At ultimate the connection achieved about 67% of the plastic moment capacity of the steel beam plus reinforcing bars in the downward direction, and about 58% of the capacity of the composite section in the upward direction.

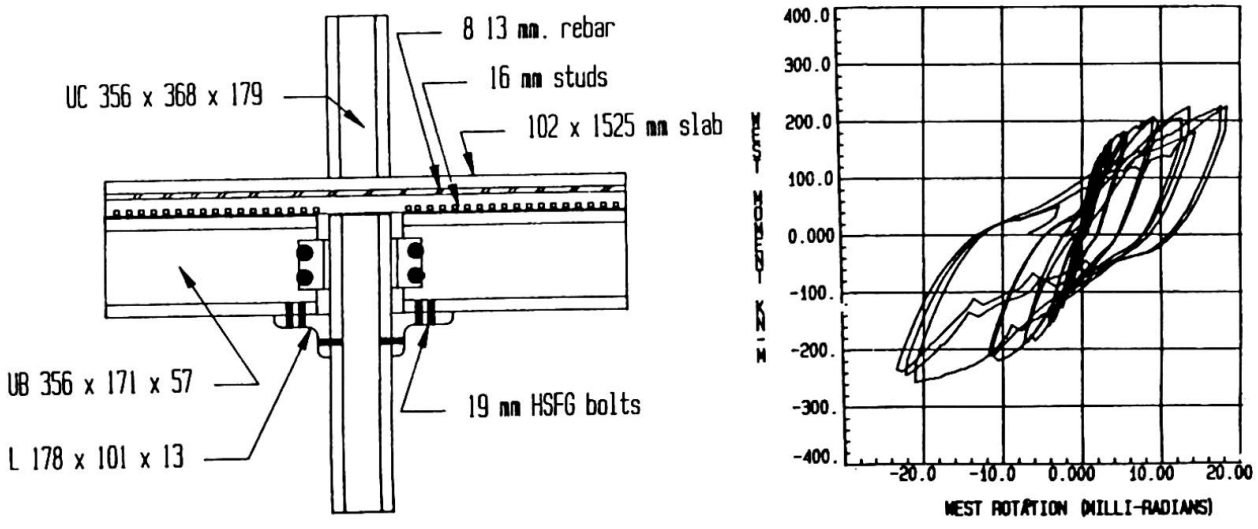


(a) Specimen details (b) Moment-rotation curve

**Figure 4 - Typical specimen tested and resulting moment-rotation curve.**

## 5. DESIGN METHODOLOGY

The design for a semi-rigid composite frame can be carried out by following the currently available criteria for Type 2 connections in allowable stress design [6] or the procedures recently proposed by Ackroyd [7]. In summary, they entail:

- Size the beams assuming ends free to rotate and based on the larger of (1) unfactored dead plus live or (2) construction loads. In general construction loads are assumed to be twice the service dead load and will govern the beam size.
- Size the columns assuming the connections are rigid and based on the larger of (1) factored gravity loads (dead plus live) or (2) factored lateral plus unfactored gravity loads. The first set of loads will provide the maximum axial loads and the latter the maximum moments. The columns should be designed as beam-columns to simultaneously satisfy both sets of forces. This will ensure that second order effects will not dominate the design.
- Analyze the structure obtained utilizing a program incorporating linear springs, and determine forces at the connection at ultimate.
- Detail connections for gravity load by providing enough slab steel within a strip equal to five times the column flange to satisfy the following equation:

$$M_n = 0.66\ A_s\ F_y\ D$$

  where $M_n$ is the nominal ultimate moment, $A_s$ is the area of the steel in the slab, $F_y$ is the yield strength of the steel, and D is the distance between the slab steel and the centroid of the bottom angle.
- If the lateral loads are not sufficient to overcome the gravity load moments, detail the seat angle to have an area equal to the bottom beam flange.
- If the lateral loads overcome the gravity load moments, size the bottom angle so the force in the leg along the beam is half of the yield force in tension, but not less than the area of the bottom beam flange.
- Provide enough bolts in the bottom angle to prevent slip of the connection and use minimum gage distances in both legs of the angle.
- Provide web cleats to carry the entire shear force.

## 6. DESIGN EXAMPLE

To demonstrate the capabilities of semi-rigid composite construction, a two-storey, three bay frame was designed utilizing the connection described in Section 4 and the experimental moment-rotation curves. The column spacing was 7.62 m and the floor heights were 4.57 m. Frames were assumed on a 6.1 m spacing. The loads were those prescribed by ANSI A58 [9]. Two plastic design load combinations were used: 1.3 (dead + live + wind) and/or 1.7 (dead + live).

The initial design exceeded the required strength, and the drift at ultimate was H/310. This was considered adequate for drift at ultimate since it satisfied the H/400 commonly assumed in the U.S. for service load design. The failure, however, was by a sway mechanism due to plastic hinge formation in the columns in the bottom storey. This was considered undesirable, and the column sizes were increased to force the formation of hinges in the beams. This required increasing the column sizes from the initial UB 254 x 146 x 33 (W10x22) exterior and UB 254 x 146 x 39 (W10x26) interior, to UB 254 x 203 x 58 (W10x 39) for all columns in the final design (Fig. 5a). Because the columns were small stiffners were provided in the column to minimize panel zone distorsions.

A comparison of the lateral load at the top of the structure vs. the total sway is shown in Fig. 5b. The design load was 13 KN, and both the rigid and semi-rigid structure exceeded this by at least a factor of 60%. The behavior

was very similar up to the design load, where the sway for the semi-rigid structure was H/450. After that the semi-rigid structure began to sway more, but even at ultimate the sway was only H/163. The structures were analyzed using a modified version of a program by Lui [8] which accounts for both the non-linear connection behavior and the stability of the structure.

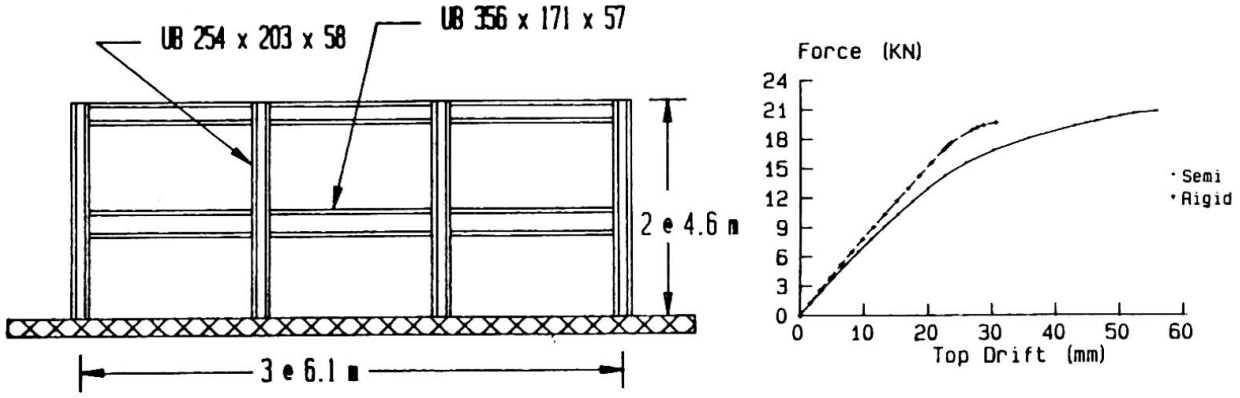


(a) Design example (b) Comparison of drift

Figure 5 - Design example and comparison of drift for rigid and semi-rigid.

## 7. CONCLUSIONS

This experimental investigation indicates that composite semi-rigid frames offer an attractive and economical solution to braced and unbraced construction up to eight or nine stories. The cost and labor for the additional reinforcing bars, shear studs, and analysis time required are more than offset by the simplicity of construction and the magnitude of the gains in strength and stiffness.

## ACKNOWLEDGEMENTS

This research was made possible through the generous financial support of the American Institute of Steel Construction.

## REFERENCES

[1] Jones, S.W., Kirby, P.A. and Nethercot, D.A., The Analysis of Frames with Semi-Rigid Connections - A State-of-the-Art Report. Journal of Constructional Steel Research, Vol. 3, No. 2, 1983.
[2] Johnson, R.P., and Law C.L.C., Semi-Rigid Joints for Composite Frames in Joints in Structural Steelwork (Howlett,J.H., et al, eds.). John Wiley & Sons, New York, 1981.
[3] American Institute of Steel Construction, LRFD Manual of Steel Construction. First Edition, AISC, Chicago, 1986.
[4] Ammerman, D., and Leon, R.T., Behavior of Semi-Rigid Composite Connections. AISC Engineering Journal, Second Quarter, June 1987.
[5] Leon, R.T., Semi-Rigid Composite Steel Frames. AISC Engineering Journal, Fourth Quarter, December 1987.
[6] American Institute of Steel Construction, Steel Construction Manual. Eighth Edition, AISC, Chicago, 1980.
[7] Ackroyd, M.H., Simplified Frame Design of Type PR Construction. Proceedings of the National Engineering Conference, New Orleans, AISC, April 1987.
[8] Lui, E.M., and Chen, W.F. Modelling of Structures with Semi-Rigid Connections. Computer and Structures, Vol. 26, No. 5, 1987.

# Influence of Details of Column Bases on Structural Behaviour

Influence des socles de colonne sur le comportement structural

Einfluß der Stützenfussplatte auf das strukturelle Verhalten

**Shigetoshi NAKASHIMA**
Lecturer
Osaka Inst. of Technology
Osaka, Japan

Shigetoshi Nakashima, born in 1943, received his Master's Degree in Eng. from Osaka Institute of Technology, Osaka. He has worked at Osaka Institute of Technology since 1965 and has been a lecturer since 1974. His researches have been concerned with strength and behaviour of steel column bases.

**Sadayoshi IGARASHI**
Professor
Osaka University
Osaka, Japan

Sadayoshi Igarashi, born in 1927, received his Doctor's Degree in Eng. from Kyoto University, Kyoto. He has worked at Osaka University since 1968 and has been a professor since that time. His researches have been concerned with strength and behaviour of steel members and connections.

**SUMMARY**
There are three types of column bases, which have been used conventionally in steel structures, namely exposed type, encased type and embedded type. In this paper, their mechanical performances will be discussed respectively. In addition, a new type column base with brackets will be introduced. It will also be shown that this new type column base has a sufficiently high degree of fixity and that its restoring force characteristics are of stable hysteretic form. Further, the relation between the column base fixity and the frame deformation will be discussed.

**RÉSUMÉ**
Trois types de socles de colonne sont utilisés dans les structures en acier: embase nue, embase fermée et embase encastrée. Les caractéristiques mécaniques de chacune sont exposées dans ce rapport. En outre, un nouveau type d'embase de colonne à cornières est présenté. Ce nouveau type d'embase présente un haut degré de rigidité et les caractéristiques de sa contrainte spécifique présentent une hystéresis stable. La relation entre la rigidité de l'embase et la déformation de la structure est abordée.

**ZUSAMMENFASSUNG**
In Stahlstrukturen werden normalerweise drei Arten von Stützenfussplatten verwendet, der freiliegende Typ, der geschlossene Typ und der eingebettete Typ. In dieser Schrift wird das Tragverhallen dieser Ausführungen verdeutlicht. Zusätzlich wird eine neue Stützenfussplatte mit Konsolen vorgestellt. Es ist auch ersichtlich, daß dieser neue Typ der Stützenfussplatte einen ausreichenden Einspanngrad sowie stabile Kraftkennlinien aufweist. Weiter wird der Zusammenhang zwischen dem Einspanngrad des Stützenfusses und der Verformbarkeit des Rahmens diskutiert.

## 1. INTRODUCTION

The column bases in a steel structure play a very important role in connecting the columns to the foundation. In Japan, steel structures, when a large lateral load is applied at the time of an earthquake, storm or the like, often collapse owing to the inadequate design and/or construction of their column bases. Column bases are composed of steel and concrete, which are foreign to each other. Unlike the connections in superstructures, the studies involving column bases had drawn little attention until quite recently when the importance of the subject began to be recognized and more papers are now being published. The Japanese seismic design standards regulate that the story deflection shall not exceed 1/200 of the story height as shown in Fig. 1. However, where the column base fixity is poor, the column member sections should be increased to satisfy this requirement. Dr. Akiyama states that in the case of a multi-story building wherein all stories have the perfect elasto-plastic type restoring force characteristics except one story that has a mixture of different restoring force characteristics (e.g. perfect elasto-plastic type and slip type), the damage would be concentrated in that one story. He also asserts that in case the second story and upward stories have the perfect elasto-plastic type restoring force characteristics and only the first story has a different type of restoring force characteristics (e.g. slip type), the damage would be concentrated in that first story [1]. Thus, the mechanical performance, such as rotation rigidity and restoring force characteristics, of the column bases greatly affects the entire structure's resistance against earthquakes. Therefore, it is very important to clarify the mechanical performance of this part of the structure. Conventionally, three types of column bases have been in use, namely 1) exposed type, 2) encased type and 3) embedded type as shown in Fig. 1. On the other hand, recently in Japan cold-formed square steel tubes are widely used as columns, but the mechanical performances of these columns in combination with column bases of different types had not been clarified sufficiently. It was under these circumstances that the authors of this paper in collaboration with their colleagues have experimentally clarified the mechanical behaviours of the column bases. As the result, it was found that the behaviours of the conventional type column bases were not satisfactory from the view point of both design and construction. Therefore, an effort was made to improve the conventional type column bases, resulting in the introduction of a new type of column base, namely 4) column base with brackets, as shown in Fig. 2. This new type column base consists of a pair of H-section steel brackets welded to the adjoining faces of the tubular column. The base and the bracket ends are fixed by the anchor bolts welded to the standardized anchor frame as shown in Fig. 3. The bracket portion is then buried in the concrete floor of the building. This type of column base has been employed in mass production housing construction and its installation method is now systematized. Lateral force was applied to full-size models of this type of column base to clarify their mechanical behaviours. Further, assuming three different structural frames, the relationship between the rigidity of column bases in the frames and the moment distributions of the frames and that between the rigidity of column bases and the horizontal deflections were clarified and the design method of this type of column base is discussed.

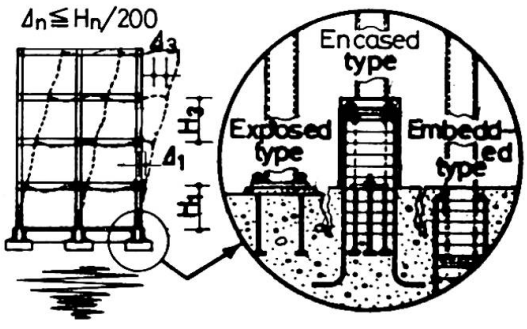


Fig.1 Three conventional type column bases

## 2. MECHANICAL BEHAVIOUR OF STEEL COLUMN BASES

Firstly, the results of the study made of the mechanical performances of the three conventional type column bases, as shown in Table 1, will be described, and thereafter the new type column base will be described.

Table 1 Mechanical characteristics of three conventinal type column bases

| | Exposed Type (R Type) | | | Encased Type (N Type)[2] | | | Embedded Type (U Type) | | |
|---|---|---|---|---|---|---|---|---|---|
| | | | | | | | Interior Column (UI Type)[3] | | Exterior (Corner) Column (UC Type)[4] |
| Test Program | B.Pl A.Bt<br>R-1 25(t) 4-M12<br>R-2 9 8-M22<br>R-3 25 12-M22<br>C-1,2 32 34-M24 | Column □-150x150x6.0<br>B.Pl 285x285 | | L/D l/D Hoop<br>N-1 2 2 35@<br>N-2 3 2 35@<br>N-3 3 2 No<br>N-4 3 2.67 35@ | Column □-150x150x6.0<br>B.Pl 160x160x19<br>A.Bt 4-M16<br>Chord Rein. 10-D13<br>Top Hoop 3-D10 25@ | | L/D<br>UI-1 1.5<br>UI-2 2.0<br>UI-3 3.0<br>UI-4 2.0 Anchor Rein. 4-D16 | Column □-150x150x6.0<br>Foundation bxd=440x600<br>Reinforcement 8-D19 | E/D<br>UC-1 1.0<br>UC-2 1.5<br>UC-3 2.0<br>UC-4 1.0 A.R.4-D13 | Column □-100x100x6.0<br>Foundation bxd=300x400<br>A.Bt 4-M12 L=2.5D<br>Chord Rein. 4-D16 Hoop<br>Top Hoop 3-D10 20@ D6 25@ |
| Mechanical Properties of Steel | σy σmax El.<br>(N/mm²) (%) | σy σmax El.<br>(N/mm²) (%) | | σy σmax El.<br>(N/mm²) (%) | σy σmax El.<br>(N/mm²) (%) | | σy σmax El.<br>(N/mm²) (%) | σy σmax El.<br>(N/mm²) (%) | σy σmax El.<br>(N/mm²) (%) | σy σmax El.<br>(N/mm²) (%) |
| | C. 348 421 35<br>B.Pl 350 465 33<br>A.Bt M12 376 522 31<br>A.Bt M22 320 470 30 | D10 371 518 21<br>D16 419 572 21 | | C. 348 421 35<br>B.Pl 300 461 33<br>A.Bt M16 322 439 31 | D 6 305 445 25<br>D10 371 518 21<br>D13 375 560 21<br>D16 419 572 21 | | C. 351 406 33<br>B.Pl 300 461 33 | D10 517 713 16<br>D16 517 743 14<br>D19 379 563 19 | C. 407 465 23<br>B.Pl 325 450 34<br>A.Bt 312 440 32 | D 6 361 485 22<br>D10 377 512 25<br>D13 367 534 22<br>D16 383 563 22 |
| P.Con. | σc 25.5(N/mm²) | σt 2.38(N/mm²) | | σc 24.2(N/mm²) | σt 2.35(N/mm²) | | σc 29.5(N/mm²) | σt 2.77(N/mm²) | σc 30.1(N/mm²) | σt 2.45(N/mm²) |
| Specimens | 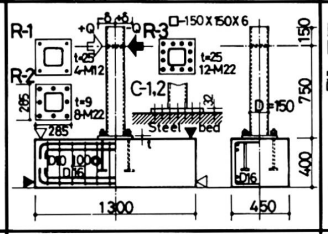 | | | 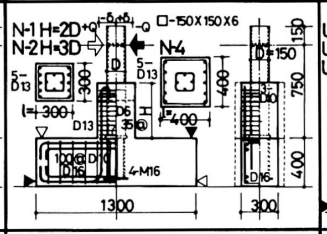 | | | 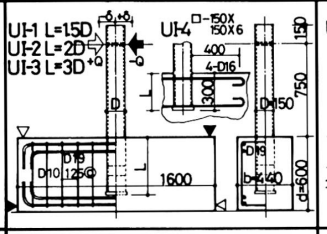 | | 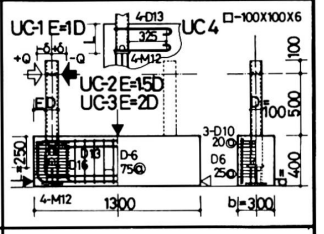 | |
| Q-δ Curves | 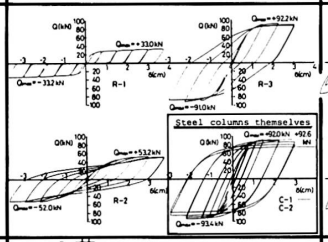 | | | 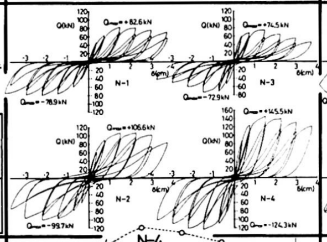 | | | 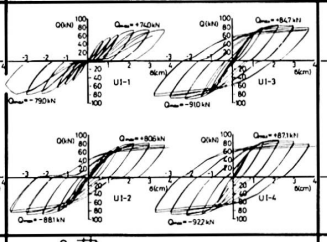 | | 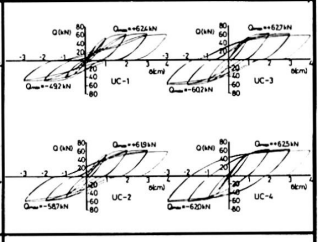 | |
| Envelope Curves of Q-δ Curves | 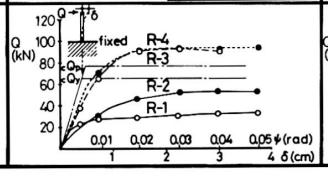 | | | 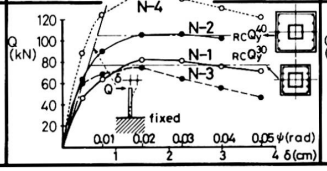 | | | 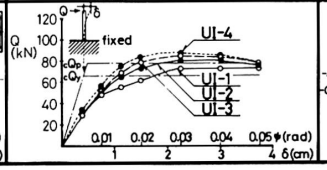 | | 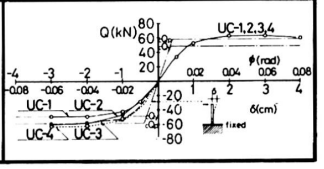 | |

### 2.1 Exposed Type Column Base (R Type)

This column base is composed of a base plate welded to the column bottom and anchor bolts. The initial rigidity is well in accord with the test result if the modulus of elasticity of the anchor bolt including the threaded connection of the anchor bolt and nut is assumed to be E/2. (E: Elastic modulus) When the anchor bolts yield, the restoring force characteristics will be of the slip type (R-1), and when the base plate yields the spindle shaped restoring force characteristics will be obtained. (R-2) If large rotation rigidity is to be obtained and a fully plastic load of the column is to be transmitted, this type of column base must have large anchor bolt sections and the base plate must be considerably thicker and the installation work will become difficult. (R-3)

### 2.2 Encased Type Column Base (N Type) [2]

This type of column base consists of a steel column base of a relatively small flexural rigidity enclosed by reinforced concrete to secure the required strength and rigidity, both of which increase as the concrete cover thickness and/or the encasement height increases. In this case, the uppermost hoop reinforcement of the encasement must be properly laid out. When the encasement height is approximately 3 times the column depth (D) and if sufficient care is given to its detail, its fixity can be considered to be perfect. (N-2,3,4) However, the restoring force characteristics of this column base type, if the concrete cover is of ordinary thickness, will be of the slip mode. (N-1,2,3,4) Further, the column base volume increased by the encasement concrete sometimes interferes with design flexibility.

### 2.3 Embedded Type Column Base (U Type) [3],[4]

The initial rigidity of this type column base is 50% to 70% of that of the steel column itself which is assumed to have been fixed to the foundation beam top. The mechanical properties are different between the interior column and the side column (or corner column) whose concrete cover is thin (UC-1). In the case of the former, even in the absence of any special reinforcement, the restoring force shows spindle shaped characteristics if the depth of embedment is sufficient (normally approx. 2.5D). (UI-2,3) In the case of the latter, it is necessary to reinforce the concrete top and the base plate level. The column, then shows the mechanical behaviours of an interior column if it is reinforced sufficiently by hoops and an end distance of at least 2D is provided. (UC-3) Efficient methods of reinforcement in this case are the use of welded anchor bars (UC-4) or U-shape bars. In the case of this column base type, difficulties are often encountered in concrete placement for the foundation beam when the embedment depth is great.

### 2.4 Bracket Type Column Base (B Type)

#### 2.4.1 Experiment Program

As mentioned before, this type column base is shown in Figs. 2 and 3. Upon this type of column base model, monotonic and repeated loads were applied by a hydraulic jack through a hinged attachment at a conceived inflection point. The experimental factors were the presence or absence of brackets (L, I) placed at right angles with the loading direction and the presence or absence of encasement concrete (R, O). In addition, two exposed type specimens without brackets (RO) and two beam type specimens (CO) were planned, of which the beam type specimens were intended for examination of the mechanical performance of the steel column itself. The results of the elemental material tests are shown in Table 3.

#### 2.4.2 Results of Experiments and Discussions

The relationships between the load (Q) applied on the column and its horizontal

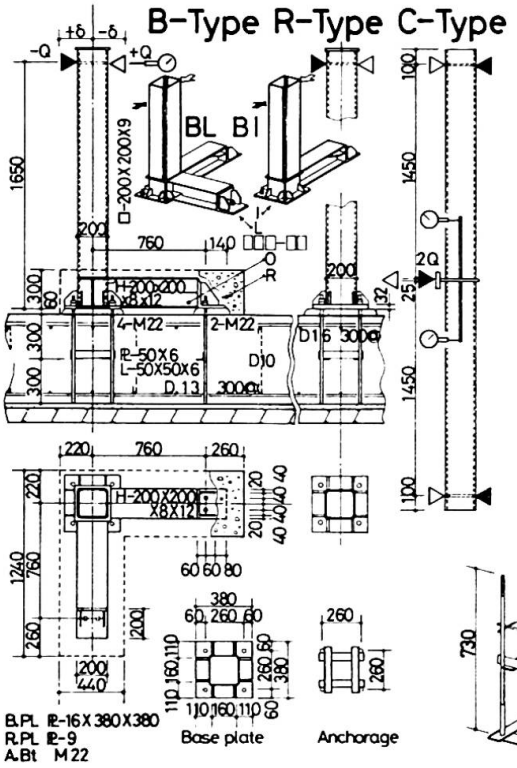


Fig.2 Test specimens

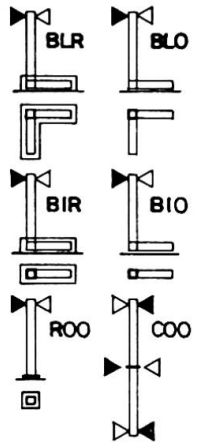


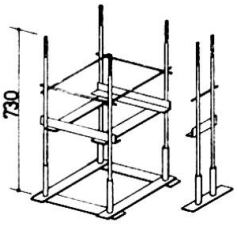


Fig.3 Anchor frames

Table 2 Test program and test results

*1 M : Monotonic load
R : Repeated load
*2 Measured at 40 kN

| Type | M or R | Sym. | Specimen Symbol | Displacement *2 + (cm) | Displacement *2 - (cm) | K (x10⁵kNcm/rad) (+) | K (x10⁵kNcm/rad) (-) | +Q*1 (kN) | -Q*1 (kN) |
|---|---|---|---|---|---|---|---|---|---|
| B | +M | A | BLR-M1 | 0.723 | —— | —— | —— | 147 | —— |
| | -M | B | BLR-M2 | 0.751 | -0.825 | —— | —— | 149 | -142 |
| | R | C | BLR-R | 0.701 | -0.834 | —— | —— | 153 | -146 |
| | | | | 0.725 | -0.830 | 72.8 | 40.5 | | |
| | +M | D | BLO-M1 | 0.860 | -0.955 | —— | —— | 150 | -147 |
| | -M | E | BLO-M2 | —— | -0.956 | —— | —— | —— | -148 |
| | R | F | BLO-R | 0.921 | -1.040 | —— | —— | 148 | -142 |
| | | | | 0.891 | -0.984 | 32.2 | 24.6 | | |
| | +M | G | BIR-M1 | 0.700 | —— | —— | —— | 152 | —— |
| | -M | H | BIR-M2 | —— | -0.750 | —— | —— | —— | -152 |
| | R | I | BIR-R | 0.757 | -0.826 | —— | —— | 147 | -141 |
| | | | | 0.729 | -0.788 | 70.7 | 49.3 | | |
| | +M | J | BIO-M1 | 0.874 | -0.971 | —— | —— | 147 | -145 |
| | -M | K | BIO-M2 | —— | -0.948 | —— | —— | —— | -136 |
| | R | L | BIO-R | 0.862 | -0.960 | —— | —— | 144 | -139 |
| | | | | 0.868 | -0.960 | 34.9 | 26.2 | | |
| R | M | M | ROO-M | —— | —— | —— | —— | 58.0 | —— |
| | R | N | ROO-R | —— | —— | —— | —— | 56.2 | - 54.0 |
| | | | | —— | —— | 9.29 | 12.7 | | |
| C | M | O | COO-M | 0.539 | —— | —— | —— | 148 | —— |
| | R | P | COO-R | 0.541 | 0.544 | —— | —— | 142 | -142 |
| | | | | 0.540 | 0.544 | —— | —— | | |

Table 3 Mechanical properties of steel and concrete

| Steel | σy (N/mm²) | σmax (N/mm²) | E (x10⁵ N/mm²) | El. (%) |
|---|---|---|---|---|
| □-200x200x9 | 395 | 446 | 1.87 | 38 |
| H-200x200x8x12 | 301 | 486 | 2.11 | 38 |
| B.PL | 322 | 493 | 2.05 | 24 |
| A.Bt (M22) | 340 | 540 | 2.10 | 26 |
| D16 | 546 | 761 | 2.15 | 10 |
| D13 | 499 | 713 | 2.10 | 13 |
| D10 | 351 | 494 | 2.13 | 12 |

| Concrete | | σc (N/mm²) | σt (N/mm²) | Ec x10⁴ (N/mm²) |
|---|---|---|---|---|
| Concrete | Foundation | 21.5 | 1.86 | 1.98 |
| | Encasement | 22.3 | 1.74 | 2.05 |
| Mortal | —— | 44.6 | 5.19 | — |

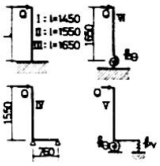


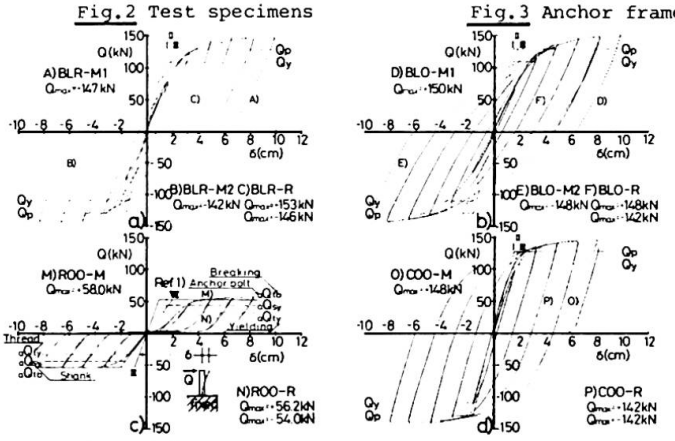


Fig.4 Q-δ curves

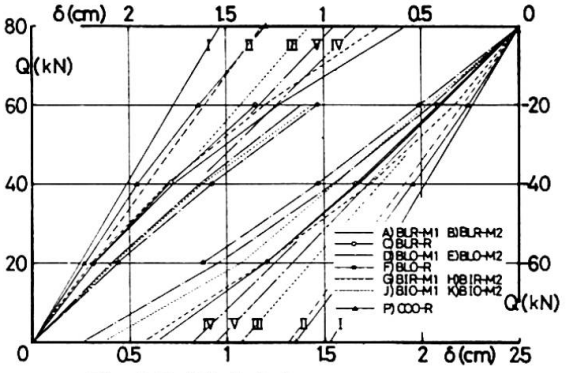


Fig.5 Initial Q-δ curves

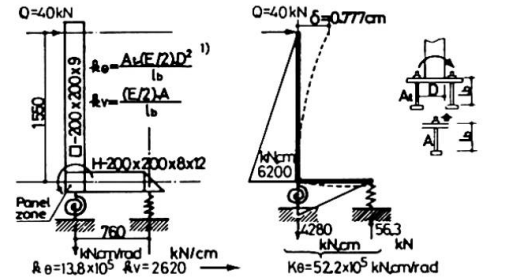


Fig.6 Structural analysis model

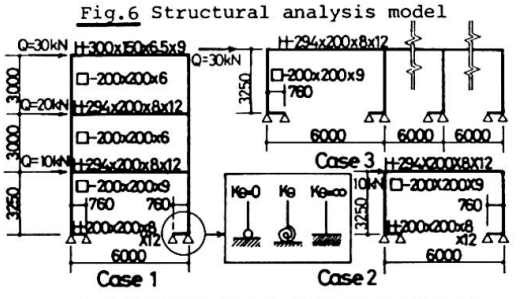


Fig.7 Three model frames conceived for structural analysis

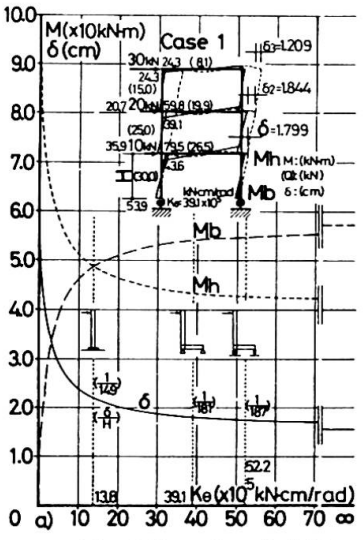


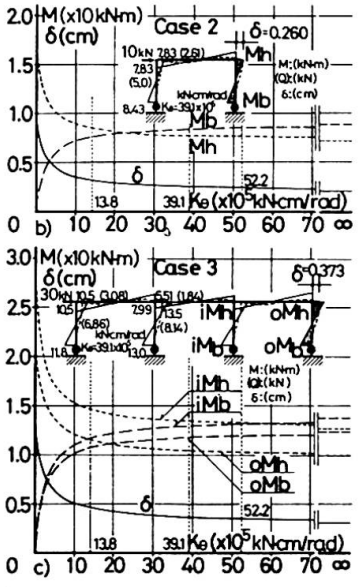


Fig.8 Moment and deflection of 1st story of analysis frames

deflection ($\delta$) are shown in Fig. 4. Fig. 4-d) shows the Q-$\delta$ curves of the steel column itself. All bracket type (BL, BI) specimens showed stabilized spindle shaped loops as shown in Fig. 4 a) and b). The initial Q-$\delta$ relationships are shown in Fig. 5, and the deflections at Q = ±40 kN and the equivalent spring constants of the column base including bracket obtained from the values of such deflections are shown in Table 2. The rotation rigidity of the column base covered with concrete was approximately two times that of the column base without concrete cover. The rotation rigidity of the exposed type column base without brackets was considerably small. The calculated values I, II and III in Figs. 4 and 5 represent Q-$\delta$ relationships of the steel column itself, and the value VI represents those where the column base and the bracket ends were assumed to have been supported with pins. The calculated value V was obtained by computer analysis through replacement of the bending moment rotation rigidity of the column base with an equivalent rotation spring in accordance with the Akiyama Method [1] and through evaluation of the bracket end expansion and contraction rigidity in terms of an equivalent expansion and contraction spring, and also with consideration of the effect of the shear deformation of the panel zone, as shown in Fig. 6. From the calculated values IV and V through the replacement of the column base including bracket with an equivalent rotation spring, ${}_{IV}K_{\theta}$ = 39.1 x $10^5$kN.cm/rad and ${}_{V}k_{\theta}$ = 52.2 x $10^5$kN.cm/rad will be obtained respectively. In the absence of a concrete cover, the rigidity by the calculated value V tends to be over-estimated, however in the presence of a concrete cover, it will be close to the value V and sufficiently safe if the design is based on the assumption of the value IV.
The relationship between the column base rotation rigidity and the column head and column base moment of the first story and also that between the column base rigidity and story deflection of the first story when a hypothetic lateral force is applied to the three model frames conceived as shown in Fig. 7 are respectively shown in Fig. 8. From these figures, it is shown that the column base with brackets may be regarded as perfect fixity. This type of column base is widely used in prefabricated house construction in Japan as it allows efficient installation with high degrees of fixity and stable restoring force characteristics.

## 3. CONCLUSION

The experiments and discussions performed have clarified the mechanical behaviours of the conventional type column bases. It was also shown from the behaviours of the structures and their components that the column base with brackets excels in rotation rigidity and restoring force characteristics as well as reliability from the standpoint of field application.

## REFERENCES

1. AKIYAMA H., Earthquakeproof Design in Steel Column Base, Gihodo Shuppan, March 1985. (in Japanese)

2. YOSHIMORI K. and NAKASHIMA S., Experimental Study on Square Steel Tubular Column Bases Consolidated with Reinforced Concrete, Proceedings of International Meeting on Safety Criteria in Design of Tubular Structures, Feb. 1987, pp. 113-120.

3. NAKASHIMA S. and IGARASHI S., Behaviour of Steel Square Tubular Column Bases Embedded in Concrete Footing, Proceedings of International Conference on Steel Structures, Part 1, Budva, Yugoslavia, Sep. 1986, pp. 119-128.

4. NAKASHIMA S. and IGARASHI S., Behaviour of Steel Square Tubular Column Bases of Corner Columns Embedded in Concrete Footings, Proceedings of the International Conference on Steel and Alminium Structures, Cardiff, U.K., July 1987, pp. 376-385.

# Liaisons dans les structures métalliques

Verbindungen in Stahlstrukturen

Connections and Steel Structures

**Reidar BJORHOVDE**
Professor
University of Pittsburgh
Pennsylvania, PA, USA

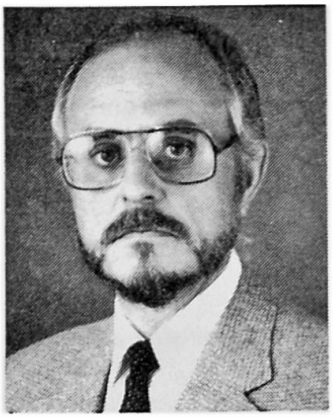

**Jacques BROZZETTI**
Directeur Scientifique
CTICM
St Rémy Les Chevreuse, France

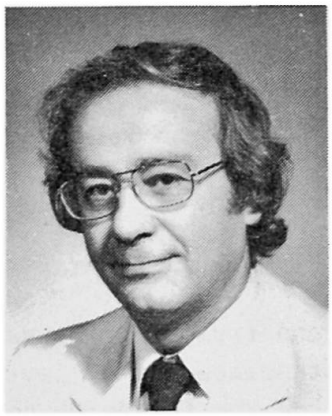

**André COLSON**
Dir. Dép. Génie Civil
Ecole Normale Supérieure
Cachan, France

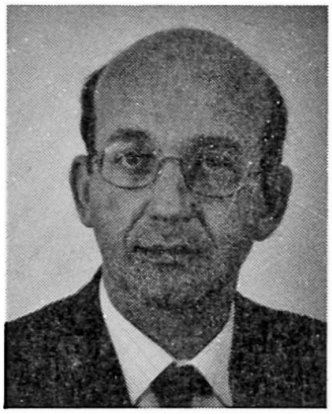

**RÉSUMÉ**
Cet article présente les principaux enseignements qui peuvent être tirés d'un colloque international organisé en 1987 à Cachan (France) sur le thème des liaisons semi-rigides dans les structures métalliques. Les connaissances scientifiques ont évolué très rapidement dans ce domaine et de nombreux résultats sont utilisables. Les travaux qui restent à développer pour une pratique industrielle courante sont définis tant en ce qui concerne les méthodes simplifiées que les états limites à adopter dans un cadre réglementaire.

**ZUSAMMENFASSUNG**
Dieser Aufsatz stellt die Haupresultate aus einem internationalen, 1987 in Cachan (Frankreich) organisierten Kolloquium über halb-starre Verbindungen in Stahlstrukturen dar. Die wissenschaftlichen Kenntnisse auf diesem Gebiet entwickelten sich sehr schnell und zahlreiche Ergebnisse sind schon zur Anwendung gekommen. Weiter zu entwickelnde Arbeiten zum Zweck von geeigneten industriellen Anwendungen wurden festgelegt sowohl was die vereinfachten Berechnungsmethoden als auch die im Rahmen der Normen anzunehmenden Grenzzustände betrifft.

**SUMMARY**
This paper presents the main conclusion of an international seminar which was held at Cachan in 1987 (FRANCE), on semi-rigid connections in steel structures. In this area, scientific knowledge has grown very quickly, and now numerous results are applicable. The work which has still to be done for a practical industrial application is presented not only for the concern of simplified methods but also for the limit states criteria to be adopted within a load and resistance factor design format.

## 1. INTRODUCTION

During the last five years much research work on semi-rigid connections has been conducted and a lot of data is now available. Partly, this is due to the computational and testing facilities which allow now studying and modeling of highly non linear and three dimensional problems that caracterize the semi-rigid connections. An International Workshop entitled "**Connections, and behaviour, strength and design of steel structures**" was held to bring together a group of researchers and designers with extensive experience in the theoretical and practical areas in order to establish a state of the art and to propose some guide-lines for design code writers.

Furthermore, it was felt that two important functions of the workshop would be :
- To identify the main topics of future research
- To organize and to set up a coherent data base to display the various resources available of reliable information among researchers, designers and code writers.

## 2. WORKSHOP ATTENDANCE AND ORGANIZATION

To achieve the most in depth, and fruitful discussions of the different aspects of the problem, the workshop attendance was by invitation limited to a relatively small group of experts from the following countries : Australia, Austria, Belgium, Canada, Denmark, France, Italy, Mexico, The Netherlands, Poland, Sweden, Switzerland, United Kingdom, United States, West Germany.

The workshop program was organized in such a manner that the maximum time was devoted for discussion in order to encourage informal exchange of ideas and information.
The following technical sessions were set up :

N°1 : Local analysis of joints
N°2A, 2B : Modeling of load-deflection behavior. Classification
N°3 : Methods of frame analysis
N°4 : Frame stability and simplified methods
N°5 : Design requirements and codes
N°6 : Data base organization.

In addition to the reporter in charge of each session, there was a research reporter whose duty was to inventory research and development needs.

## 3. TECHNICAL SESSIONS : TOPICS AND DISCUSSIONS

### 3.1 Local analysis of joints

This session was intended for a review of current theoretical and experimental research dealing with the local behavior of actual connections including all

connecting parts, fasteners, welds and so on. The expected outcomes were the understanding of the failure mechanisms and the identification of the load-deformation controlling parameters.

The main remarks and conclusions are :

- From the theoretical and numerical point of view, the recent finite element methods allow now for the analysis of one, two and three dimensional problems. Material and geometrical properties are considered, as well as contact and slip resistant problems. The separation of individual effects is possible which is of first interest for parametric investigations. Nevertheless some calibration tests are necessary to support and to make operational these methods.

- In the field of experimental work it is recognized the importance of the three dimensional analysis of the behavior of the connections, which are now assessed by new testing facilities. This covers the connections as well as the material itself. Also the unloading behavior should be more systematically studied.

- Concerning the design detailing and code requirements the main need resides in unified concepts and criteria for serviceability and ultimate limit states of the connecting part as well as for the global connection. For example it was thought more adequate to use the ultimate strength of the material rather than the yield stress to determine the strength capacity within an ultimate limit state design format.

- A particular attention was given to the prying force in end plate type of bolted connections. There is a consensus to incorporate the prying effect on the load side of the design equation.

3.2.1. Modeling of load deflection behavior

It was recognized that the global modeling (i.e. moment-rotation curve) is the only possible way to analyse frames with semi-rigid connections.

Many global connection models have been developed and presented. However, the need for assessing the influence of various details was stressed during the discussion. For example the use of slotted holes, to facilitate the erection work, have a significant role in the moment-rotation characteristics which must be taken into account in the modeling.

Although it was agreed that it is preferable to utilize global connections models, it is still necessary to determine carefully the main parameters such that initial stiffness and ultimate strength. Moreover, some global models in use refer specifically to these parameters.

Column footing connections bring up a lot of specific questions regarding unilateral contact problem, anchor bolt bound failure, grouting, crushing of concrete more especially under cyclic loading. In spite of these uncertainties it was recognized that column footing connections are able to have a sufficient amount of end restraint capacity.

Regarding the cyclic loading in general it subsits some particular complex problems with regard to the behaviour of the connection within the range of reversal loading.

### 3.2.2. Classification

A special sub-session was devoted to the classification of connections into categories such as flexible, semi-rigid, rigid from both experimental and theoretical standpoint. It was largely agreed that a classification system must be given in terms of STRENGTH, STIFFNESS and DEFORMATION CAPACITY. Among these three main parameters the initial stiffness is recognized as the most important controlling parameter for the frame analysis and behavior. So it is necessary to define it more precisely and particularly regarding the perturbation which may happen due to the testing procedure at the start of the loading which may alter the moment-rotation curve definition.

The unloading stiffness seems to be the same that the one in loading, this point have to be checked for a large range of connection types and sizes. This is important for the stiffness definition, on the one hand, and for the stability of frames on the other hand.

With regard to the definition of initial stiffness and ultimate strength some suggestions for simplified moment rotation curve were made (bilinear or trilinear).

As an outcome of the workshop the authors propose a classification system for the beam to column connections based on a reference length and ultimate strength of the connected beam.

## 3.3. Frame analysis

Different frame analysis computer programs were presented, all taking into account the P - $\Delta$ effects. Differences reside in the way the global response of the connection is treated, either discrete plastic hinges, or gradual spread plastification in the members, and so on. Despite these differences the analytical results correlate very well. These programs are mostly research tools and it is still necessary to develop additional design-oriented programs.

The use of semi-rigid connections generally induces lateral drift in the frame, which is the controlling factor in the design process. However, it is possible to find economical solutions which satisfy the drift limitation requirements.

Numerous points were raised regarding the use of composite girders which result in a more flexible bare frame if the slab stiffness and continuity is not taken into account in the calculation. In fact, composite action is able to provide a significant amount of end restraint.

### 3.4. Frame stability and simplified methods

There are now practical and design-oriented approaches to column and frame stability with semi-rigid connections. From experimental studies it was found a good correlation between the stability problems of individual columns and columns in subassemblages and frames. More particularly, the column stability solution seems to have a wide application area.

Concerning the simplified methods it was pointed out that they are the only way to bring effectively the semi-rigidity concepts into practice. In these methods the initial stiffness is of first importance. However the initial stiffness for the column footing connections depends on the moment-axial load interaction, longterm effect and cyclic loading. So additional research is needed to clarify the importance of these effects.

### 3.5. Design requirements and codes

There is a general agreement to recognize that the only practical way to make use, and to design semi-rigid connections was to refer to limit states design format.

It was pointed out that revised drift limits would have to be developed for frames with semi-rigid connections and that the commonly used limit of 1/400 for the ratio of building drift to building height have been established for structures with rigid joints taking implicitly into account the deformability of the connections. More accurate evaluation of lateral displacement leads to define more realistic drift limits. As said in the local analysis session, the limit states requirements for individual fasteners have to be known and fixed precisely.

Another question is to know if it is possible to introduce new steel quality and grades in the current design standards which are mainly based on the mild structural steel properties. There is a consensus to give a positive answer as long as, yield ratio, ductility ratio and weldability are warrantied. In the same way it is suggested that design standards should establish in parallel scopes and knowledge dissemination documents to establish or justify their background information.

### 3.6. Data base organization

There is a general agreement to recognize that this subject is of significant interest for a proper organizational structure allowing exchanges of information as well as avoiding any duplication of work. The first task of this organization is to provide a data sheet format available for researchers and designers for actual construction projects. This data sheet must contain all information for material properties of members and connectors, drawings of connections and testing devices, loading and measurement procedures and so on. The results have to be given in load-deflection curve indicating serviceability and ultimate load as well as initial stiffness which may be obtained by a partial unloading path. In the future this data base organization could be implemented and processed through a computer network such as E.A.R.N.

The contact persons for the data base organization are :

Reidar Bjorhovde (USA) and Jacques Brozzetti (France) for the beam to column connections.
Frans Bijlaard (The Netherlands) and Denis Beaulieu (Canada) for the column footing connections.

## 4. CONCLUSION

For the participants, the first benefit of this workshop is a better knowledge of each other through truly in-depth exchanges of opinions, methods, procedures, results and future directions and this for a wide number of countries.

There were agreements on the necessity of :
- improving the limit states design codes for allowing a better account of the semi-rigid connection concepts.
- setting up new simplified, and accurate, methods.
- a classification system of connections with regard to their main behavior.
- a data base organization.

A large number of propositions has been done to achieve these goals both with the identification of the more interesting research and development needs.

## 5. ACKNOWLEDGEMENTS

Financial support of the workshop was provided by a grant from the French government (Ministère de la Recherche et de l'Enseignement Supérieur).

## 6. BIBLIOGRAPHY

[1]. BJORHOVDE R., BROZZETTI J., COLSON A.
Connections in Steel Structures : Behaviour, Strength and Design. Proceedings of the Cachan workshop. 25-27 May 1987.
Elsevier Applied Science Publishers.

# Influence of Structural Connecting Details on the Load Carrying Capacity of Girders

Influence des assemblages sŭr la charge ultime des poutres

Der Einfluß von Anschluß-Details auf die Traglast von Biegeträgern

**Joachim LINDNER**
Prof.Dr.
Techn.Univ. Berlin
Berlin

Joachim Lindner, born in 1938, worked in the structural steel fabricating industry and later with an industrial scaffolding company. Since 1974, he has been Professor for steel structures at the Technical University, Berlin. His main research activities centre on the area of stability.

**SUMMARY**
If the compression flange of a beam in bending is not supported laterally the beam may fail by lateral torsional buckling. Investigation of this stability problem usually assumes simple support. In reality often notched ends are used. By this real support condition the beam becomes weaker which is unfavourable especially with respect to the torsional rigidity. On the other hand a partial fixing in the lateral direction is given by the commonly used bolted connections. It is reported on tests which were carried out to investigate these two effects.

**RÉSUMÉ**
Au cas où la membrure comprimée d'une poutre fléchie n'est pas supportée latéralement, la ruine de la poutre peut se produire à cause du flambement par flexion-torsion. L'étude de ce problème de stabilité présuppose en général un appui simple. Mais il y a très souvent, des entailles, qui réduisent la rigidité de la poutre. D'autre part, les assemblages, conventionnels par boulons assurent une certaine rigidité latérale. Ces deux effets ont fait l'objet d'essais, présentés dans ce rapport.

**ZUSAMMENFASSUNG**
Wenn der Druckgurt eines Biegeträgers seitlich nicht gehalten ist, kann der Träger durch Biegedrillknicken (''Kippen'') versagen. Bei der Berechnung dieses Stabilitätsproblems wird üblicherweise eine Gabellagerung angenommen. Tatsächlich sind jedoch häufig Ausklinkungen vorhanden. Diese vermindern die Steifigkeit des Trägers, ergeben durch die Schrauben am Anschluß jedoch auch eine teilweise seitliche Einspannung. Es wird über Versuche zur Klärung dieser Effekte berichtet.

## 1. GENERAL

The theory of lateral torsional buckling was investigated by many researchers in the past. As the most appropriate method, the utilization of the theory of elasticity has been established. The plasticity of steel is then being incorporated by way of special design-procedure.

In building structures commonly connections are used which provide ease of design, fabrication and erection. Some typical configurations for beam to column and beam to beam connections are shown in Fig. 1.

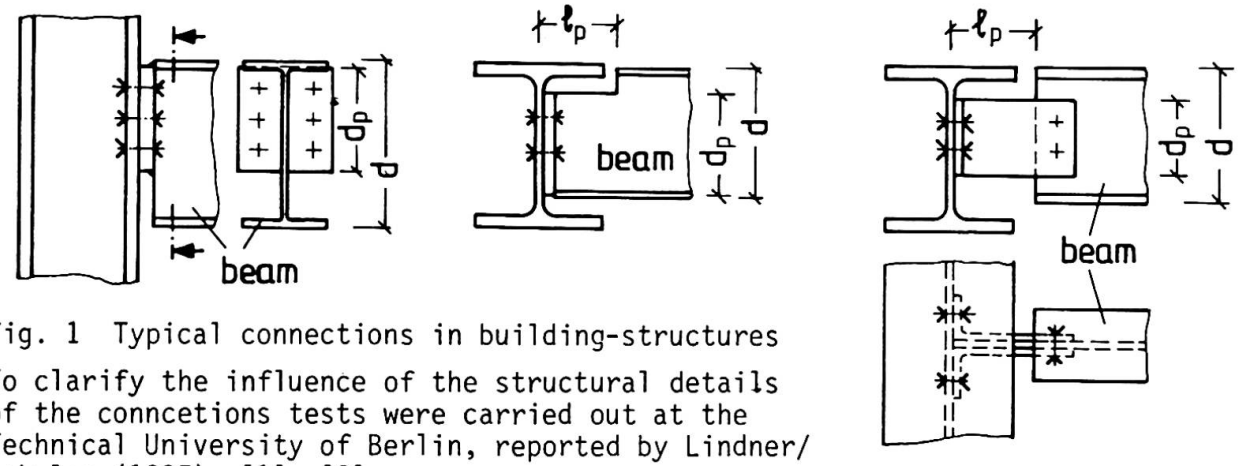


Fig. 1 Typical connections in building-structures

To clarify the influence of the structural details of the conncetions tests were carried out at the Technical University of Berlin, reported by Lindner/ Schulze (1985), [1], [2].

## 2. TEST SPECIMEN

Single-span girders were chosen for the test-programme:
- IPE (UB) 160/St 37, beam length 2,20 and 3,80 m,
- IPE (UB) 300/St 37, beam length 3,80 and 5,60 m.

A concentrated load at mid-span was applied 10 mm above the top-flange. It was inserted with a lateral load eccentricity of L/1000 with respect to the web. This eccentricity was chosen in such way that the displacements summed up caused by the out-of-straigthness and the eccentricity.

Three different types of connections were investigated; Fig. 1: 1. end plates with reduced depth, 2. notched ends, 3. web cleats which result in a special type of notched ends. The connections mainly were chosen from a publication of the German Steel Association, [3]. The nomenclature in Table 3 followed [3]. The bolt grade was chosen as 4.6 and 10.9, in the latter case with a partial tightness of 50%. High strength bolts were used for tests A3, T4 (Table 1), ISH connection type (Table 2), all tests (Table 3).

The geometrical and material properties of each beam were measured as well as the out-of-straigthness.

The section properties differed slightly from the nominal values. The yield stress $\sigma_y$ was higher than the nominal value:
- IPE 160: $\sigma_y$=253 .. 332 N/mm$^2$ (MPa), - IPE 300: $\sigma_y$:267 .. 286 N/mm$^2$ (MPa).
Using the measured section properties and the measured yield stresses the following full plastic moments $M_p$ were calculated
- IPE 160: $M_p$=32,6 .. 40,3 kNm, - IPE 300: $M_p$:164,0 .. 174,2 kNm.

## 3. TEST RIG AND TESTING PROCEDURE

The test rig was described by Lindner (1977), [4]. The load was applied by a jack over a movable loading frame in such way that any restraining effect of the applied load was eliminated. The support construction of the jack moved by ball bearings on a small transverse beam in cases when the tested beam was twisting and deflecting. So the complete loading arrangement ensured that the applied

| Test No. | Profil IPE | L [m] | Connection $\ell_p/d$ | Connection $d_p/d$ | $\kappa = \frac{M_{test}}{M_p}$ | Test No. | Profil IPE | L [m] | Connection $\ell_p/d$ | Connection $d_p/d$ | $\kappa = \frac{M_{test}}{M_p}$ |
|---|---|---|---|---|---|---|---|---|---|---|---|
| A1 | 160 | 2,2 | 0,67 | 0,67 | 0,538 | T4 | 160 | 2,2 | 0,67 | 0,78 | 0,962 |
| A2 | 160 | 2,2 | 0,67 | 0,67 | 0,604 | T5 | 160 | 2,2 | 0,67 | 0,78 | 0,782 |
| A3 | 160 | 2,2 | 0,67 | 0,67 | 0,521 | | | | | | |

Table 1 Test results for notched beams
type A: both flanges notched, type T: upper flange notched

| Test No. | Profil IPE | L [m] | Connection type | Connection $d_p/d$ | $\kappa = \frac{M_{test}}{M_p}$ | Test No. | Profil IPE | L [m] | Connection type | Connection $d_p/d$ | $\kappa = \frac{M_{test}}{M_p}$ |
|---|---|---|---|---|---|---|---|---|---|---|---|
| 1 | 300 | 5,6 | ISH 204 | 0,80 | 0,647 | 14 | 160 | 3,8 | IS 164 | 0,75 | 0,651 |
| 2 | 300 | 5,6 | ISH 204 | 0,80 | 0,576 | 15 | 160 | 3,8 | IS 164 | 0,75 | 0,701 |
| 3 | 300 | 5,6 | ISH 202 | 0,40 | 0,534 | 16 | 160 | 3,8 | ISH 162 | 0,63 | 0,668 |
| 4 | 300 | 5,6 | ISH 202 | 0,40 | 0,535 | 17 | 160 | 3,8 | IS 162 | 0,44 | 0,596 |
| 5 | 300 | 5,6 | IS 204 | 0,50 | 0,508 | 18 | 160 | 3,8 | IS 164 | 0,75 | 0,658 |
| 6 | 300 | 5,6 | IS 202 | 0,27 | 0,480 | 19 | 160 | 3,8 | ISH 162 | 0,63 | 0,670 |
| 7 | 300 | 3,8 | IS 204 | 0,50 | 0,659 | 20 | 160 | 2,2 | ISH 162 | 0,63 | 0,708 |
| 8 | 300 | 3,8 | ISH 202 | 0,40 | 0,712 | 21 | 160 | 2,2 | ISH 162 | 0,63 | 0,727 |
| 9 | 300 | 3,8 | ISH 202 | 0,40 | 0,699 | 22 | 160 | 2,2 | IS 162 | 0,44 | 0,711 |
| 10 | 300 | 3,8 | ISH 202 | 0,40 | 0,732 | 23 | 160 | 2,2 | ISH 164 | 0,75 | 0,777 |
| 11 | 300 | 3,8 | ISH 204 | 0,80 | 0,755 | 24 | 160 | 2,2 | ISH 164 | 0,75 | 0,769 |
| 12 | 300 | 3,8 | ISH 204 | 0,80 | 0,756 | 25 | 160 | 2,2 | IS 164 | 0,75 | 0,765 |

Table 2 Test results for end plate connections with reduced depth

| Test No. | Profil IPE | L [m] | Connection $\ell_p/d$ | Connection $d_p/d$ | $\kappa = \frac{M_{test}}{M_{pl}}$ | Test No. | Profil IPE | L [m] | Connection $\ell_p/d$ | Connection $d_p/d$ | $\kappa = \frac{M_{test}}{M_p}$ |
|---|---|---|---|---|---|---|---|---|---|---|---|
| W1 | 160 | 2,2 | 0,13 | 0,75 | 0,900 | W13 | 300 | 3,8 | 0,50 | 0,77 | 0,676 |
| W2 | 160 | 2,2 | 0,13 | 0,75 | 0,951 | W14 | 300 | 3,8 | 0,50 | 0,77 | 0,659 |
| W3 | 160 | 2,2 | 0,63 | 0,63 | 0,995 | W15 | 300 | 3,8 | 0,33 | 0,77 | 0,687 |
| W4 | 160 | 2,2 | 0,63 | 0,63 | 0,900 | W16 | 300 | 3,8 | 0,33 | 0,77 | 0,667 |
| W5 | 160 | 2,2 | 0,63 | 0,75 | 0,995 | W17 | 300 | 3,8 | 0,33 | 0,53 | 0,619 |
| W6 | 160 | 2,2 | 0,63 | 0,75 | 0,976 | W18 | 300 | 3,8 | 0,33 | 0,53 | 0,702 |
| W7 | 160 | 3,8 | 0,63 | 0,63 | 0,632 | W19 | 300 | 5,6 | 0,33 | 0,77 | 0,516 |
| W8 | 160 | 3,8 | 0,63 | 0,63 | 0,702 | W20 | 300 | 5,6 | 0,33 | 0,77 | 0,502 |
| W9 | 160 | 3,8 | 0,63 | 0,75 | 0,627 | W21 | 300 | 5,6 | 0,33 | 0,53 | 0,472 |
| W10 | 160 | 3,8 | 0,63 | 0,75 | 0,657 | W22 | 300 | 5,6 | 0,33 | 0,53 | 0,452 |
| W11 | 160 | 3,8 | 0,94 | 0,63 | 0,648 | W23 | 300 | 5,6 | 0,50 | 0,77 | 0,494 |
| W12 | 160 | 3,8 | 0,94 | 0,63 | 0,612 | W24 | 300 | 5,6 | 0,50 | 0,77 | 0,482 |

Table 3 Test results for connections with web cleats (L 200•100•10)

load remained vertical.

The load on the specimens was held constant at convenient increments throughout the test so that the various data readings could be taken after the specimen -

had stabilized itself at that load level.

## 4. TEST RESULTS AND EVALUATION

The test results are given in Tables 1, 2, 3. In order t evaluate these results the design procedure of the European Recommendation (1978) by the ECCS was used.

$$\lambda_{eq} = \sqrt{M_p/M_E} \qquad (1)$$

$$\kappa_M = \left[\frac{1}{1+\lambda_{eq}^{2n}}\right]^{1/n} \quad , \quad n = 2{,}0 \quad , \quad M_u = \kappa_M \cdot M_p \qquad (2)$$

where $M_E$ = elastic critical lateral torsional buckling moment

$n$ reduced system factor, following [5].

For each test specimen this evaluation was carried out using the individual section properties and yield stress. For calculation of the value $M_E$ computer programms were used taking into account different assumptions:

E1. constant stiffness across the beam length, no cross section deformation,[6],

E2. reduced stiffness at the support due to the connection type, no cross section deformation, [6],

E3. reduced stiffness at the support due to the connection type, warping stiffness of the end plate and cross section deformations are considered, [7], [8], [9].

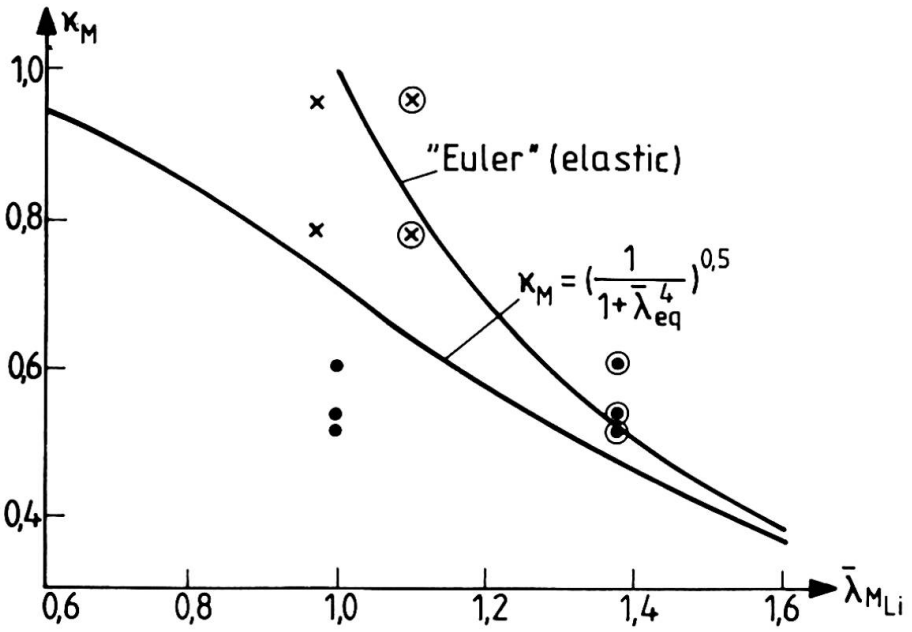


Fig. 2 Notched ends, evaluation of test results
•/x: assumption E1, •/x:assumption E3, [9]

Some of the results can be seen in Figs. 2 to 4, where the test results are plotted versus the equivalent slenderness $\lambda_{eq}$ of equ. (1).

The following general conclusions can be drawn from these results:

1. Notched beams

1.1 The reduced stiffness and the cross section deformation in the notched region must be taken into consideration.

1.2 A significant effect of partial fixing with regard to the minor axis can be seen in the case of one flange notching.

2. End plate connections with reduced depth

2.1 The reduced stiffness due to the end plates is significant for beams of higher depth (here IPE 300).

2.2 A partial fixing with regard to the minor axis leads to a higher load carrying capacity especially for the smaller profiles (here IPE 160).

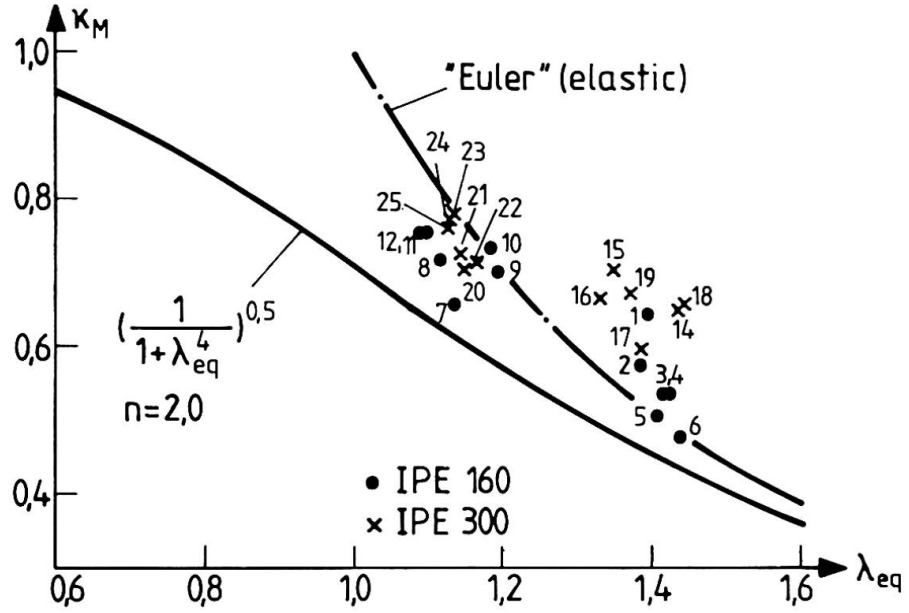


Fig. 3 Evaluation of test-results using assumption E3 - connection with end-plates

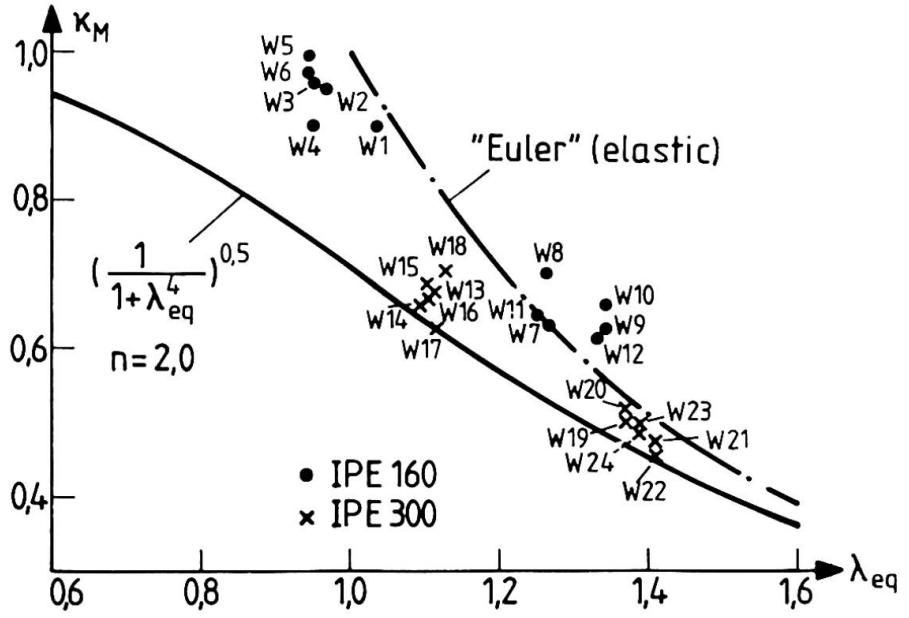


Fig. 4 Evaluation of test-results using assumption E2 - connection with web cleats

## 3. Connections with web cleats

3.1 The reduced stiffness in the support region is of minor influence. But this depends especially on the torsional stiffness of the cleats themselves which is relatively high in the cases tested here.

3.2 A partial fixing with regard to the minor axis leads to a higher load carrying capacity especially for the smaler profiles (here IPE 160).

The load deflection curves for the lateral displacement of the upper flange have shown to be very similar in all tests showing a satisfying rotation capacity. Bolt grade seems not to be a significant factor neither for the load carrying capacity nor for the flexible behaviour of the connections.

## 5. CONCLUSION

Further investigations under way concentrate on the influence of partial fixing with regard to minor axis. This effect depends especially on the type of cross section investigated.

## 6. ACKNOWLEDGEMENT

The author would like to express his appreciation to the "Deutsche Forschungsgemeinschaft" for providing financial assistance and to Dipl.-Ing. G.Schulze/ TU Berlin for conducting the tests.

## REFERENCES

[1] Lindner,J. und Schulze,G.: Biegedrillknickuntersuchungen an ausgeklinkten Trägern unter Berücksichtigung der Quereinspannung. Bericht VR 2073, Institut für Baukonstruktionen und Festigkeit, Technische Universität Berlin, 1985.

[2] Lindner,J. und Schulze,G.: Einfluß von Quer-Einspannungen auf die Gabellagerung. Bericht VR 2065, Institut für Baukonstruktionen und Festigkeit, Technische Universität Berlin, 1987. (Abschlußbericht DFG-Forschungsvorhaben Li 351/2-2).

[3] Typisierte Verbindungen im Stahlhochbau. Ringbuch des DASt/DSTV 2.Auflage. Stahlbau-Verlags-GmbH Köln, 1978 und Ergänzungsblätter vom Oktober 1984.

[4] Lindner,J.: Developments on lateral torsional buckling. 2nd International Colloquium on Stability, Washington D.C., May 1977, pp. 532-539.

[5] Draft DIN 18800 Part 2: Stahlbau, Stabilitätsfälle; Knicken von Stäben und Stabwerken. (Steel structures, Stability; buckling of bars and system of bars), 1988.

[6] Lindner,J. und Bamm,D.: KIBL2-Programm zur Berechnung der Verzweigungslasten beliebig gelagerter gerader Stabsysteme. Technische Universität Berlin, 1986.

[7] Gietzelt,R.: Grenztragfähigkeit von querbelasteten Trägern mit I-Querschnitt unter Berücksichtigung wirklichkeitsnaher Lagerungsbedingungen an den Trägerenden. Dissertation (Ph.D. thesis), Technische Universität Berlin, 1982.

[8] Lindner,J. und Gietzelt,R.: Influence of End-Plates on the Ultimate Load of Laterally Unsupported Beams. In: Instability and plastic Collapse of Steel Structures, pp 538-546. (M. Horne Conference). London/Toronto/Sydney/ New York, Granada 1983.

# Single-Bolt Semi-Rigid Connections in Space Frames

Assemblages semi-rigides à un boulon dans les structures spatiales

Flexible Einschraubenanschlüsse beim Bau räumlicher Stabwerke

**Herbert KLIMKE**
Dr.-ing.
MERO-Raumstruktur GmbH & Co
Würzburg, Fed. Rep. of Germany

Herbert Klimke, born 1939 received his civil engineering degree 1966 at the TU Berlin and his doctors degree 1976 at the TH Karlsruhe. Since 1974 he is head of the MERO-Raumstruktur computer center.

**Torsten HÖGLUND**
Professor
Royal Inst. of Technology
Stockholm, Sweden

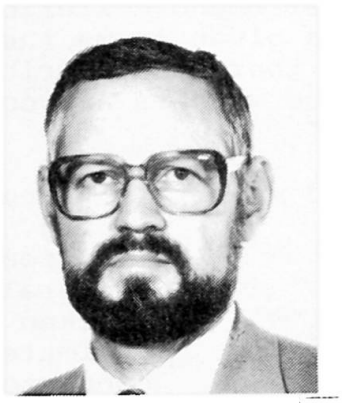

Torsten Höglund, born 1936 received his civil engineering degree 1963 and his doctors degree 1972 at the Royal Institute of Technology, Stockholm. After eight years as a consulting engineer, he is since 1982 professor of steel structures.

**SUMMARY**
Analysis of space structures normally assumes ideal spherical hinges at the intersections of member axes. However, no building system provides these ideal joints. Offset-connections must actually have some bending stiffness in order to prevent node rotations, especially if members are transversally loaded. The design of single-bolt semi-rigid joints for directly loaded rectangular hollow members and some physical tests are the topic of discussion in this paper.

**RÉSUMÉ**
L'analyse des structures spatiales présuppose normalement des articulations sphériques idéales à l'intersection des axes des membrures. Il n'existe cependant aucun système offrant ces assemblages idéaux. En fait, ces liaisons doivent présenter une certaine rigidité à la flexion afin d'éviter la rotation des noeuds, particulièrement si les membrures sont chargées transversalement. L'article présente le projet d'assemblages semi-rigides à un boulon pour des membrures rectangulaires creuses sous charges axiales. Des essais sont rapportés.

**ZUSAMMENFASSUNG**
Die Berechnung von Raumfachwerken beruht auf der Annahme idealer Kugelgelenke in den Schnittpunkten der Stabachsen. Tatsächlich besitzt kein reales Raumfachwerksystem diese idealen Verbinder. Zur Vermeidung von Knotenrotationen dürfen die exzentrischen Anschlüsse an die Knoten, insbesondere bei querbelasteten Stäben, keine Gelenke sein. In diesem Beitrag wird ein Bemessungskonzept für flexible Anschlüsse von direkt belasteten Rechteck-Hohlquerschnitten und die versuchstechnische Prüfung des Konzeptes diskutiert.

## 1. BASIC CONCEPTS

The analysis of general space frames can be distinguished by the stability criterion according to Föppl [1]. Those frames in accordance with Föppl's stability requirements are space trusses, i.e. they require no bending-resistant connections for the analysis of (axial) member forces.

The normal procedure of analysis is to assume ideal spherical hinges at the intersections of the member axes. In reality no building system provides a true spherical hinge at the intersection of member axes, i.e. the real offset-connections have to provide bending stiffness even in the ideal analytical model.

Because the magnitude of the connections rigidity remains unknown, no bending moments can be calculated for the connections by a full frame analysis. The only possible solution is found by the ultimate load concept, e.g. the upper and lower bound criteria as described by Feinberg (1948), Greenberg and Prager (1949) and Horne (1950).

Neal [2] states the lower bound criterion: "For any distribution of bending moments for a given frame the loading is less than the ultimate load, provided that the distribution is statically allowable and nowhere the members and connectors ultimate capacities are exceeded".

A typical MERO top chord member is represented by a model as shown in fig. 1. The bending moment at position a for the given loads $\gamma P$ (lateral) and $\gamma D$ (axial) is to be checked with respect to the ultimate bending capacity of the connectors (c)

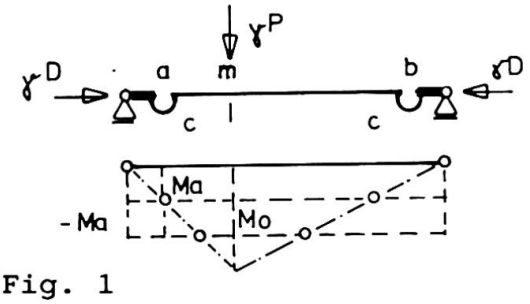

Fig. 1

$$M_a < M_{ult,c} \qquad (1)$$

The ultimate bending capacities and the spring rigidity c itself are related to the axial force. The check (1) is a straight forward application of the lower bound criteria, but does not explain the magnitude of nodal bending moments in the "real" structure: it only indicates that they cannot be greater than twice the ultimate bending capacity of the connection (resp. the sum of reverse bending capacities for non symmetric joints, see below).

## 2. DERIVATION OF A RATIONAL DESIGN CONCEPT BASED ON THE LIMIT STATE

Rectangular hollow sections (RHS) are most appropriate for the design of transversely loaded members in space frames. To interconnect them in a physical connector, a single bolt arrangement is used with the MERO-PLUS system. It offers the most advantages for fabrication and erection, including replacement of single members (fig. 2).

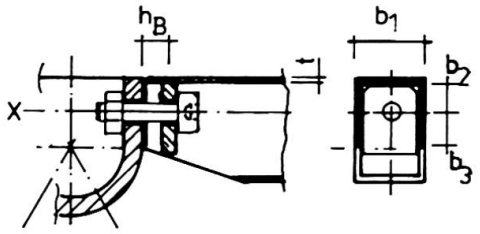


Fig. 2 Mero-Plus connector

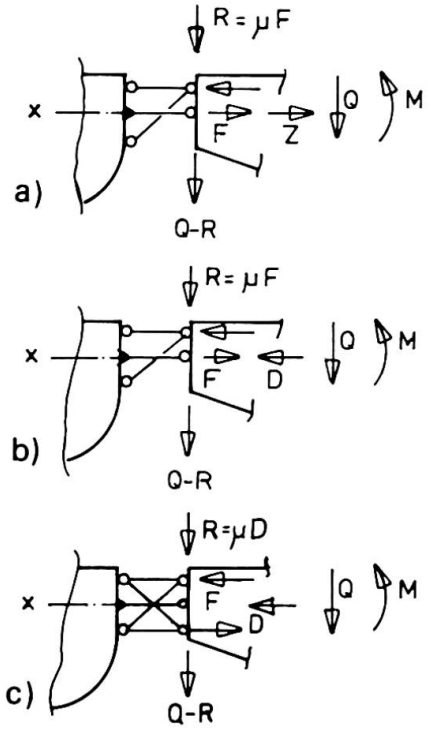


Fig. 3 Limit state models

Three different limit states can be distinguished (fig. 3). For the derivation of the design method some basic limit values are in common:

- the bolt tension capacity

$$Z_{Tr,B} = \beta_{Tr,B} \, A_{Bs}$$

where $\beta_{Tr,B}$ is the bolt yield stress and $A_{Bs}$ the bolt stress area;

- the bolt bending capacity

$$M_{Tr,B} = 0,24 \, \beta_{Tr,B} \, A_B^{3/2}$$

where $A_B$ is the gross section area;

- the bolt shear capacity

$$Q_{Tr,B} = M_{Tr,B}/h_B,$$

$h_B$ after fig. 2;

- the member contact surface compression capacities

$$D_{Tr,i} = \beta_{Tr,St} \, b_i \, t$$

where $\beta_{Tr,St}$ is the steel yield stress and $b_i$ (i=1,2,3) and t are according to fig. 2.

Using the above definitions, the ultimate loads can be derived for varying loading conditions, considering the limit state models in fig. 3. For each model further case separations have to be observed, as the sign of bending moments (M > 0, M < 0), the bolt strength ($Z_{Tr}$-Z, $Z_{Tr}$+D) and surface compression capacities ($D_{Tr,i}$) are governing the failure criterion. The derivation shall be shown as an example for case a in fig. 3 for a negative moment (M < 0) and the surface compression capacity limiting the connectors capacity (representing the obviously most critical situation): $Z_{Tr,B} - Z > D_{Tr,3}$ (fig. 4).

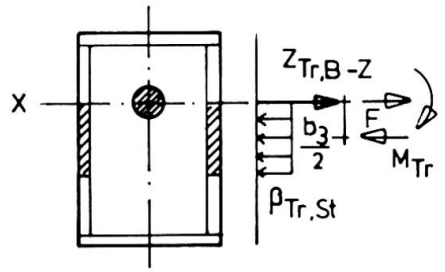


Fig. 4 Ultimate load stress distribution

The equilibrium equation for axis x yields with $F = D_{Tr,3}$ (fig. 2):

$$M^*_{Tr} = D_{Tr,3} \, b_3/2 + M_{Tr,B}\left(1 - \frac{Z + D_{Tr,3}}{Z_{Tr}}\right) \quad (2)$$

The related ultimate shear load is found according to (2) conservatively

$$Q^*_{Tr} = Q_{Tr} \, (1 - Z/Z_{Tr}) \quad (3)$$

where $Q_{Tr} = \text{Min}(0.9 \, Q_{Tr,B}, \, \mu \, Z_{Tr})$,

i.e. 0.9 $Q_{Tr,B}$ is the limit shear force that can be taken simultaneously with $M_{Tr,B}$ and vice versa.

In the same manner all possible combinations of loads and capacities as discussed above can be treated, yielding eventually a set of design formulae.

Still the question remains, whether the single bolt connections are providing enough ductility (rotational capacity) to allow for an application of the limit state concept. Tests under axial and transverse load have been performed to study the rotation of the connections.

## 3. TESTS CONFIRMING THE RATIONAL ANALYSIS CONCEPTS

Four tests were conducted at the Royal Institute of Technology, Stockholm, two in compression and two in tension. The tested construction simulated a top cord of the Stockholm Globe Arena and consisted of one rectangular hollow section top chord member bolted to two cup-shaped connectors. Details of a connector are shown in fig. 5a. The main purpose of the tests was to study the U-shaped connection area between the connectors and the space frame members. See fig. 5b.

Fig. 5c shows the four tests and table 1 gives some test results. The transverse load Q was in direct proportion to the axial load N. The load combination was chosen to be unfavourable for the contact region, not for the member as a whole. Therefore the compression members are acted upon by a transverse load corresponding to wind suction and the tension members to wind compression or snow load.

The material in the 150*100 hollow sections was St 52-3 with yield stress 387 N/mm$^2$ and ultimate stress 540 N/mm$^2$ according to coupon tension tests. The member thickness was 7,91 mm. The mean value of the ultimate load for the M27 10.9 bolts was 491 kN.

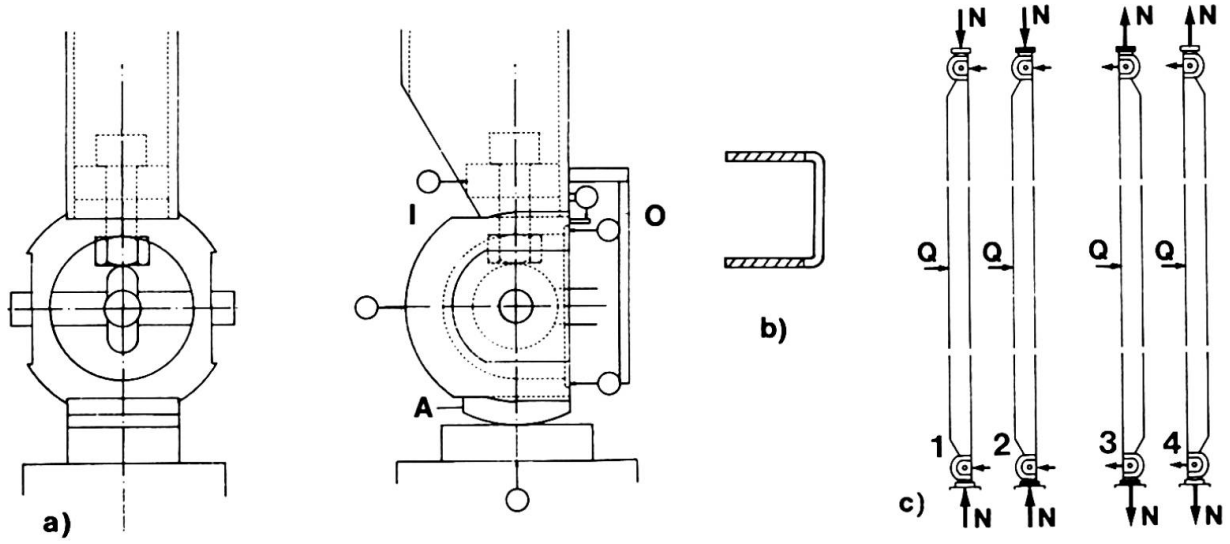


Fig. 5 a) Connector b) Contact area c) Tests

Table 1 Test results.

| Test no | Load direction | $\frac{Q}{N}$ | Support | Ultimate load N[kN] | Q[kN] | Failure mode |
|---|---|---|---|---|---|---|
| 1 | compression | 0.045 | simple | 710 | 32 | Yielding in contact region |
| 2 | compression | 0.045 | fixed | 950 | 43 | |
| 3 | tension | 0.060 | fixed | 470 | 28 | Failure of tension bolt |
| 4 | tension | 0.12 | simple | 480 | 58 | |

## 3.1 Test no. 1

The cylindrically formed supporting plate (A in fig. 5a) was given a radius with the center coincident with the center of the connector. The normal force acts through the center of the supporting connector even when it is rotated. In the beginning of the tests both inner and outer sides (I and O, see fig. 5b) were in compression, see fig. 6a. At larger loads there becomes a gap at the outer side and a local compression of the inner side. Only the legs of the U-formed end of the hollow section member were carrying the axial and shear load. At the ultimate load, 710 kN, the calculated nominal stress on the contact area was 660 N/mm$^2$ which is 1.2 times the ultimate stress 540 N/mm$^2$ given by the coupon tension tests.

Most of the yielding took place close to the connecting surface. No yielding of the connector was observed. The transverse load seemed to have neglectable influence on the contact pressure.

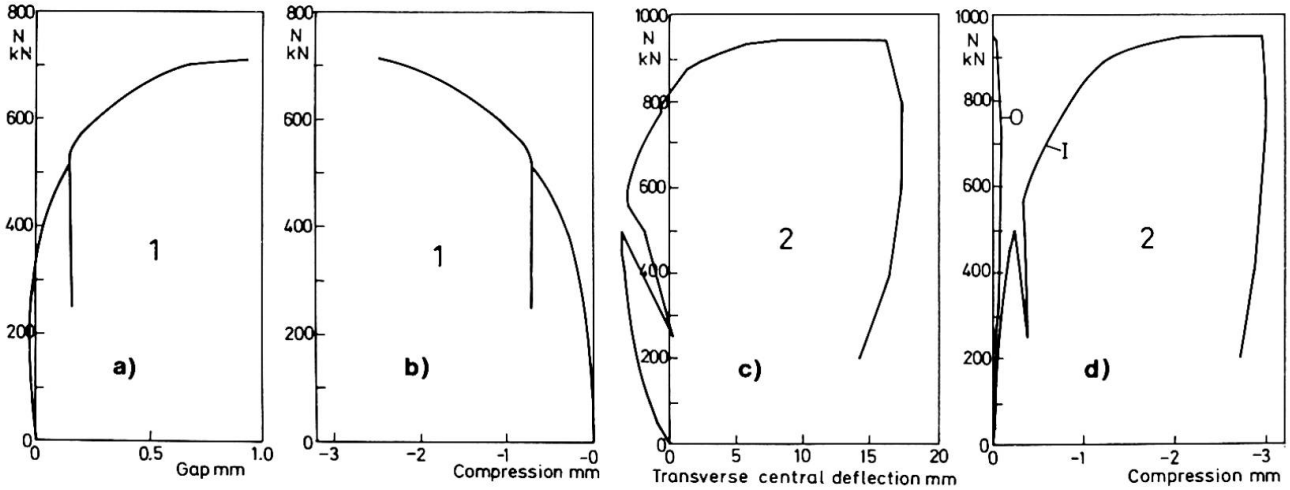


Fig. 6 a) Gap at outer side O and b) local compression at inner side I. Test no 1. c) Central deflection and d) local compression at inner side I and outer side O. Test no 2

## 3.2 Test no. 2

The connectors were fixed to the testing machine by bolts and rectangular plates. Both ends of the member were fixed. In the beginning, the direction of the transverse deflection coincided with the direction of the transverse load. At about 500 kN the transverse deflection changed sign and at the ultimate load the

maximum deflection was about 17 mm in the opposite direction. See fig. 6c.

Both sides of the connection area were in compression during the testing but the compression on the outer side was very small, almost zero at the ultimate load. See fig. 6d. The local compression at the inner side was about 3 mm. If all the U-shaped area was supposed to be in compression then the average stress would be 490 $N/mm^2$. If only the legs where in compression then the calculated stress would be about 860 $N/mm^2$ compared to 660 in test no 1.

### 3.3 Tests no. 3 and 4

Both tests were fixed to the testing machine by the same type of bolts (M27 10.9) as between the connectors and the hollow section member.

At small loads there was a gap only at the outer side but at about 200 to 350 kN gaps also arose at the inner side. See fig. 7. The final mode of action was the same for the two tests although the transverse load was twice as much in test 4 as in test 3. The ultimate load was 473 and 483 kN respectively. In both tests the uppermost bolt failed by thread stripping at loads close to the bolt tension strength 491 kN.

The transverse shear load was 14 and 29 kN which apparently had a minor influence on the ultimate load.

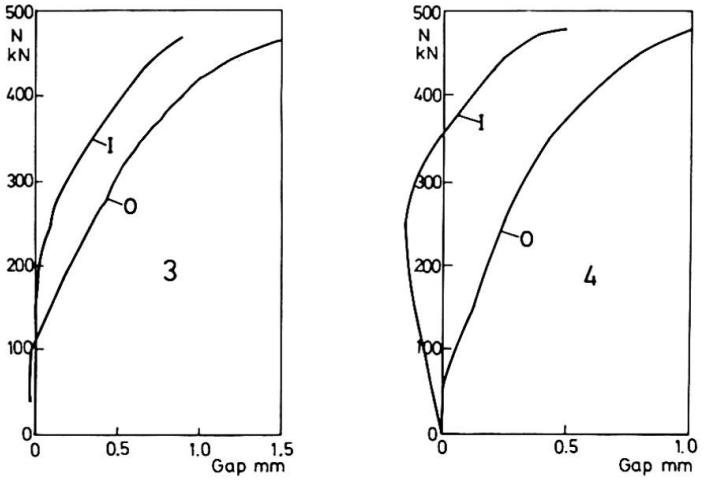


Fig. 7 Gap at the inner and outer side of the intersection between the connector and the member. Tests no. 3 and 4

## 4 CONCLUSION

The theory is in good agreement with the tests except that due to partially restrained lateral expansion of the member ends the ultimate compression capacity is larger than the theoretical capacity based on the yield stress. In a hyperstatic space frame there is a reserve in compression strength of the connector and possibilities of redistribution of forces after local yielding.

[1] Föppl A. Das Fachwerk im Raume, Teubner, Leipzig 1928.
[2] Neal B.G. Die Verfahren der plastischen Bemessung biegesteifer Stahlstabwerke, Springer, Berlin 1958.

# Assessing Alternative Details in Beam/Column Connections

Evaluation des détails constructifs d'assemblages poutres-colonnes

Bewertung verschiedener bewehrter Rahmenknoten

**R. H. SCOTT**
Lecturer
University of Durham
Durham, England

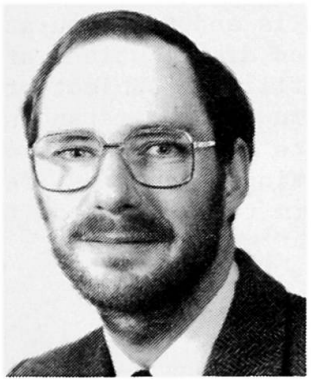

Dr. Scott graduated from the University of London in 1968, and then spent ten years with a Consultant and Local Authority. He joined the School of Engineering and Applied Science at the University of Durham in 1978 as a lecturer with special interests in concrete structures.

**P.A.T. GILL**
Senior Lecturer
University of Durham
Durham, England

Dr. Gill has degrees in mechanical engineering from Nottingham and Southampton Universities. He worked in the aero engine industry before joining Durham University in 1967. His principal interests are stress analysis and dynamics.

**SUMMARY**
Test on three reinforced concrete beam/column connection specimens are described, each having a different reinforcement layout. Reinforcement strain distributions were measured by internally strain gauging the reinforcement; electric resistance strain gauges were installed in each specimen. The effects of the detailing arrangements on the overall structural behaviour are discussed, and an indication given of future tests in the programme.

**RÉSUMÉ**
Des essais ont été réalisés sur trois assemblages poutres-colonnes en béton armé, chacun ayant un renforcement de configuration différente. On a mesuré la répartition des tensions dans le renforcement en y introduisant des indicateurs de tension à résistance électrique. On discute les effets de la configuration des détails sur le fonctionnement de la structure en général et l'on esquisse les grandes lignes des essais envisagés pour la suite du programme.

**ZUSAMMENFASSUNG**
Es werden Tests mit drei verschiedenen Rahmenknoten beschrieben, jede mit einer anderen Bewehrungsführung. Die Verteilung der Bewehrungsspannungen wurde mit Dehnmessstreifen bestimmt. Bis zu 230 Dehnmessstreifen wurden in die Knoten einbetoniert. Die Wirkung der jeweiligen Anordnung auf das verhalten der Gesamtstruktur wird diskutiert und es wird auch auf zukünftige Tests in diesem Programm hingewiesen.

## 1. INTRODUCTION

The connections between beams and columns are often the most critical sections in a reinforced concrete structure. The connection zones are in a state of multi-axial stress due to the combined actions of axial load, bending moment and shear forces, and these effects can be particularly severe in the case of an external connection where the beam is present on one side of the joint only. It is well known that the reinforcement detailing in the connection zone has a profound effect on the joint behaviour; typically in external connections the beam tensile rods are bent either up or down into the column, or bent into a 'U' to form the beam compression reinforcement. Tests have been conducted in many countries to assess these details and to formulate guidelines for good detailing practice. However, the detailed distributions of strain along the reinforcement in the connection zone are still the subject of some speculation and here a significant area of ignorance in the understanding of connection behaviour still exists. The authors decided to address this problem by conducting a series of tests in the laboratory using specimens reinforced with strain gauged reinforcement. These tests form the subject of this paper.

## 2. SPECIMEN DETAILS AND TEST PROCEDURE

Three external beam/column connections have been tested to date. Each had a beam 850 mm long framing at mid-height into one side of a column 1700 mm high. The column cross-sections were all 150 mm × 150 mm and the beams 210 mm deep and 110 mm wide. Both the beam and the column were loaded, the former downwards at a point 100 mm from the free end; the tension steel was thus at the top of the beam's cross-section. The columns were each reinforced with four 16 mm diameter high yield rods (Torbar) and 6 mm diameter mild steel links at 150 mm centres; this included a link at the mid-height of the beam. The beams were reinforced with a pair of 12 mm diameter high yield rods top and bottom with 6 mm diameter mild steel links at 100 mm centres. In the connection zone the beam reinforcement fitted between the column reinforcement, but the two sets of rods touched where they became adjacent. The rods on one side of the specimen were specially machined to permit the installation of electric resistance strain gauges (gauge length 3 mm) for strain measurement. Three different detailing arrangements were studied. With Specimen 1, the beam tension reinforcement was bent down into the column, with Specimen 2 it was bent up into the column, and with Specimen 3 it was bent into a 'U' to form the beam compression reinforcement; with specimens 1 and 2 straight rods were used for the beam compression reinforcement.

The strain gauges were mounted in a duct 4 mm wide × 4 mm deep running longitudinally through the centre of the reinforcement, as described in reference 1. Up to 230 strain gauges were installed in the beam and column reinforcement, including the bent beam rods (which were machined after bending). The gauging layouts were designed to give both an overall picture of the specimen's behaviour plus very detailed information in the connection zone itself; the minimum gauge spacing was 12.5 mm.

The column was loaded first to 275 kN in increments of 25 kN. This produced a compressive strain of around 500 microstrain in the column reinforcement which was considered to be a typical working load situation. The column load was then held whilst the beam was loaded in 1 kN increments until failure occurred. At each load stage a full set of strain gauge readings was recorded using a computer controlled data acquisition system. This also logged the applied loads, column shear forces and the load carried by a prop provided at the beam end to control sidesway. Where possible, increments of deflection were applied to the beam after joint failure had occurred.

## 3. RESULTS

The strain distributions along the beam tension reinforcement are shown in Figures 1, 2 and 3 for specimens 1, 2 and 3 respectively. The rods have been "straightened" for ease of interpretation with a key being provided with each figure to show its context within the specimen. The loads indicated are those applied to the beam; the column load is always 275 kN.

Loading the column to 275 kN produced compressive strains of about 500 microstrain both in the column reinforcement and in the vertical leg of the beam tension reinforcement, including the 'U' bar of specimen 3. The Poisson ratio effect caused by the column shortening led to small tensile strains being recorded in the bottom beam rods where they crossed the connection zone. Loading the beam soon eliminated these and caused a steady increase in tension of the top beam reinforcement and compression in the bottom beam reinforcement in all three specimens. The distribution of tension in the top beam reinforcement exhibited a series of peaks as cracks developed in the beam. A progressive movement into the connection zone of the point of zero strain was observed at each load stage as an increasing length of the top beam rod became tensile.

Diagonal cracking in the connection zone was first apparent at loads of 17.1, 18.9 and 19.9 kN for the three specimens respectively, at which time maximum strains in the beam tension rods, at the face of the column, were 1891, 2547 and 2442 microstrain. In specimens 1 and 2 the top beam rods were now in tension throughout the connection zone, whilst with specimen 3 tension had penetrated around both bends of the 'U' bar.

Up to this point in the tests - the onset of diagonal cracking - the behaviour of the three specimens had been broadly similar. However, marked differences were observed as the beam loads were increased further. With specimen 1, the effect was to cause an increasing length of the vertical leg of the top beam rod to become tensile at each load stage until, when failure occurred at 26.2 kN there were no compressive strains in the rod at all, even though its vertical leg abutted a column rod which was always in compression. This detail allowed the full moment of resistance of the beam to be developed and peak tensile strains at the column face were in excess of 20,000 microstrain; the reinforcement was either at, or near to, its yield stress well into the connection zone.

Specimen 2 was more brittle as it failed at 21.5 kN, only 2.6 kN above the load for the first diagonal crack. Failure was characterised by a sudden propogation of the tension zone along the vertical leg of the top beam rod when a vertical crack formed along the line of the adjacent column rod. The maximum strain was 5782 microstrain but there was little plasticity in the connection zone.

Specimen 3 exhibited behaviour similar to specimen 1 in that the advance of tension around the 'U' bar was progressive as the load was increased. Failure was at 25.9 kN, by which time the tension zone had extended back out into the bottom of the beam. The beam was able to develop its full moment of resistance but there was less ductility than with specimen 1 as the strains in the connection zone were lower. A small peak was discerned in the strains at the point where the rod re-entered the beam, believed to be caused by the effects of the diagonal cracking. A similar, but rather more marked, effect had previously been observed in the bottom beam rods of specimens 1 and 2, the strain distributions for the latter being shown in Figure 4. Peak tensile strains of 168 and 1207 microstrain were recorded for these two specimens respectively; with specimen 2, near to the column, both the top and the bottom rods in the beam were in tension at the end of the test.

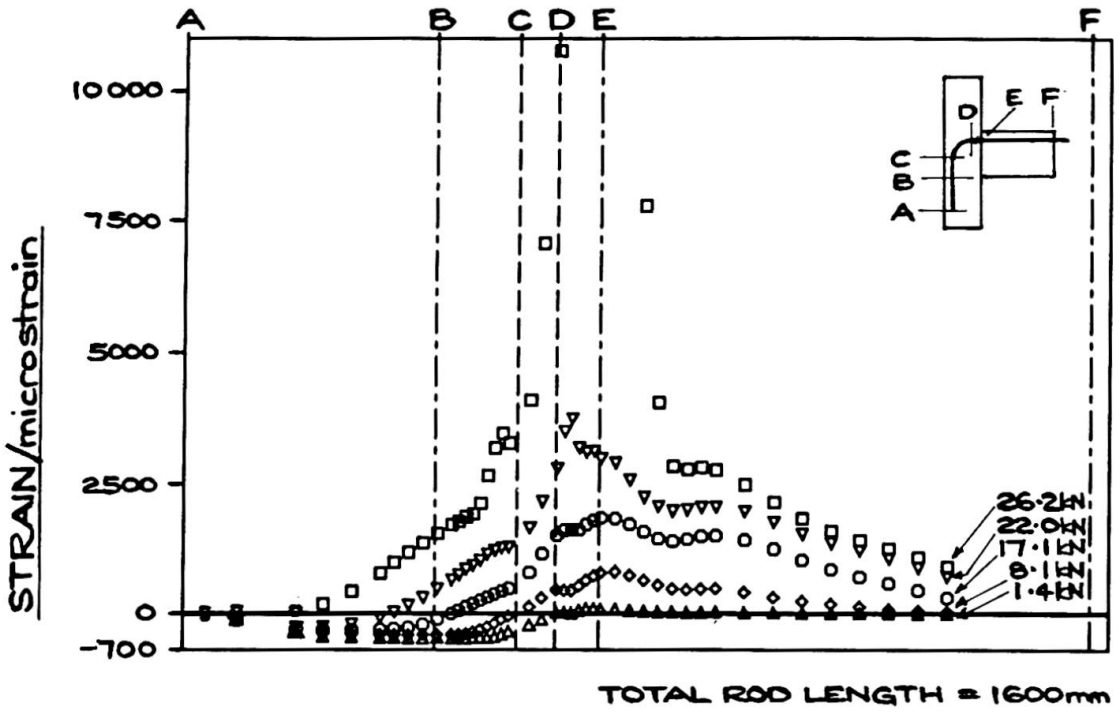


Fig.1: SPECIMEN 1 – TOP BEAM ROD

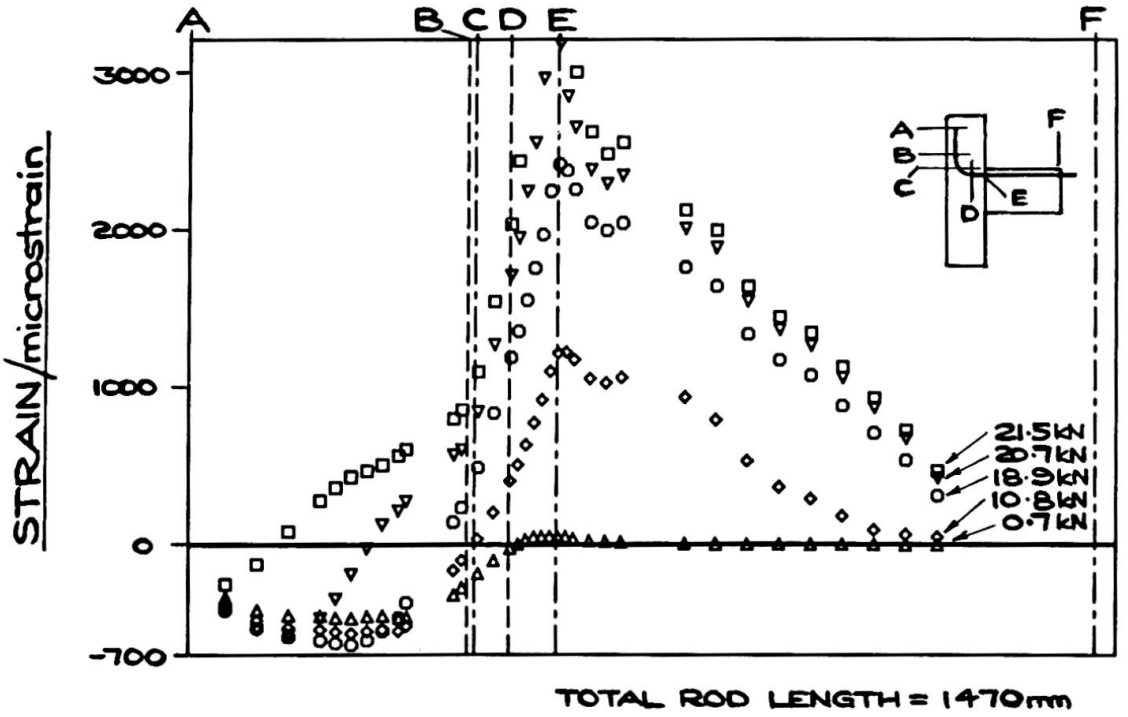


Fig2: SPECIMEN 2 – TOP BEAM ROD

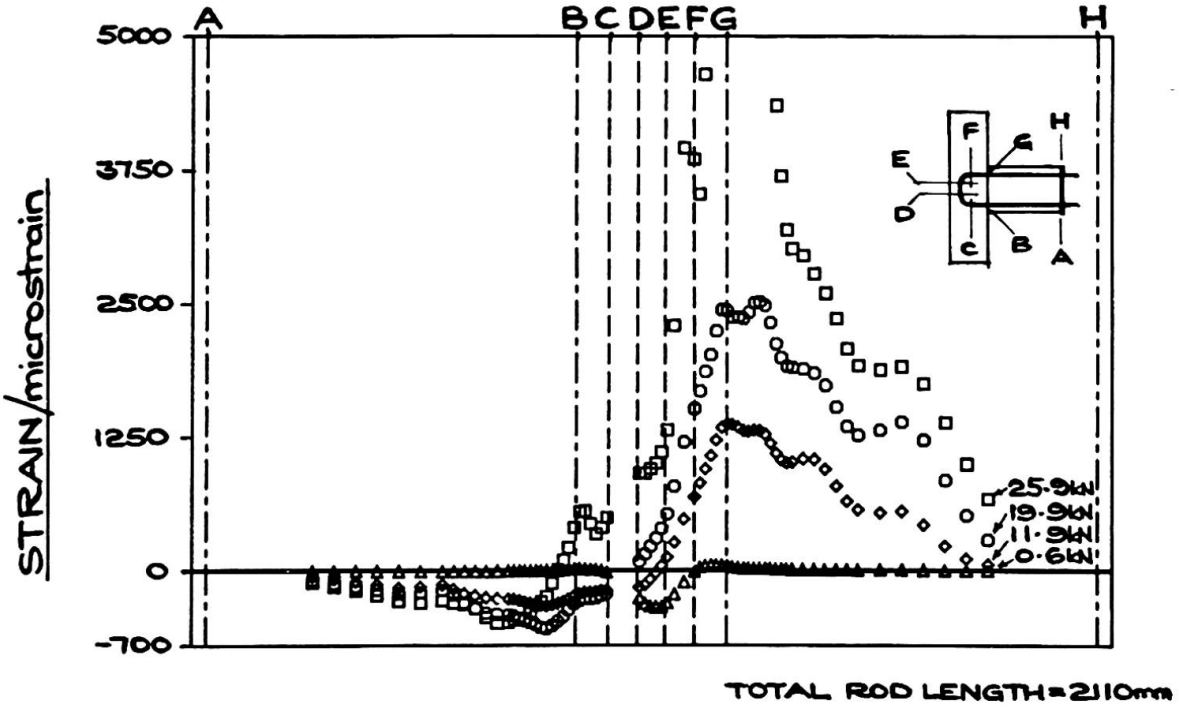


Fig3: SPECIMEN 3 – 'U'-BAR

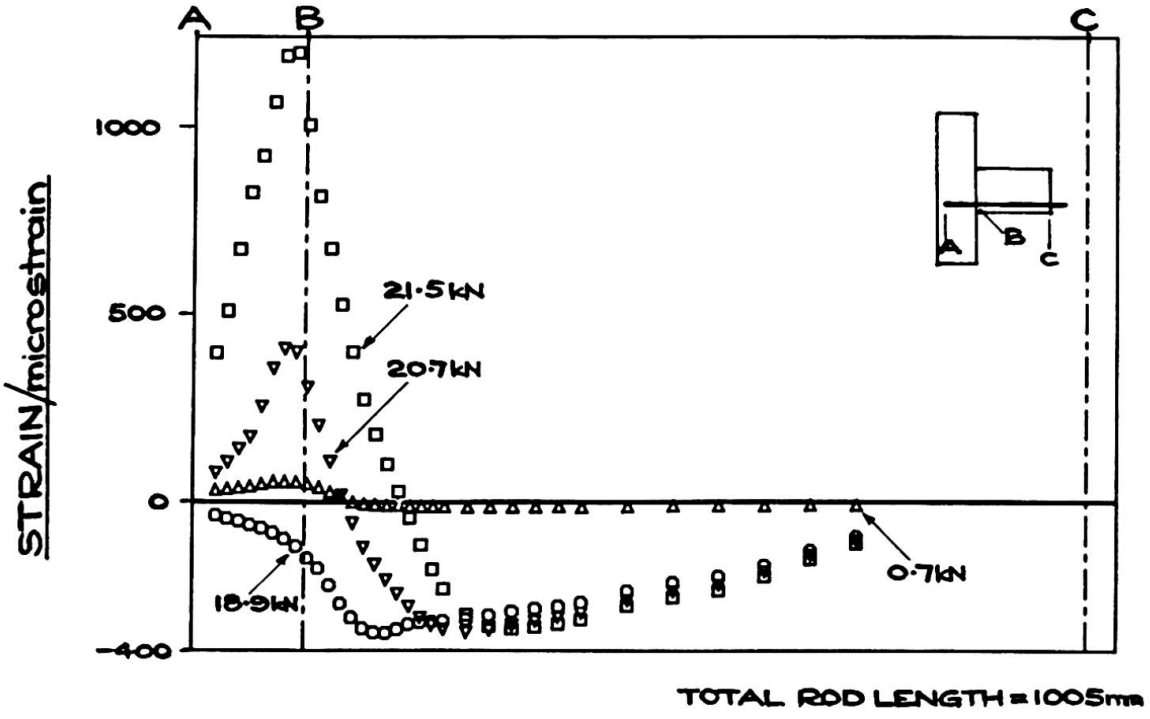


Fig4: SPECIMEN 2 – BOTTOM BEAM ROD

## 4. DESIGN IMPLICATIONS

Some preliminary implications regarding overall structural behaviour may be drawn from these tests. The detailing system of specimen 1 - beam reinforcement bent down into the column - is capable of developing considerable ductility and thus would permit a considerable redistribution of moments throughout a structure at the ultimate limit state. However, as the beam tension steel is at or near to its yield stress throughout much of the connection zone under these conditions, then consideration should be given to increasing its anchorage length in the column since bond stresses in the connection zone will be very low. The 'U' bar detail of specimen 3 also performed well but was rather less ductile than specimen 1, whilst the marked lack of ductility in specimen 2 - beam reinforcement bent up into the column - would be a severe hindrance should moment redistribution be found necessary due, say, to an accidental overload. The presence of surprisingly large tensile strains in the bottom beam reinforcement suggests that the column link in the connection zone may be quite highly stressed under ultimate conditions and so have an important role in tying the connection zone together.

## 5. FURTHER WORK

This paper has described the first phase of a comprehensive programme of tests. Currently, an examination of the effects of a higher reinforcement percentage is in progress by using two 16 mm diameter rods for the beam tension steel. Further tests will induce more bending in the column by using a lower column load, and an attempt will be made to measure directly the strains in the beam and column links. Associated with the experimental work is a comprehensive programme of data analysis using purpose-written inter-active colour graphics software.

## 6. CONCLUSIONS

A detailed picture of the reinforcement strain distributions in three reinforced concrete beam/column connections has been established using internally strain gauged reinforcement. The style of the reinforcement detailing had a profound effect on the behaviour of the specimen by controlling the degree to which ductility could be developed in the connection; this has implications for the redistribution of moments around a structure at the ultimate limit state. Consideration should be given to increasing anchorage lengths in some instances.

## 7. ACKNOWLEDGEMENTS

The technical support of Mr. S.P. Wilkinson and the financial support of the Science and Engineering Research Council are both gratefully acknowledged.

## 8. REFERENCE

1. SCOTT R.H. and GILL P.A.T., Short-Term Distributions of Strain and Bond Stress Along Tension Reinforcement. The Structural Engineer, Vol. 65B, No. 2, June 1987, pp. 39-43.

# Imperfections of Structural Details and Behaviour of Steel Frames

Imperfections des détails de construction et comportement de cadres métalliques

Imperfektionen von Konstruktionsdetails und Verhalten von Stahlrahmen

**Miklós IVÁNYI**
Prof. Dr. Sc.
Technical University
Budapest, Hungary

Miklós Iványi, born in 1940, received his civil engineering degree at Technical University, Budapest, 1963, where he is Professor of Structural Engineering and Head of the Department of Steel Structures. His main fields of activity are the stability of steel structures and plastic design in steel.

**SUMMARY**
Within a development program of mass-produced simple industrial steel structures a series of full-scale failure tests has been carried out. Effects of change in geometry, local instability and initial imperfections were analyzed.

**RÉSUMÉ**
Des essais à la ruine en vraie grandeur ont été effectués au cours d'un programme de développement de constructions industrielles en acier, simples produites en série. Les effets du changement de forme de la structure, du voilement local et des imperfections initiales ont été examinés.

**ZUSAMMENFASSUNG**
Im Verlaufe eines Entwicklungsprogramms für Serienfertigung einfacher industrieller Stahlbauten wurden Bruchversuche im Originalmasstab durchgeführt. Einflüsse von Biegemomenten zweiter Ordnung, Plattenbeulung, Kippen und Anfangsimperfektionen wurden analysiert.

## 1. INTRODUCTION

The increasingly powerful experimental and computational tools of structural design require a well-defined design philosophy. As its basis generally the concept of limit states is accepted in many countries. Limit states are usually divided into the two following groups:

1st group - limit states of carrying capacity / ultimate limit states /
2nd group - limit states of seviceability

Checking serviceability at -working load level the traditional and well tried out methods of structural analysis are used. The quite frequent tests on original structures show as a rule a relatively good accordance with calculated stress patterns or even better with predicted deflections /apart from the occasional effect of lack of fit at connections/.

On the other hand, structural response in the vicinity of peak load can be extremely complex. The early and very simple methods of plastic limit analysis /based on the concept of rigid-plastic materials which are in principle completely insensitive regarding any forms of initial imperfections/ are confined to a very limited class of structures, built up of bulky elements. As soon as global and even more as local instability plays role in failure,

- the effect of initial geometric imperfections is enhanced,
- the residual stresses /remaining regularly latent at lower loads, interacting with growing active stresses/ result in premature plastic zones, and /last but not least/
- the usual and widely accepted tools of analysis - as beam theory /based on Bernoulli-Navier hypothesis/, small deflection theory of plates and so on - cannot describe exactly enough the structure's response at failure.

The simplified model is not elaborate enough to reflect real structural behaviour, so that a secondary, more detailed local model is introduced to depict the mostly critical part of the structures, by which more realistic quality parameters can be deduced from the already known primary parameters.

Because of the interaction of local and global behaviour this pattern cannot be followed in the case of hyperstatic structures, as the additional information gained by the secondary, local model is to be fed back to the calculation of primary parameters as well. For this purpose, if - as very often - the secondary model can be analysed by numerical methods or only experimentally, the results have either to be re-interpreted to obtain mathematically treatable, simple enough rules, or the secondary model has to be simplified to get well-usable results. In both cases the validity or accuracy has to be proved by /usually very expensive/ failure tests on the whole structures.

To sum up, it seems that because of frequent uncertainties in predicting failure load, the double check of structures - at different load levels - not only reflects different aspects of stuctural behaviour, but contributes to a safer design procedure as well.

## 2. TEST PROGRAM

The experimental research project was carried out in the Laboratory of the Department of Steel Structures, Technical University, Budapest.

Fig. 1. gives a brief summary of the full-scale tests and dimensions of the specimens, indicating the loads and the characteristics of the loading process. [2]
The second part of the program was a representative part of a multi-purpose, pinned, pitched roof industrial hall: a building section consisting of 3 frames, bracings with pinned elements, light gage purlins and wall beams with corrugated steel sheeting. /Fig. 2./ [4]

## 3. COMPUTATIONAL MODEL

Instead of the plastic hinge the "interactive plastic hinge" has been introduced for mounting base constructed from plates which are of a much higher degree of freedom than the previous ones as they also embrace the effects of strain hardening of the steel material, of the residual deformation, as well as of the plate buckling bringing about the "descending" characteristics. [3]
The element of the bar is considered to be built up of plate elements /following the pattern of steel structures/ instead of a compact section.

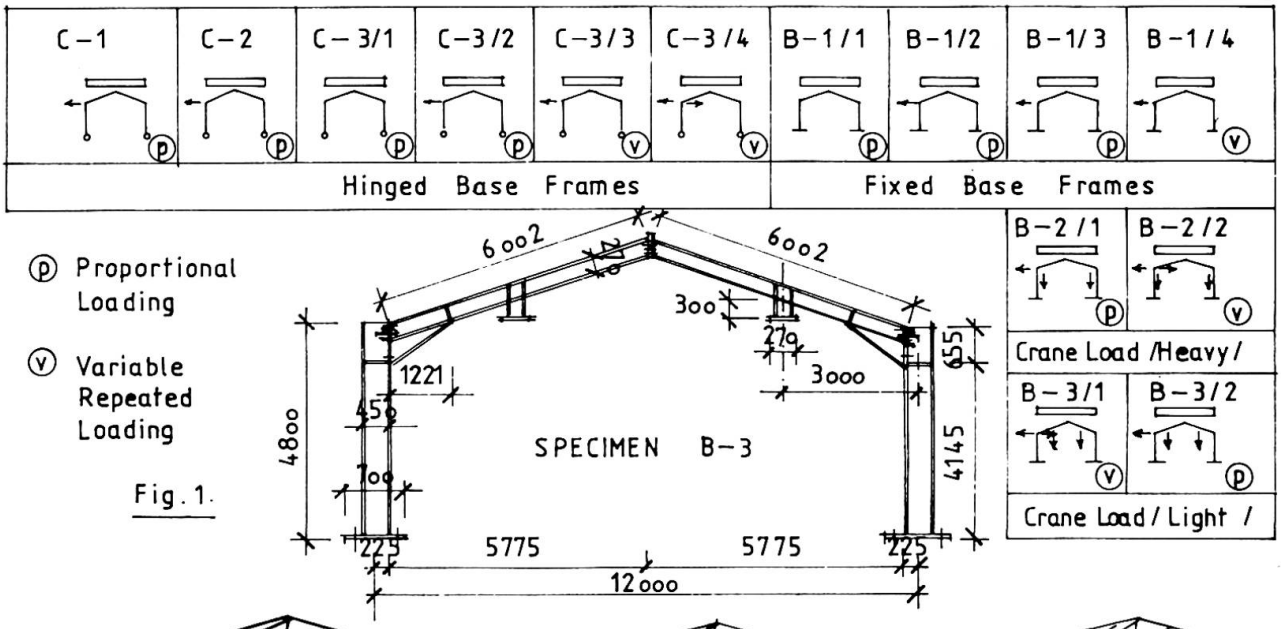


Fig. 1.

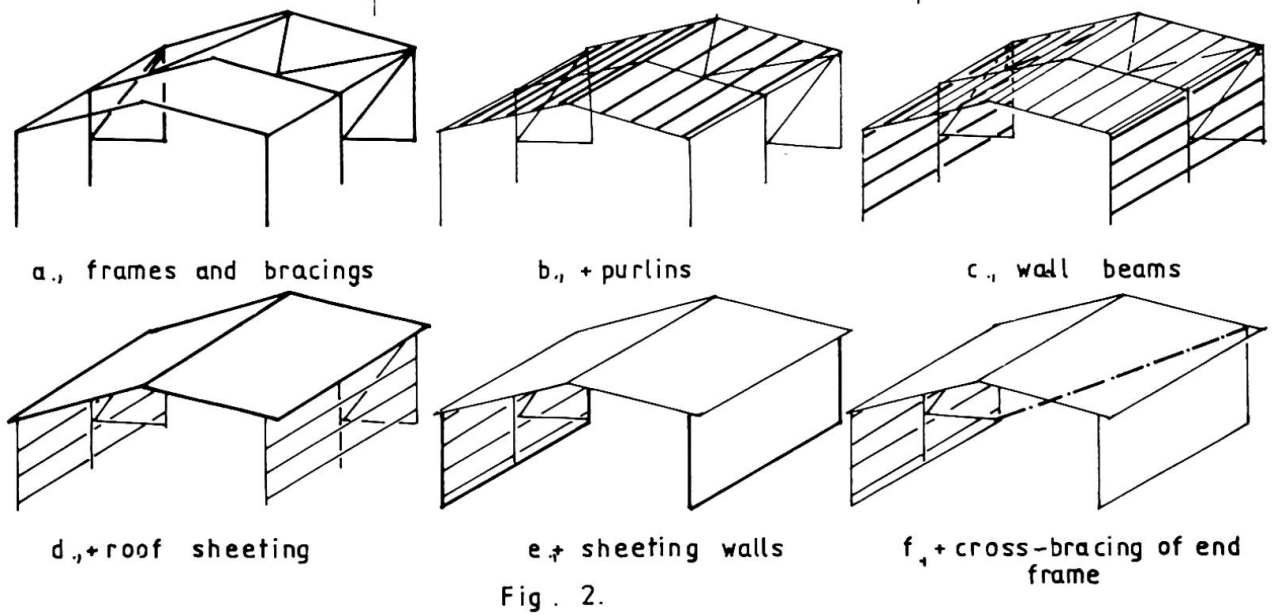


Fig. 2.

The interactive plastic hinge model is suitable for computer computations. The failure of a frame which had been investigated experimentally was simulated by the computer.[1] /Fig. 3./

## 4. EFFECT OF FABRICATION AND ERECTION

Effect of incorrect geometry was investigated by introducing different initial lateral displacements. Consequences are illustrated by Fig. 4.
The effect of the different values of residual stresses is shown in Fig. 5. The medium curve was in coincidence with test results.
The presented method for the complex analysis of frameworks takes several effects into consideration. /Fig. 6./

## 5. EFFECT OF STRUCTURAL DETAILS

It seems worthwhile to draw attention to the occasional decisive role of minor differences in structural details on failure as well. Some of the results are reproduced below.

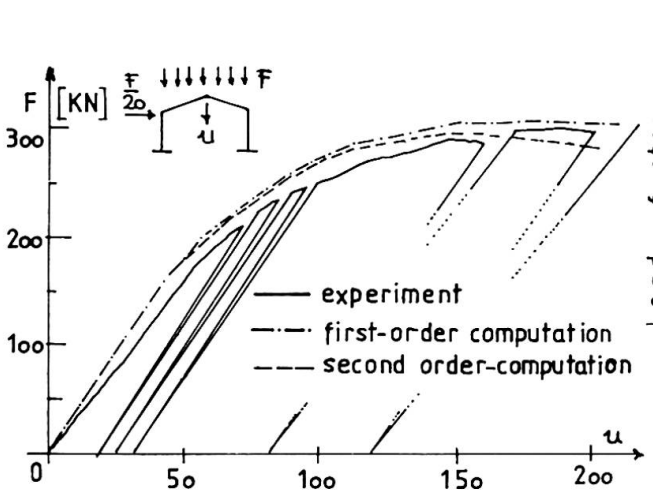


Fig. 3.

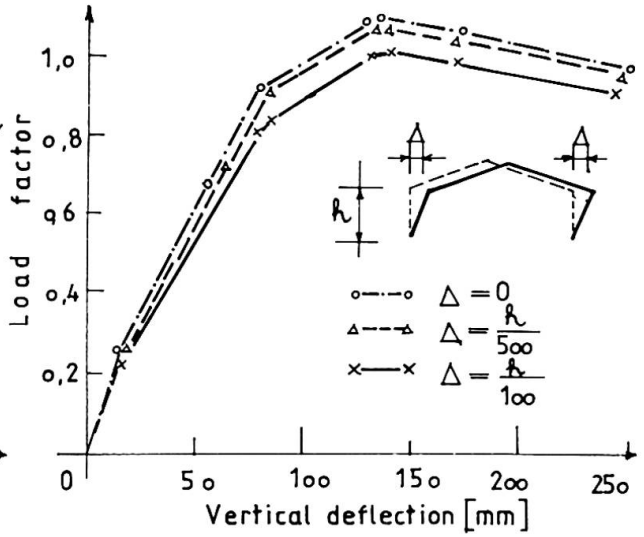


Fig. 4.

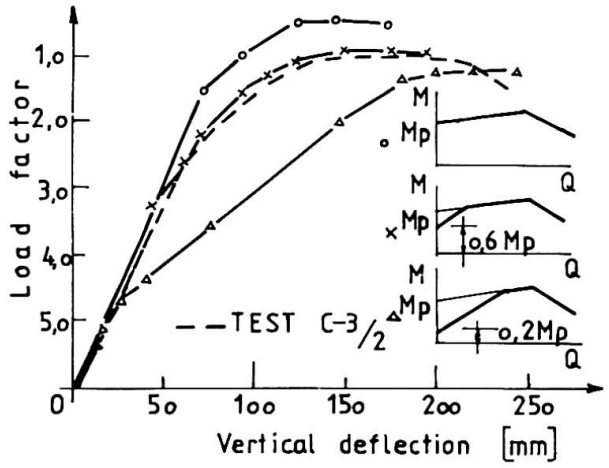


Fig. 5.

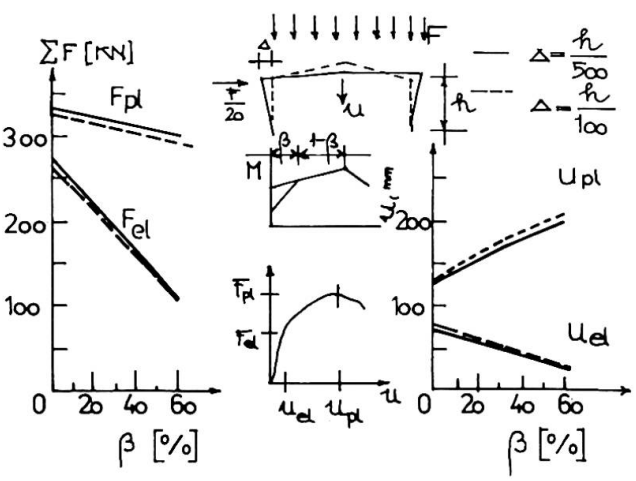


Fig. 6.

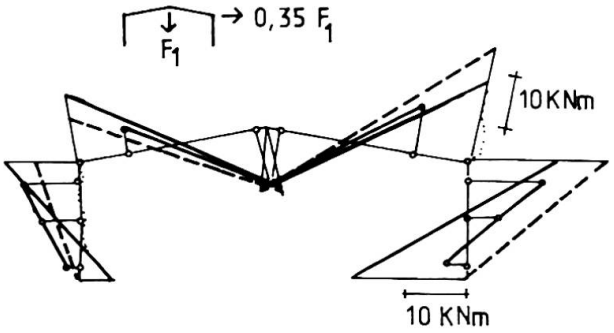


Measured and calculated bending moments

Fig. 7.

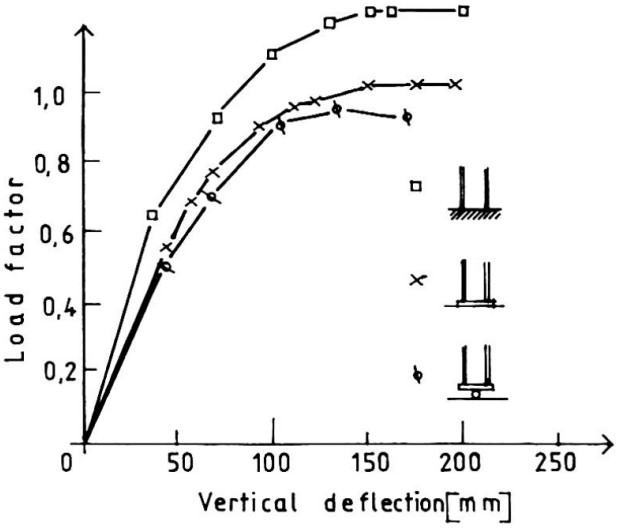


Fig. 8.

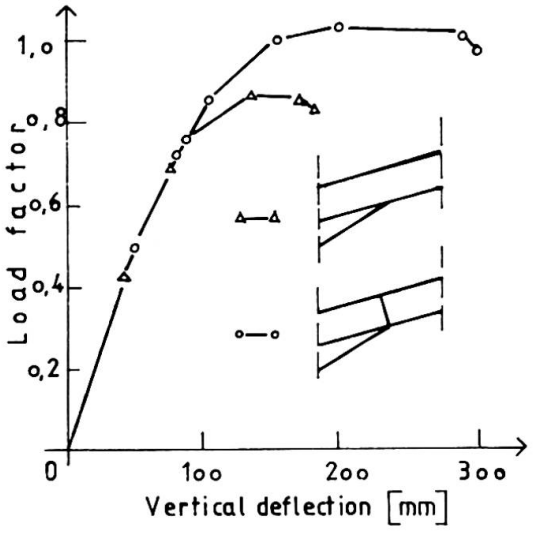


Fig. 9.

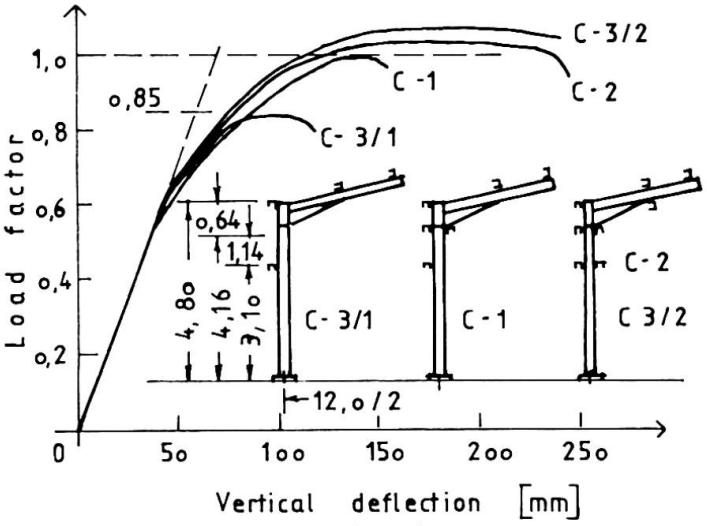


Fig. 10

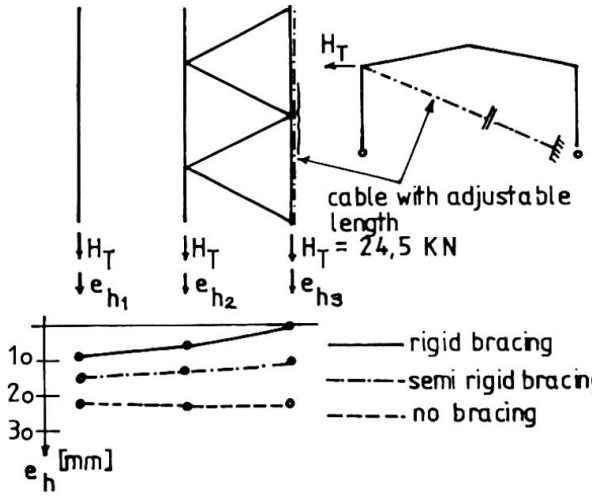


Fig. 11.

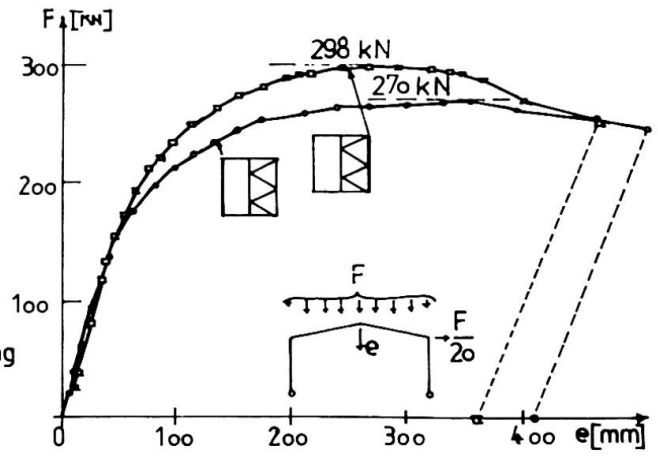


Fig. 12

5.1 Column bases
Column bases were fixed or hinged. The hinges were not ideal : columns could have been rather supported by a bigger base-plates. Fig. 7. compares the measured bending moment due to vertical and horizontal load to the calculated ones assuming pinned /dashed line/ and fixed /solid line/ frame. The corresponding moment-rotation diagram of column base was checked experimentally, its adaption to an interactive plastic hinge, indicating the load-deflection diagrams obtained by different end conditions. /Fig. 8./

5.2 Web-stiffeners
Some secondary elements /such as web-stiffeners/ can be of importance too. Form of failure with and without stiffener is indicated Fig. 9.

5.3 Lateral supports
Spacing and efficiency of lateral supports proved to be of basic importance. Their effect is illustrated by Fig. 10.

5.4 Cross-bracing of the end frame
Measured eaves deflections from uniform horizontal loads are shown on Fig. 11. representing the effect of both semi-rigid and rigid cross-bracing of the end frame.

5.5 Horizontal and vertical bracing system
Finally, load-displacement diagrams of incremental collapse tests are shown in Fig. 12. Ultimate loads are influenced by local loss of stability, previous loadings and the layout of frame-horizontal and vertical bracing connections.

6. CONCLUSION

It seems that because of frequent uncertainties in predicting the failure load of structures approximate models and procedures limited to special structures have to be used, and there is a need for regular experimental checks.

REFERENCES

1. BAKSAI R., IVANYI M., PAPP F., Computer Program for Steel Frames Taking Initial Imperfections and Local Buckling into Consideration. Periodica Politechnica, Vol. 29., Nos 3-4 1985.
2. HALASZ O., IVANYI M., Tests with Simple Elastic-Plastic Frames. Ibid, Vol.23., Nos 3-4 1979.
3. IVANYI M., A New Concept in Limit Design of Steel Structures. Colloquium on "Stability of Metal Structures", Paris. 16-17 nov. 1983, Final Report
4. IVANYI M., KALLO M., TOMKA P., Experimental Investigation of Full-Scale Industrial Building Section. Colloquium on "Stability of Steel Structures", Hungary 25-26 sept. 1986, Final Report

# Fatigue of Cross Beam Connections in Steel Bridges

Fatigue des liaisons traverses-poutres principales des ponts en acier

Ermüdung der Querträger-Anschlüsse bei Stahlbrücken

**Ichiro OKURA**
Res. Assoc.
Osaka University,
Osaka, Japan

Ichiro Okura, born 1955, received his B. Sc., M. Sc. and Dr. Eng. degrees in civil engineering from Osaka University in 1977, 1979 and 1985.

**Yuhshi FUKUMOTO**
Prof. of Civil Eng.
Osaka University,
Osaka, Japan

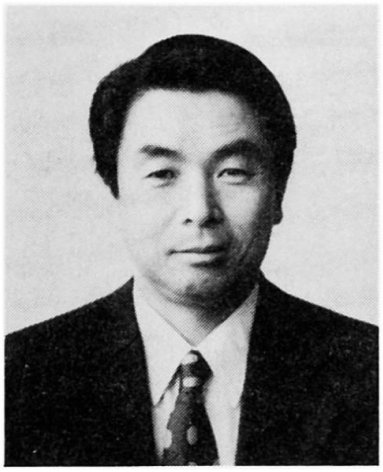

Yuhshi Fukumoto, born 1932, received his M. Sc. degree in civil engineering from Kyoto University and Ph. D. degree from Lehigh University. He has held professorship at Nagoya University from 1963 to 1986.

## SUMMARY

Fatigue cracks are often initiated at the connections of cross beams to main girders in plate girder bridges. The stress states at the cross beam connections are revealed by the static loading test of an actual plate girder bridge. The local stresses which induce fatigue cracks are related quantitatively to the three-dimensional behavior of the bridge.

## RÉSUMÉ

Les fissures de fatigue apparaissent souvent dans les liaisons entre les traverses et les poutres principales de ponts à poutres métalliques. L'état des contraintes dans la liaison est donné par un essai de charge statique d'un pont en service. Les contraintes locales qui provoquent les fissures de fatigue dépendent du comportement tridimensionnel du pont.

## ZUSAMMENFASSUNG

Bei Vollwandbalkenbrücken sind zwischen den Quer- und den Hauptträgern oft Ermüdungsrisse vorhanden. Die Spannungszustände wurden im statischen Belastungsversuch an einer Vollwandbalkenbrücke im Gebrauchszustand untersucht. Die lokalen Spannungen, die die Ermüdungsrisse hervorrufen, hängen qualitativ mit dem dreidimensionalen Verhalten der Brücke zusammen.

## 1. INTRODUCTION

In many steel bridges, fatigue cracks are observed at the connections of main members with secondary members such as cross beams, sway bracings and lateral bracings [1]. Such fatigue cracks are caused by locally induced stresses not generally considered in the bridge design practice. Usually it is very difficult to predict the local stresses, because they are produced by the three-dimensional behavior of the bridge.

This paper deals with the relation between the local stresses and the three-dimensional behavior of plate girder bridges. In plate girder bridges, as shown in Fig.1, the following four types of fatigue cracks are detected at the connections of cross beams to main girders [2]:

Type 1: This is initiated either on the bead or at the toe of the end return of the fillet weld between the connection plate and the top flange of the main girder.
Type 2: This is initiated at the upper scallop of the connection plate, and grows diagonally through the connection plate itself.
Type 3: This is initiated at the toe of the end return of the fillet weld connecting the connection plate to the main girder web, and grows downward along the toe on the connection plate side.
Type 4: This is initiated and grows along the toe on the web side of the fillet weld between the top flange and the web of the main girder.

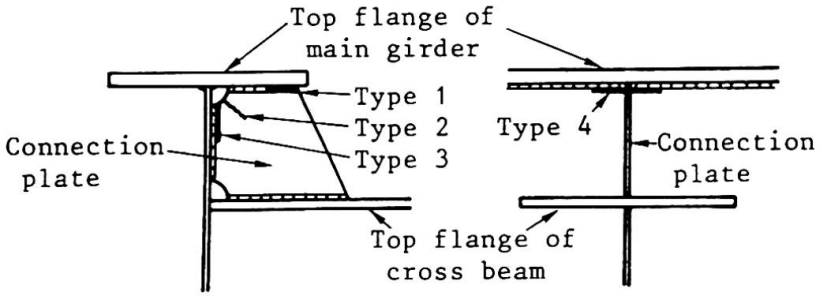


Fig.1 Fatigue cracks at cross beam connection

The difference in vertical displacement between main girders and the deformation of a concrete slab are pointed out as the main cause of the fatigue cracks [3,4]. However, until now it is not clear how these factors are related to the local stresses which induce the fatigue cracks.

## 2. STRESS MEASUREMENT OF PLATE GIRDER BRIDGE

### 2.1 General View of Plate Girder Bridge

In order to know the stress states at cross beam connections in plate girder bridges, stress measurement of an actual plate girder bridge shown in Fig.2 has been carried out [5]. It is a simply-supported composite plate girder bridge with a span length of 28.4 m and total width of 17.6 m, which was designed by the Japanese Specification for Highway Bridges. The bridge has five main girders, a cross beam in the middle of the span and six sway bracings. The concrete slab is 180 mm thick. The bridge was opened to traffic in 1970. Repair and reinforcement works for the slab were done in 1979. A steel plate 4.5 mm thick was attached to the bottom surface of the slab, and some stringers were installed, as shown by dotted lines in Fig.2.

The loading truck and its loading positions are shown in Figs.3 and 4, respectively. Four cases of A, B, C and D were considered according to the intervals

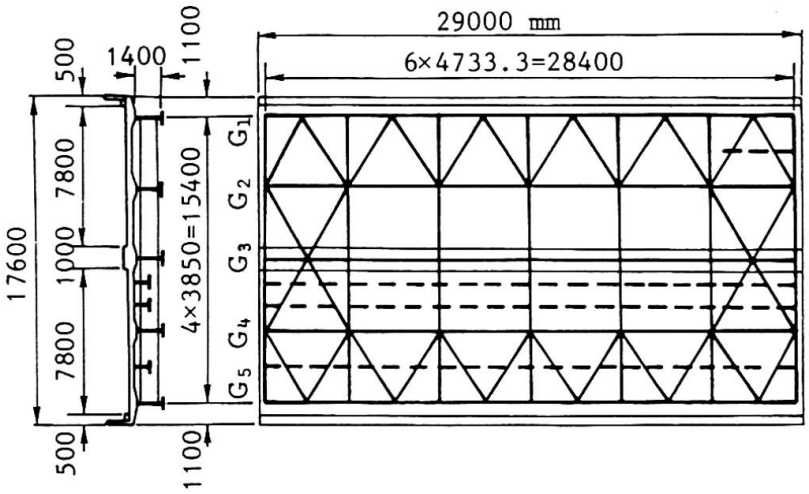


Fig.2 General view of plate girder bridge

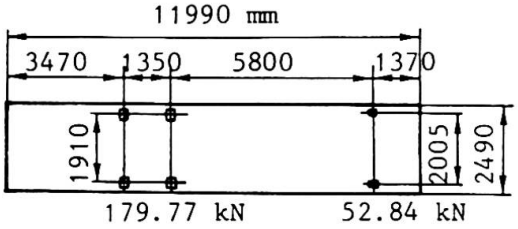


Fig.3 Loading truck

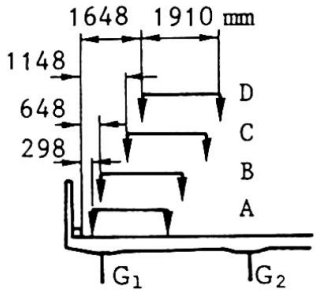


Fig.4 Loading positions of truck

between the coping and the center of the rear double-tires on the left side. The static stress measurement was done at 11 locations in the longitudinal bridge-axis direction for each loading case. 24 one-directional, 214 two-directional and 126 three-directional strain gauges were attached on the cross beam connections at $G_1$ and $G_2$ girders.

## 2.2 Stress States at Connection Plates

The stress measurement results show that the plate-bending strains are much smaller than the membrane ones at the connection plates. Accordingly, the membrane stress is considered to be influential for the initiation of Types 1, 2 and 3 fatigue cracks. Figure 5 shows the principal membrane stresses when the center of the rear two wheel axles exists just above the cross beam in the loading case D. A relatively large compressive principal stress occurs around the

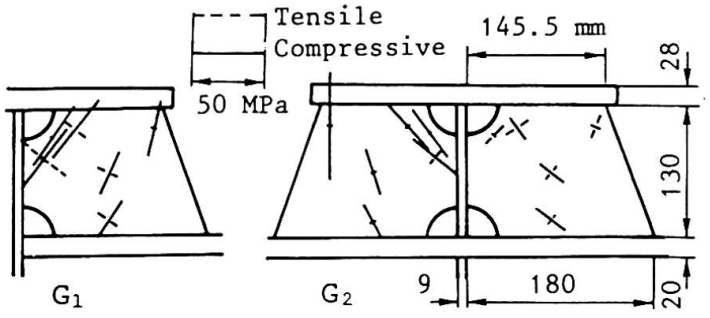


Fig.5 Principal membrane stresses of connection plates

scallop of the connection plate of $G_1$ girder and also at the left edge of the left connection plate of $G_2$ girder. The direction of the principal stress at the connection plate edge is almost vertical, and it is perpendicular to the direction of the propagation of Type 1 fatigue crack.

## 2.3 Stress States at Main Girder Webs

Referring to Fig.6, the components of plate-bending stress $\sigma_{by}$ and membrane stress $\sigma_{my}$ are significant for Type 4 fatigue crack, because they act perpendicularly to the direction of the propagation of the crack. Figure 7 shows the distributions of $\sigma_{by}$ and $\sigma_{my}$ along the x-axis at y=16 mm from the bottom surface of the flange plate. The plate-bending stress $\sigma_{by}$ takes the large values between the connection plate at x=0 and the tip of the top flange of the cross beam at the section I-I (x=225 mm), and increases gradually toward the connection plate. The membrane stress $\sigma_{my}$ changes sharply from compressive to tensile stress in the very vicinity of the connection plate. The ratios of $\sigma_{my}$ to $\sigma_{by}$ at the point of x=24.5 mm and y=16 mm where the strain gauges were glued nearest to the connection plate, vary from 20 % to 26 % depending on the loading cases.

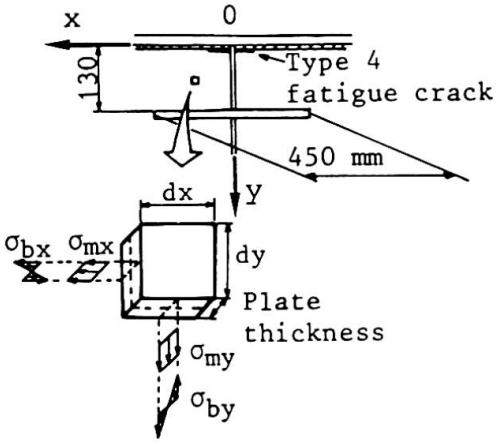


Fig.6 Stress components near Type 4 fatigue crack

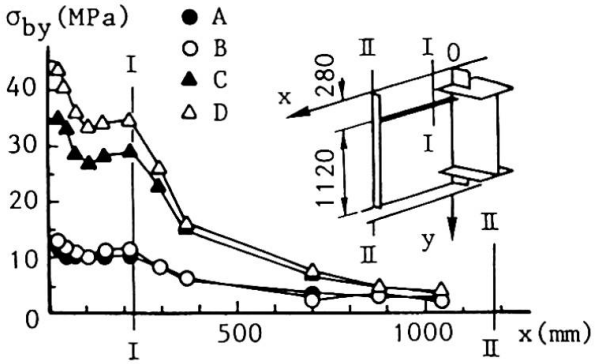


(a) Distribution of $\sigma_{by}$

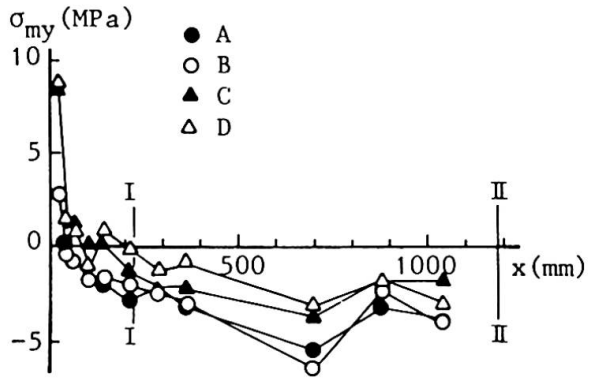


(b) Distribution of $\sigma_{my}$

Fig.7 Distributions of $\sigma_{by}$ and $\sigma_{my}$ along the x-axis at y=16 mm of $G_1$ girder web

## 3. ESTIMATION OF LOCAL STRESSES

From the stress measurement of a plate girder bridge, the membrane stress $\sigma_{my}$ and the plate-bending stress $\sigma_{by}$ illustrated in Fig.8 are the governing stresses for the initiation of Types 1 and 4 fatigue cracks, respectively. Referring to Fig.9, they are caused by the respective rotations $\theta_s$ and $\theta_g$ of the concrete slab and cross beam and by their respective horizontal displacements $u_s$ and $u_g$. Through the plate-bending analysis of the slab and the three-dimensional F.E.M. analysis of the whole bridge, the equation to estimate the local stresses of

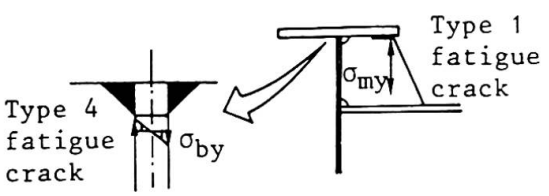


Fig.8 Fatigue crack types and local stresses

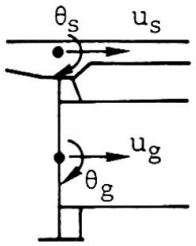


Fig.9 Notation

$\sigma_{my}$ and $\sigma_{by}$ has been obtained as follows:

$$\begin{bmatrix}\sigma_{my}\\ \sigma_{by}\end{bmatrix} = \begin{bmatrix}k_{m1} & k_{m3}(\gamma - k_{m123})\\ k_{b1} & k_{b3}(\gamma - k_{b123})\end{bmatrix}\begin{bmatrix}\theta_{s0}\\ \theta_g\end{bmatrix} \qquad (1)$$

where $\theta_{s0}$ is the rotation of a slab due to its plate-bending deformation excluding the deformation of the slab produced by the different vertical deflections of main girders, $\theta_g$ is the rotation of a cross beam caused by the different vertical deflections of main girders, $\gamma$ is a coefficient defined by $(u_s - u_g)/\theta_g$ and it takes different values depending on the positions of the truck loading along the width of the roadway, and $k_{m1}$, $k_{m3}$, $k_{m123}$, $k_{b1}$, $k_{b3}$ and $k_{b123}$ are coefficients which relate the local stresses $\sigma_{my}$ and $\sigma_{by}$ to the corresponding rotations $\theta_{s0}$ and $\theta_g$ [6] .

Figure 10 shows a comparison of the values estimated by Eq.(1) with the measured ones when the loading truck moves along the longitudinal bridge-axis in the loading case D. It can be seen that Eq.(1) is very close to the measured values.

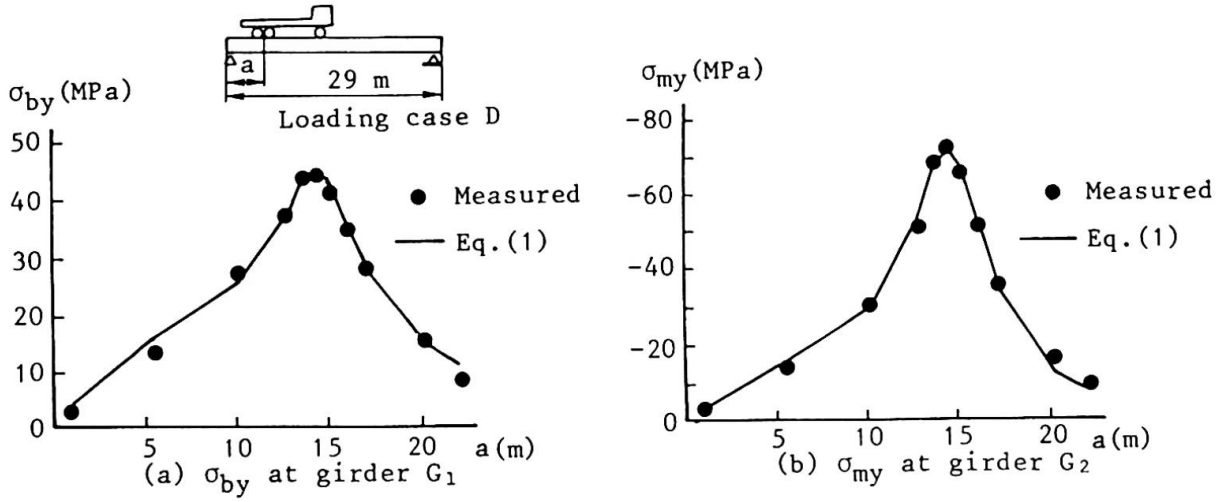


Fig.10 Comparisons between the values by Eq.(1) and the measured ones

Figure 11, which has been theoretically obtained by Eq.(1), shows the effects of the rotations $\theta_{s0}$ and $\theta_g$ on the local stresses $\sigma_{by}$ and $\sigma_{my}$ when a concentrated load P=9.81 kN moves on the slab along the cross beam between $G_1$ and $G_2$ girders. When the load is in the middle part between $G_1$ and $G_2$ girders, $\sigma_{by}$ can be mainly induced by the term $\theta_{s0}$, and on the contrary, when it moves near $G_1$ or $G_2$ girder, $\sigma_{by}$ mainly induced by the term $\theta_g$. The membrane stress $\sigma_{my}$ is mainly induced by the term $\theta_{s0}$. That is, the rotations of a slab due to its plate-bending deformation and of a cross beam caused by the different vertical deflections of main girders are equally influential for Type 4 fatigue crack, while only the former has a great influence on Type 1 fatigue crack.

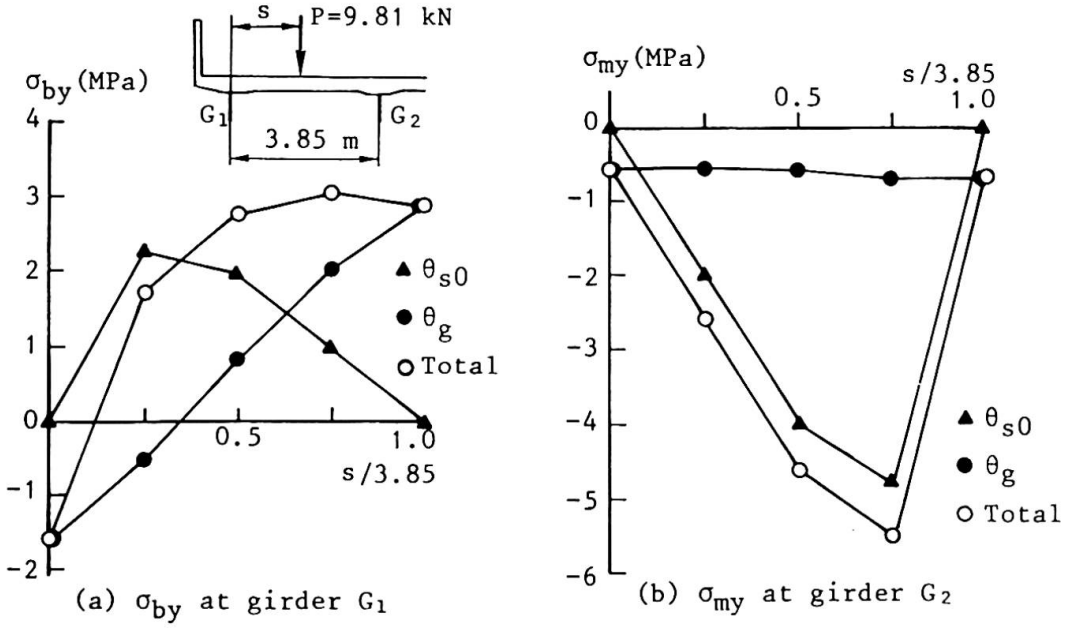


Fig.11 Effects of $\theta_{s0}$ and $\theta_g$ on $\sigma_{by}$ and $\sigma_{my}$

## 4. CONCLUSIONS

In this paper, the stress states at the connections of cross beams to main girders in plate girder bridges were revealed by the static loading test of an actual plate girder bridge. The local stresses which induce fatigue cracks were related quantitatively to the three-dimensional behavior of the bridge.

## REFERENCES

1. FISHER J.W., Fatigue and Fracture in Steel Bridges, John Wiley & Sons, Inc., 1984.

2. HANSHIN EXPRESSWAY PUBLIC CORP. and NAIGAIKOEI CO., LTD., Classification of Fatigue Cracks at Member Connections in Plate Girder Bridges, Mar., 1985. (in Japanese)

3. FISHER T.A., FISHER J.W., KOSTEM C.N. and MERTZ D.R., Design and Retrofit for Fatigue Damage in Web Gap, IABSE Colloquium, Lausanne, 1982, pp.535-543.

4. KATO S., YOSHIKAWA O., TERADA H. and MATSUMOTO Y., Studies on Fatigue Damages Based on Strain Measurements of a Highway Bridge, Proc. of JSCE Struct. Eng./ Earthq. Eng., Vol.2, No.2, 1985, pp.445s-454s.

5. OKURA I., HIRANO H. and YUBISUI M., Stress Measurement at Cross Beam Connections of Plate Girder Bridge, Technol. Repts. Osaka Univ., Vol.37, No.1883, 1987, pp.151-160.

6. OKURA I., YUBISUI M., HIRANO H. and FUKUMOTO Y., Local Stresses at Cross Beam Connections of Plate Girder Bridges, Submitted to Proc. of JSCE Struct. Eng./ Earthq. Eng.

# Parametric Study on Seismic Ties of Boiler House

Etude paramétrique d'attaches anti-sismiques d'une chaudière

Parameterstudie über seismische Verbindungsglieder in einem Kesselhaus

**Sadao UCHIYAMA**
Archit. Engineer
Electric Power Dev. Co., Ltd.
Tokyo, Japan

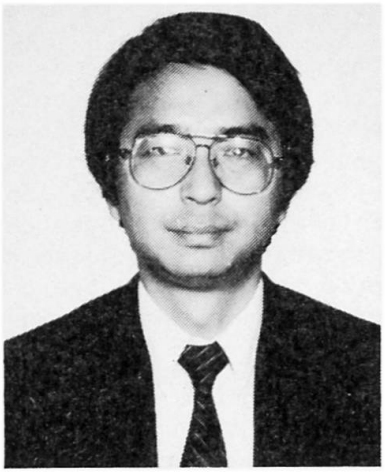

Sadao Uchiyama, born 1954, received his architectural degree of master at Tohoku University, Sendai, Japan. For eight years he was involved in structural design and supervision of Electric Power Facilities.

**SUMMARY**
The seismic ties of the boiler house of a thermal power station have the function of fastening the boiler body to the boiler house. In particular, the mechanical properties of the seismic tie are expected to exert significant influence on the seismic response of the boiler and boiler house system. This paper evaluates quantitatively the influence the seismic tie exerts on the seismic response of the boiler house. This evaluation reflects the parametric study carried out by varying the mechanical properties (gab, yield strength and initial rigidity) of the seismic tie.

**RÉSUMÉ**
Les attaches anti-sismiques d'une chaudière dans une centrale thermique ont pour fonction de fixer le corps de la chaudière au bâtiment. Il est admis que dans le cas d'un séisme important, les caractéristiques mécaniques des attaches anti-sismiques ont une influence remarquable sur le comportement du système de la chaudière et du bâtiment. Cette étude concerne l'évaluation quantitative de l'influence de différentes caractéristiques mécaniques des attaches anti-sismiques sur la réponse sismique du bâtiment de chaudière.

**ZUSAMMENFASSUNG**
Die seismischen Verbindungsglieder in Kesselhäusern von Heizkraftwerken dienen der Befestigung des Kessels am Kesselhaus. Das Verhalten bei schweren Erdbeben kann jedoch dadurch beeinträchtig werden, daß das Erdbebenverhalten des Systems zusammen mit dem Kesselhaus stark beeinträchtigt wird. Die Studie schätzt diesen Einfluß quantitativ aufgrund einer Parameterstudie unter Veränderung der mechanischen Eigenschaften des seismischen Gliedes (Fugenbreite, Nachgiebigkeit, Anfangsfestigkeit) ab.

## 1. INTRODUCTION

The boiler house of a thermal power station is the structure that supports the power generating boiler by means of the top girder. The boiler weight of the Takehara Thermal Power Station Unit No. 3 amounts to 12,000 tons and accounts for 40 percent of the total weight of the boiler house as a whole. Its configuration is outlined in Figure 1. The boiler is fastened to the boiler house by means of a device called a seismic tie. This device has the function of restraining the boiler in the boiler house to prevent excessive shaking during an earthquake. On the other hand, the seismic tie is devised so that the boiler remains free with regard to deformation caused by its deadweight and by heat on ordinary condition (refer to Figure 2).

It may safely be said that the function of the seismic tie has been neglected thus far in connection with the aseismic design of the boiler house, irrespective of the static or dynamic design method adopted in this connection. In other words, the boiler house formerly was given an aseismic design by assuming that the seismic tie has infinite rigidity, and that an earthquake force due to the boiler is transmitted to the boiler house through the seismic ties as they share. The mechanical strength of the seismic tie was previously determined from the earthquake force they have to bear. Furthermore, the rigidity of the boiler itself was neglected for aseismic design of the boiler house.

It must be remembered, however, that the boiler and the boiler house have vibration characteristics very different from each other if they are regarded as independent vibrating systems. It is obvious, therefore, that the mechanical properties of the seismic tie exert a significant influence on the force working on the both in the case of an earthquake, since the both are coupled each other by the seismic ties.

In this paper the author carries out a parametric study of the mechanical properties of the seismic ties in a coupled vibration model of boiler and boiler house whose validity was proved by a simulation analysis of earthquake response for the boiler house of Takehara Thermal Power Station Unit No. 3. The study aims to improve aseismic design method for the boiler house as a structure. The flow of this study is shown in Figure 3.

## 2. PARAMETRIC STUDY

### 2.1 Analytical Model

The analytical model used for the sake of this parametric study is a sixteen-lumped-mass model. This is obtained by simplifying the accurate model (pseudo-three-dimension model) that consists of representing each member of the columns, beams and braces of the boiler house as well as the boiler itself and the seismic tie with finite elements. In this model the boiler is supported at the top of the boiler house by means of a hanging spring. Boiler weight is represented by mass concentrated at each floor. Boiler rigidity is represented by elastic springs valuating the axial and bending rigidity. On the other hand, the seismic tie is represented as a nonlinear spring taking into consideration of such factors as the gap and the yielding. The coupled vibration model of boiler and boiler house mentioned in the foregoing is called a seismic tie model (refer to Figure 4(a)).

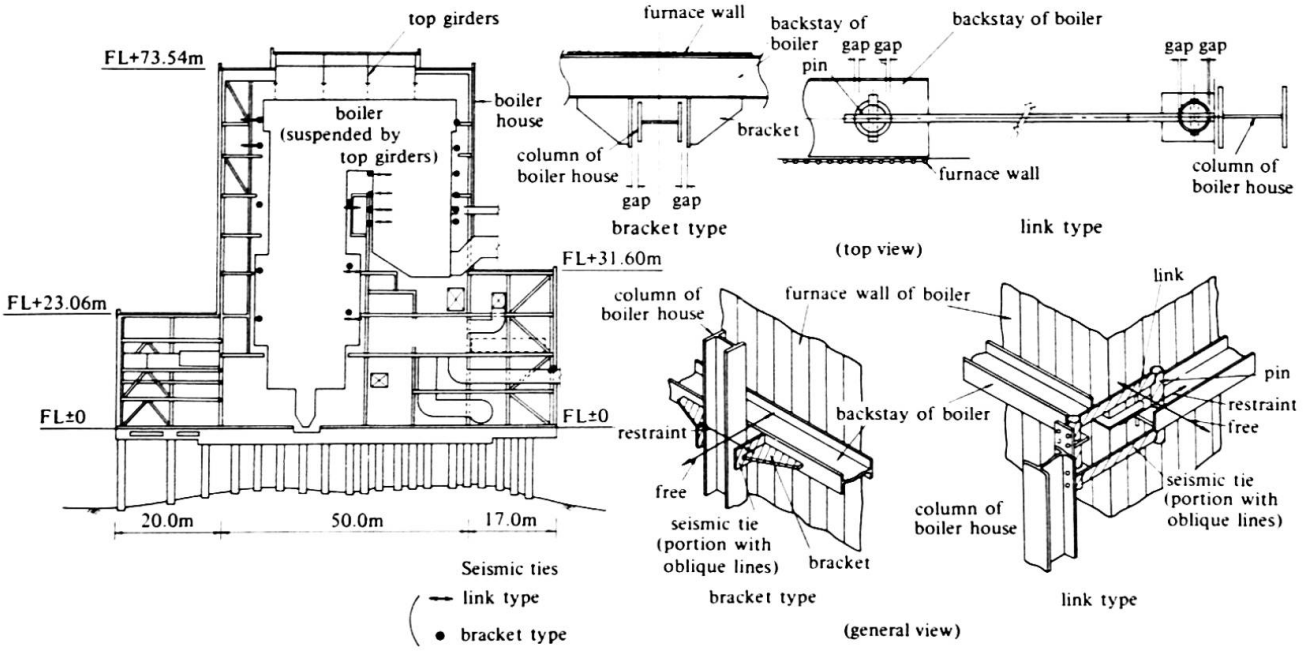


Fig. 1 Section of Boiler House (Takehara Thermal Power Station Unit No. 3)

Fig. 2 Structure of Seismic Ties

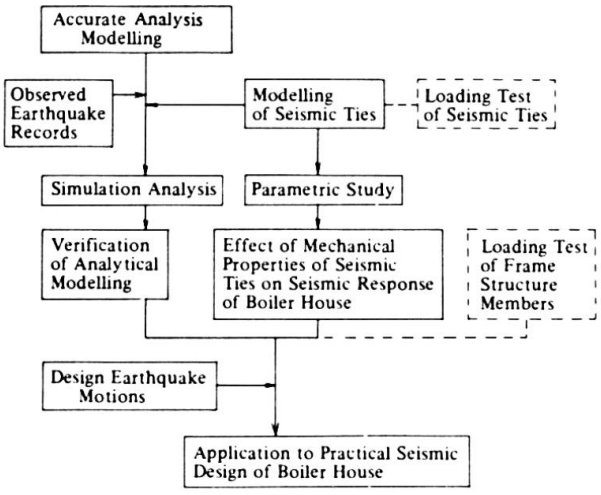


Fig. 3 Flow of Study

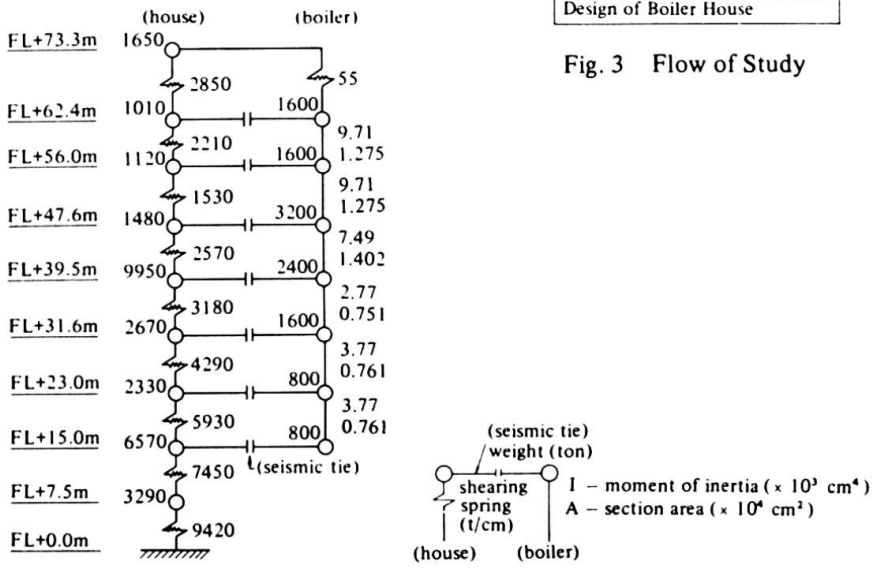


Fig. 4 (a) Analytical Model (Seismic Tie Modei)

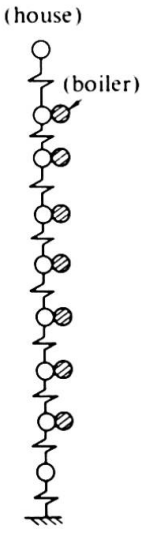


Fig. 4(b) Analytical Model (One-Body Model)

A conventional model, called a one-body model hereafter, is illustrated in Figure 4(b) that is for comparing with the results of the above-mentioned seismic tie model. This is obtained in the same manner as above except that the mass point corresponding to the boiler weight is added to the mass point at each floor, i.e. with seismic ties of infinite rigidity and neglecting rigidity of the boiler itself.

## 2.2 Parameters

Two distinct types of seismic ties, classified in terms of their hysteresis characteristics, are taken into consideration in this study.

(1) Gap-slip type (in which the gap widens concurrently with the plastic deformation. It corresponds to the bracket type shown in Figure 2).

(2) Gap-bilinear type (in which the gap continues to remain constant after the yield. It corresponds to the link type shown in Figure 2).

The hysteresis characteristics of each type are shown in Figure 5.

The initial gap amount, the initial rigidity and the yield strength are selected as the main parameters representing the mechanical properties of these two types of seismic ties. These parameters are varied as shown in Table 1, based on the value actually adopted in the Takehara Thermal Power Station Unit No. 3 as standard one. When one parameter is varied, the standard value is adopted for the other two parameters.

## 2.3 Earthquake Response Analysis

The earthquake response analysis is carried out by adopting the El Centro 1940 (NS) as input ground motion and by normalizing the maximum acceleration at 200 gals. As for distribution of max. response shear force of boiler house and max. response relative displacement between boiler and boiler house, Sendai 038 (NS) by Miyagi Ken Oki earthquake of July 12, 1978 is applied for supplement. 3 percent of internal viscous damping is assumed to occur in correspondence to the first natural mode of the boiler house.

## 2.4 Results

The parametric study by means of the earthquake response analysis was carried out in conformity with the conditions mentioned in Sections 2.1 through 2.3 above. The results obtained are outlined as follows.

### 2.4.1 Influence of the analytical model and the hysteresis characteristics

(1) Distribution of the Maximum response shear force for each story of the boiler house

Figure 6 shows the distribution of the maximum response shear force of the boiler house. Comparing the gap-slip type and gap-bilinear type seismic ties in terms of hysteresis characteristics, there is no much difference in the distribution of the maximum response shear force. It is, therefore, concluded that there is no difference attributable to the hysteresis characteristics.

On the other hand, the maximum response shear force of the seismic tie model is reduced to 60 percent through 80 percent of the response of the one-body model in both cases (gap-slip type seismic tie and gap-bilinear type seismic tie).

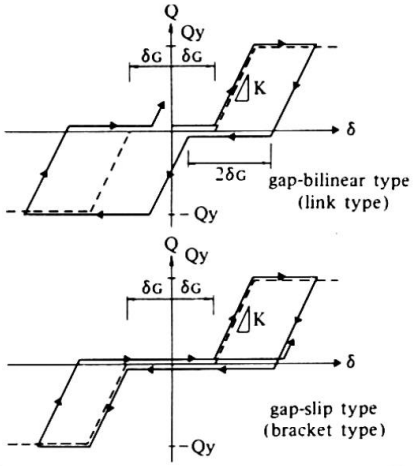


Fig. 5 Hystereses Models of Seismic Ties

| | S.V ×1/3 | Standard Value (S.V) | S.V ×5/3 |
|---|---|---|---|
| δG (cm) | 0.3 | 0.9 | 1.5 |
| * K (t/cm) (total value) | 2400 | 7200 | 12000 |
| * Qy (ton) (total value) | 1200 | 3600 | 6000 |

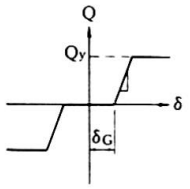


δG : initial gap amount
K : initial rigidity
Qy : yield strength

* total value of all seismic ties

Table 1 Parameters of Study

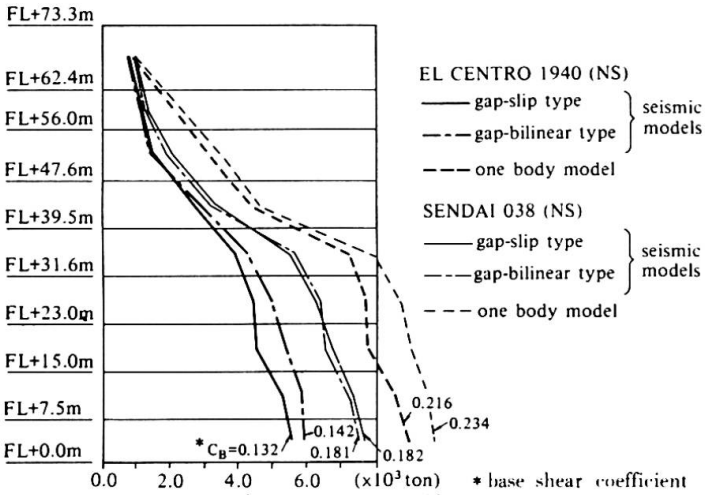


Fig. 6 Distribution of Max. Response Shear Force of boiler house

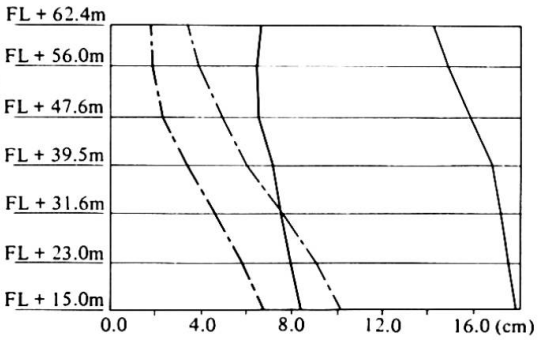


Fig. 7 Max. Response Relative Disp. between Boiler and Boiler House

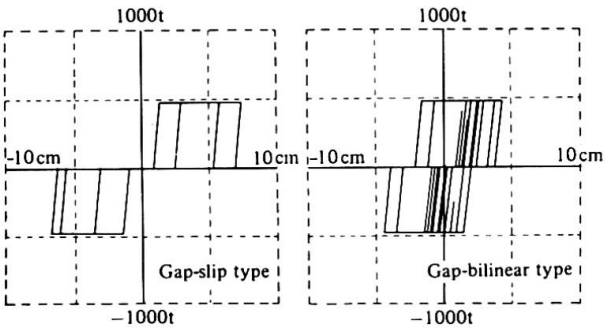


Fig. 8 Hystereses of Seismic Ties by Analysis

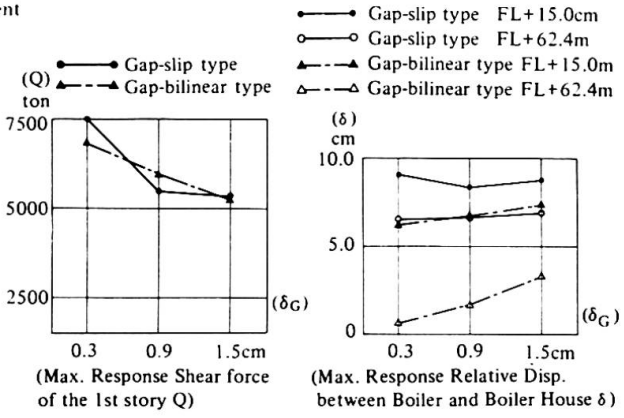


(Max. Response Shear force of the 1st story Q)

(Max. Response Relative Disp. between Boiler and Boiler House δ)

Fig. 9 Effect of Initial Gap Amount ($\delta_G$)

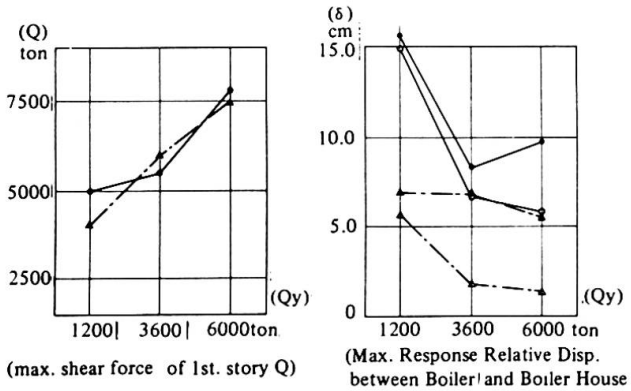


(max. shear force of 1st. story Q)

(Max. Response Relative Disp. between Boiler and Boiler House δ)

Fig. 10 Effect of Yield Strength (Qy)

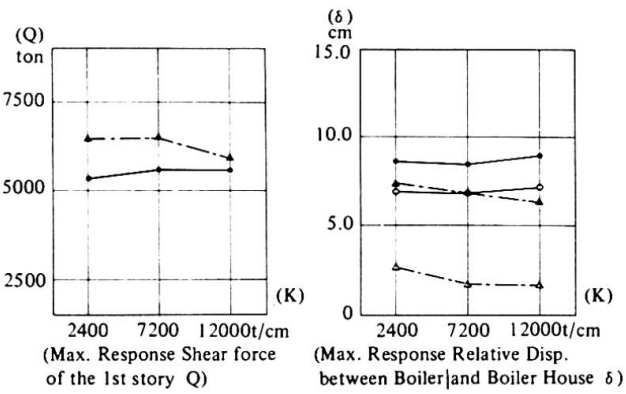


(Max. Response Shear force of the 1st story Q)

(Max. Response Relative Disp. between Boiler and Boiler House δ)

Fig. 11 Effect of Initial Rigidity (K)

(2) Maximum response relative displacement between boiler and boiler house

Figure 7 shows the maximum response relative displacement between boiler and boiler house. As can be seen, the relative displacement occurring in the gap-slip type is approximately twice as much in the gap-bilinear type.

The said difference occurs because whereas in the gap-bilinear type seismic tie the gap remains constant, in the gap-slip type seismic tie the gap increases concurrently with the progress of yield. And this characteristic is clearly explained by the hysteresis loop of the seismic tie of FL + 31.6 shown in Figure 8 as an example.

2.4.2 Influence of the mechanical properties of the seismic tie

(1) The maximum response shear force occurring in the first story of the boiler house and (2) the maximum response relative displacement between boiler house and boiler when the mechanical properties of the seismic tie are varied - with the El Centro wave adopted as input ground motion - are shown in Figure 9 through 11.

(1) Maximum response shear force in the first story of the boiler house

The larger the initial gap the smaller the maximum response shear force, and the smaller the yield strength the smaller the maximum response shear force. The relationship is practically linear. When the initial gap $\delta_G$ is 1.5 cm the extent of reduction is approximately 10 percent as compared with the standard value ($\delta_G$ = 0.9 cm). When the yield strength $Q_y$ is 1200 t the extent of reduction is of the order of 30 percent compared with the standard value ($Q_y$ = 3600 t). It is presumed that the said fact occurs because of the increasing hysteresis damping effect. This is attributed to the frequent response in the plastic range resulting from the lower value of the yield strength. Differences in the initial rigidity seem to exert practically no influence.

(2) Maximum response relative displacement

Contrary to the tendency mentioned above, the larger the initial gap the larger the maximum response relative displacement, and the smaller the yield strength the larger the maximum response relative displacement. A quite large relative displacement caused by plastic deformation occurs when the yield strength $Q_y$ is 1200 ton. Differences in initial rigidity seem to exert practically no influence in response relative displacement as well as in response shear force.

## 3. CONCLUSION

Seismic ties are useful for reducing earthquake force of boiler house as well as for restraining the large relative displacement between boiler and boiler house during an earthquake by providing appropriate mechanical properties such as gap amount, yield strength and ductility. For evaluating the effect above-mentioned properly, analysis model representing the mechanical properties of seismic tie such as seismic tie model is essential.

# Application of Friction Damper to Highrise Buildings

Application d'un amortisseur à friction pour un gratte-ciel

Anwendung von Reibungsdämpfern in Hochbauten

**Takayuki TERAMOTO**
Chief Struct. Eng.
Nikken Sekkei Ltd.
Tokyo, Japan

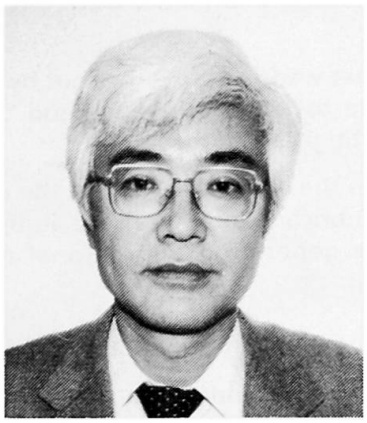

Takayuki Teramoto, born 1948, obtained his master of engineering at the Tokyo Institute of Technology, JAPAN. He was involved in the structural design of mainly highrise buildings. He is now the Chief of Structural Department of the firm.

**Haruyuki KITAMURA**
Senior Struct. Eng.
Nikken Sekkei Ltd.
Tokyo, Japan

**Kenji ARAKI**
Assist. to Gen. Mgr.
Sumitomo Metal Industries, Ltd.
Osaka, Japan

**Kiichi TAKADA**
Res. Eng.
Sumitomo Metal Industries Ltd.
Tokyo, Japan

**SUMMARY**
This paper introduces the fundamental characteristics of a new type of friction damper and describes some experiments of the damper itself and a frame with a damper under static and dynamic loading. The friction dampers are used in the highrise building in order to decrease horizontal displacements caused by earthquakes.

**RÉSUMÉ**
Ce papier pésente les caractéristiques fondamentales d'un nouveau type d'amortisseur à friction et décrit quelques essais de l'amortisseur lui-même et d'un encadrement avec un amortisseur sous une charge statique et dynamique. Les amortisseurs à friction sont utilisés dans un édifice à 31 étages afin de diminuer des déplacements horizontaux occasionnés par des secousses sismiques.

**ZUSAMMENFASSUNG**
Die vorliegende Abhandlung erklärt die Grundeigenschaften eines neuen Reibungsdämpfertyps und beschreibt Versuche, mit diesem Dämpfer allein und im Zusammenhang mit einem Bauwerk unter statischen und dynamischen Belastungen. Diese Reibungsdämpfer werden in einem 31 Stockwerke hohen Gebäude verwendet, um die Horizontalverschiebung bei Erdbeben niedrig zu halten.

## 1. INTRODUCTION

In the structural design of a highrise building, its seismic design is made by fully studying its expected behavior during a big earthquake. It has become hard to economically reduce the displacement during an earthquake because of its longer natural period. To reduce the building's displacement, it is effective to install dampers. The dampers effectively reduce the seismic input into the structure, finishing materials, etc., and the sway due to small- to medium-scale earthquakes or usual wind, improving the psychological effect on inhabitants of the building. Mainly to reduce the displacement and imprvove the vibration characteristics in a highrise building, friction dampers were installed on each floor and in each direction to produce certain frictional damping.

## 2. FRICTION DAMPER MECHANISM

Fig. 1 shows the friction damper's mechanism. The damper consists of a rod, nuts and a cup spring through which the rod passes, a friction part consisting of an inner wedge and a cotter outer wedge, and a steel outer cylinder.

The frictional force is obtained by pressing the inner wedge onto either nut by means of the cup spring and generating a compressive force between the cotter outer wedge and the steel outer cylinder interior. Its value is controlled by means of the nut tightening torque.

A piece of copper alloy is used as a friction part in the contact portion of the cotter outer wedge with the steel outer cylinder. Many pieces of solid lubricant (graphite) are imbedded to give a stable frictional force and to prevent abnormal noise generation at frictional movement. An oil-less mechanism is adopted.

### 2.1 Method of Test

Fig. 2 shows the method of loading. The steel outer cylinder was fixed with a pin and sine-wave vibration by deformation control was applied from the rod side. The measured items were the damper's input load (frictional force), the friction part's sliding amount, and the steel outer cylinder's temperature. The test was conducted after vibration of about 750 cycles (amplitude 1 mm, frequency 1 Hz) in order to adjust the friction face's initial condition.

Vibration was applied as shown in Table 1 to study the effects of the vibration speed, the vibration cycle and the friction face temperature on the damper's dynamic characteristics.

### 2.2 Test Results

A slight drop in frictional force is observed at the moment when the friction part starts sliding (e.g. the ○ mark in Fig. 3). It is considered to be a transitional phenomenon when sliding shifts from static to dynamic friction.

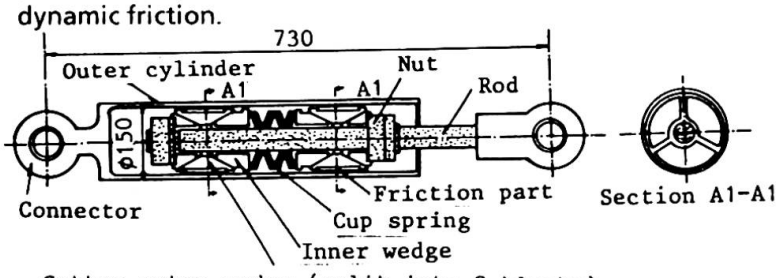


Fig. 1 Friction Damper's Mechanism

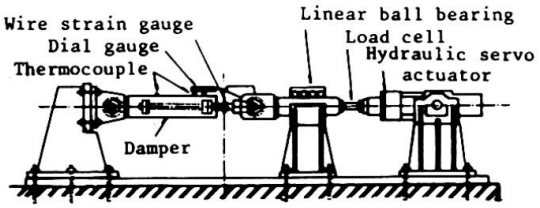


Fig. 2 Method of test

| Amplitude δ: mm | Frequency f: Hz | Vibration speed*1 V: cm/sec. | N150*2 : cycle |
|---|---|---|---|
| 1 | 1 | 0.63 | 15000 |
| 3 | 0.33 | 0.63 | |
| 5 | 5 | 15.71 | 250 |
| 10 | 0.33 | 2.09 | |
| 10 | 1 | 6.28 | 550 |
| 10 | 2 | 12.57 | 270 |
| 20 | 0.2 | 2.51 | 700 |
| 20 | 0.33 | 4.19 | |
| 20 | 0.5 | 6.28 | 500 |
| 20 | 2 | 25.13 | |
| 30 | 0.33 | 6.28 | |
| 38 | 0.33 | 8.38 | 350 |

*1 Speed at sliding displacement 0 position

*2 Repetition cycles at which outer cylinder temperature reaches T = 150°C

Table 1 Content of Vibration Test

Effects of vibration speed: Fig. 3 shows the effects of the vibration speed on restoring force characteristics. Fig. 5 shows the relationship between the vibration speed and the energy absorbed by the damper. It is evident that, as vibration speed v increases, the sliding load increases in the static friction range and drops a little in the dynamic friction range and that the damper's restoring force characteristics shift from a rectangular to concave shape. It is possible to consider, however, that such increase and decrease of the sliding load offset each other, so that the absorbed energy per cycle is nearly proportional to the sliding amount and is not affected by the vibration speed.

Effects of friction part temperature: Fig. 4 shows the effects of the friction part temperature on restoring force characteristics and Fig. 6 shows the relationship between the friction part temperature and the absorbed energy. It is evident that, as the friction part temperature rises, the sliding load increases a little in the static friction range and drops in the dynamic friction range. While the absorbed energy also drops as the temperature rises, the drop rate of the absorbed energy at friction part temperature T = 105°C is about 7% of that at T = 30°C.

Effects of vibration cycle: Test results showed the effects of the vibration cycle on restoring force characteristics. The friction part abrasion is a maximum of 0.1 mm in diameter after various vibration tests (total repetition is about 20,000 cycles). Considering that an abrasion of 0.1 mm represents a drop in frictional force of about 3% according to calculation, the friction damper can be judged as having sufficient durability under practical conditions.

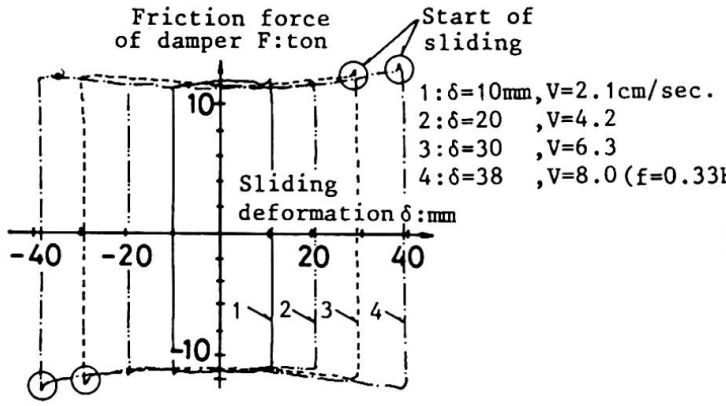


Fig. 3 Effects of Vibration Speed

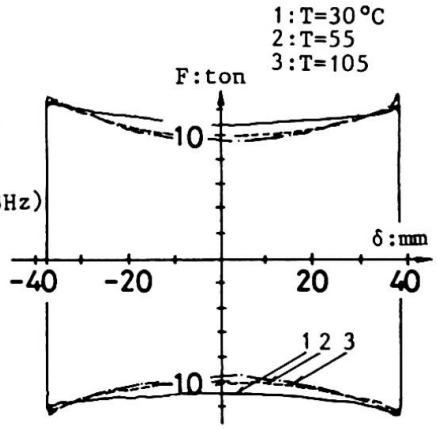


Fig. 4 Effects of Damper Temperature

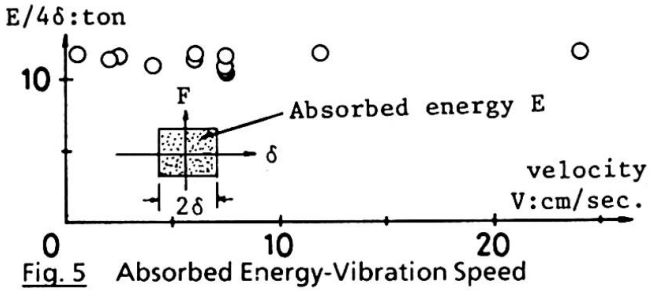


Fig. 5 Absorbed Energy-Vibration Speed

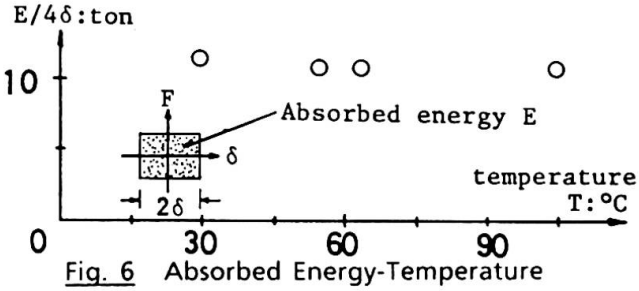


Fig. 6 Absorbed Energy-Temperature

## 3. EXPERIMENTS OF A FRAME WITH FRICTION DAMPER

After the tests of the friction damper itself, the static and dynamic loading tests for a steel frame with the friction damper were conducted. These tests were planned to ascertain the damper performance under practical conditions prior to putting it into use for a building.

### 3.1 Contents of Test

Fig. 7 shows the dimensions of the test frame. A damper of frictional force 10-ton and sliding length ± 60mm was installed between a upper steel beam and the top of a precast concrete wall. The precast concrete wall was fixed to the steel underbeam in 2 places at its bottom to create such a mechanism that a frictional force is generated in the damper via the precast concrete wall as the steel frame is subjected to story drift.

Loading Method: Fig. 7 shows the loading method. The steel frame was supported on the test bed, and static and dynamic horizontal forces were applied to it by means of an actuator.

Loading Procedure: Table 2 shows the loading procedure. For the dynamic loading test, the damper friction part's sliding amount and vibration period were taken as test parameters.

Measuring Procedure: The steel frame's story drift and the damper friction part's sliding displacement were measured with the dial gauge (D.G.) shown in Fig. 7 and the damper rod's strain (for detecting the damper's frictional force) was measured with the wire strain gauge (W.S.G.).

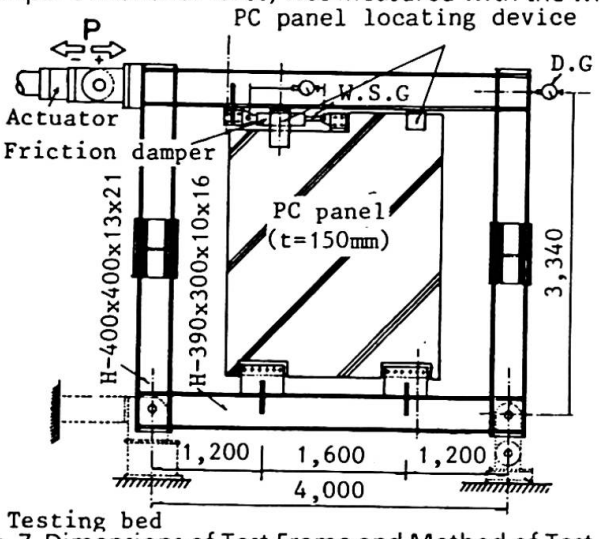


Fig. 7 Dimensions of Test Frame and Method of Test

| Loading Step | Content of Loading |
|---|---|
| (1) | Static load: Gradually increased repetition of P = ±50 tonf |
| (2) | Dynamic load: Sine-wave vibration of T = 1, 2, 3, 4 sec., respectively, at δ = ±2, ±5, ±10, ±15 mm |
| (3) | Static load: Controlled from P = ±60 tonf to δ = 60 mm by the damper's sliding amount δ at △δ = 15 mm pitch |
| (4) | Dynamic load: Since-wave vibration of T = 3 sec. at δ = ±10, ±30 and T = 5 sec. at δ = ±50 |

Table 2 Loading Procedure

## 3.2 Test Results

Static Loading Test: Fig. 8 shows the test frame restoring force characteristics and Fig. 9 shows the damper frictional force-sliding displacement relationship. It is evident that the test frame restoring force characteristics are bi-linear as calculated even if the steel frame is in the elastic range. It can be seen that while the damper's frictional force is slightly more than 11 ton at the beginning of sliding (the ○ mark in the figure), it continues sliding at a stable frictional force of slightly more than 10 ton for the entire sliding length after starting to slide.

Dynamic Loading Test: Fig. 10 shows the test frame restoring force characteristics and Fig. 11 shows the damper frictional force-sliding displacement relationship as examples of their respective test results. Meanwhile, Fig. 12 shows the damper absorbed energy-vibration speed relationship.
It is evident that the test frame restoring force characteristics are bi-linear just as in the static loading test. There is no fluctuation in the frictional force of the damper at the beginning of sliding observed during the static loading test. The sliding load in the dynamic friction range drops in the vibration range of v = 6.2 cm/sec. or more. The damper restoring force characteristics shift from a rectangular to concave shape. The damper absorbed energy also tends to fall as vibration speed v rises. The drop rate of the absorbed energy at v = 8.7 cm/sec. was about 10% of that at v ≦ 3 cm/sec.

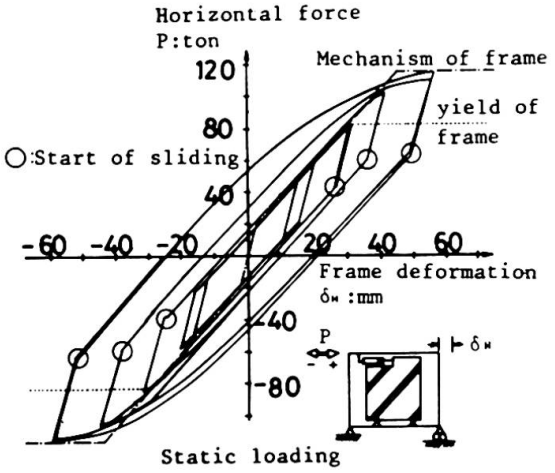


Fig. 8 Test Frame Restoring Force Characteristics

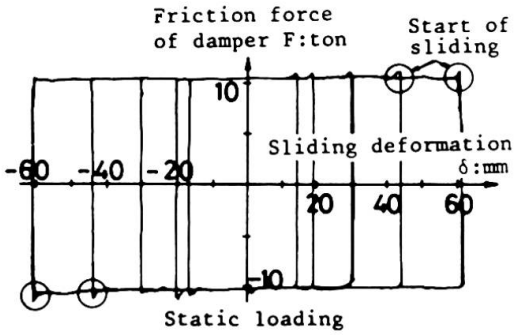


Fig. 9 Damper Characteristics

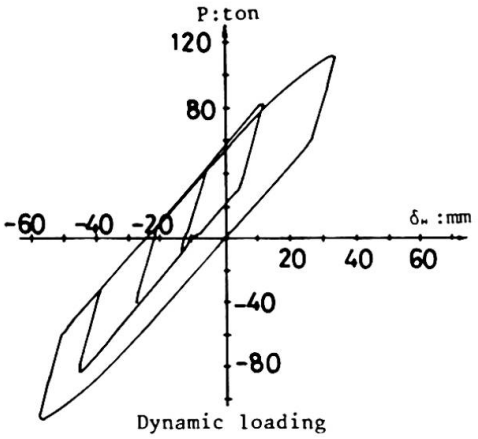


Fig. 10 Test Frame Restoring Force Characteristics

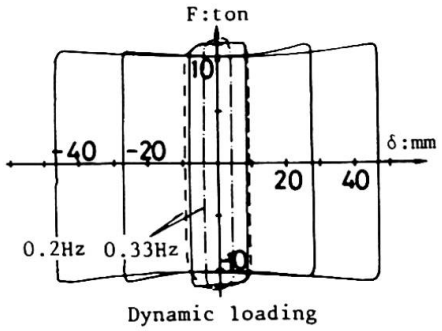


Fig. 11 Damper Characteristics

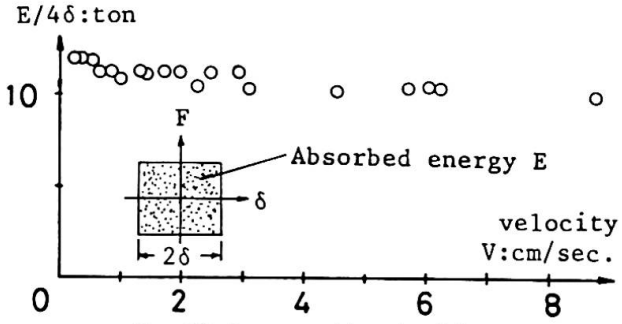


Fig. 12 Damper Absorbed Energy

## 4. APPLICATION OF FRICTION DAMPER TO HIGHRISE BUILDING

Friction dampers were installed in the Industrial Culture Center office building in Omiya, Japan, a 31-story steel-framed structure (Fig. 13).

The dampers were installed at the locations shown in Fig. 13. They were arranged almost symmetrically around the core wall. In the vertical direction, they were installed on all of the 1st ~ 31st floors. The number of pieces installed for each story was: X-direction, A1 x 4 pcs. and Y-direction, B2 x 2 pcs., for a total of 4 dampers each direction. Fig. 14 shows the details of the damper installation. Story drift is transmitted to the damper via the precast concrete wall, which generates a frictional force in the damper.

### 4.1 Dynamic Analysis

As the vibration model, a 32-mass shear model was used to represent the building. For the model, the design rigidity and restoring force of the frame was used. The damper restoring force characteristics were as described in Section 3.2. Table 3 shows the vibration model natural periods. While the initial rigidity increases due to the presence of the damper and the natural periods have become a little shorter, the difference is only about 10% in terms of the 1st period. As the input earthquake motion, El Centro 1940 NS was used. Table 4 shows the five types of intensity of input seismic motion adopted. In the case of small to medium earthquake motions, the building damping was estimated to be 1%, and in 25 & 50cm/sec. motions to be 2%.

Table 5 and Fig. 15 show the response results in the X-direction to seismic motions of 50~150 gal, while Table 5 and Fig. 16 show the results under ground motions of 25 & 50cm/sec. Therefore, the following conclusions are obtained.

(1) There is little difference in the response distribution between with or without dampers, so the response distributions look quite similar.

(2) Under small to medium earthquake motions, the overall response of the building is reduced about 20% by the effect of the dampers.

(3) The building overall response is reduced about 10% in the case of 25cm/sec. motions.

(4) In the case of 50 cm/sec. motions, the damper has little effect.

## 5. CONCLUSION

The above results show that a significant reduction in building sway was achieved, particularly in the case of small- to medium-scale earthquake motions. We have introduced above one example of a friction damper. Various mechanisms are conceivable for this type of energy absorption, and developments allowing this technique to be widely used can be expected in the future.

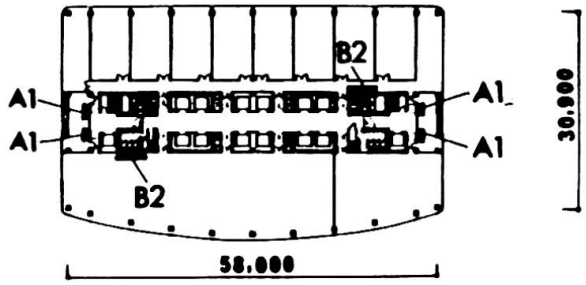


Fig. 13 Typical Floor Plan

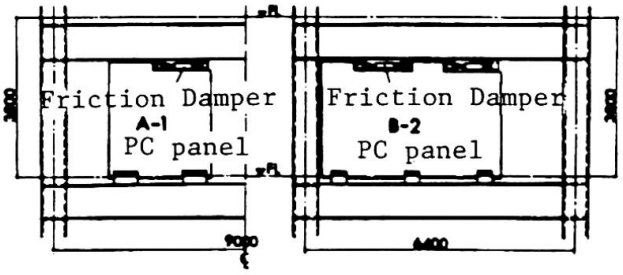


Fig. 14 Details of Damper Installation

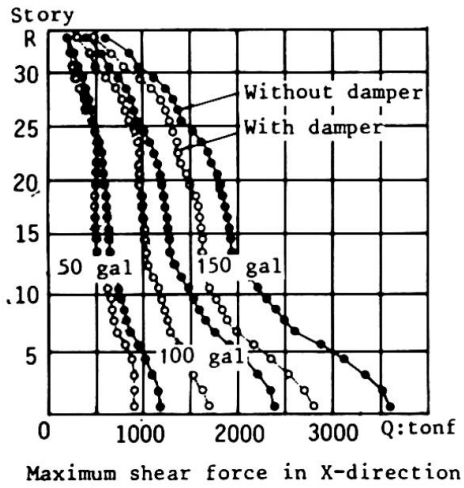


Fig. 15 Response Results at Ground Motion 50~150 gal

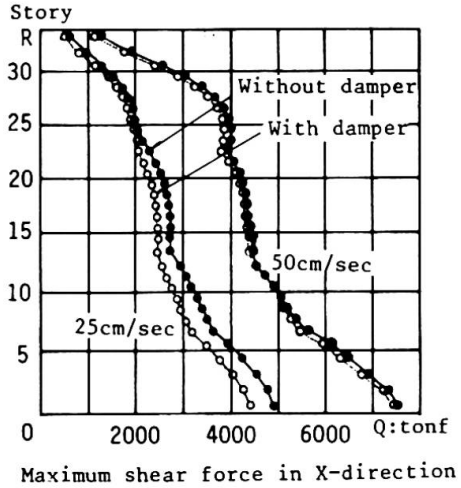


Fig. 16 Response Results at Ground Motion 25 & 50 cm/sec

| | | 1st | 2nd | 3rd |
|---|---|---|---|---|
| X-direction | Without damper | 3.12 | 1.17 | 0.77 |
| | With damper | 2.88 | 1.07 | 0.71 |
| Y-direction | Without damper | 3.06 | 1.12 | 0.73 |
| | With damper | 2.76 | 1.02 | 0.66 |

Table 3 Natural Periods (sec)

| | Input Level | Acceleration (gal) | Building Damping (%) | Response Time (sec.) |
|---|---|---|---|---|
| 1 | Small to medium earthquake motions | 50 | 1.0 | 20.0 |
| 2 | Small to medium earthquake motions | 100 | 1.0 | 20.0 |
| 3 | Small to medium earthquake motions | 150 | 1.0 | 20.0 |
| 4 | 25 cm/sec. | 259 | 2.0 | 20.0 |
| 5 | 50 cm/sec. | 518 | 2.0 | 20.0 |

Table 4 Input Seismic Motion

| Input Level | 50 gal | | | 100 gal | | | 150 gal | | | 25 cm/sec. | | | 50 cm/sec | | |
|---|---|---|---|---|---|---|---|---|---|---|---|---|---|---|---|
| | Without | With | With/ Without | Without | With | With/ Without | Without | With | With/ Without | Without | With | With/ Without | Without | With | With/ Without |
| 1st floor Q (t) | 1206 | 925 | 0.77 | 2412 | 1730 | 0.72 | 3618 | 2830 | 0.78 | 4945 | 4470 | 0.90 | 7537 | 7450 | 0.99 |
| 10th floor Q (t) | 746 | 638 | 0.86 | 1491 | 1180 | 0.79 | 2237 | 1730 | 0.77 | 3203 | 2800 | 0.87 | 4940 | 4920 | 1.00 |
| 1st floor δ (cm) | 0.24 | 0.18 | 0.77 | 0.47 | 0.34 | 0.72 | 0.71 | 0.55 | 0.78 | 0.97 | 0.87 | 0.90 | 1.85 | 1.79 | 0.97 |
| 10st floor δ(cm) | 0.36 | 0.30 | 0.86 | 0.71 | 0.56 | 0.79 | 1.07 | 0.82 | 0.77 | 1.53 | 1.33 | 0.87 | 2.73 | 2.71 | 0.99 |
| Top displacement (cm) | 8.07 | 6.40 | 0.79 | 16.1 | 12.8 | 0.79 | 24.2 | 19.9 | 0.82 | 35.8 | 32.8 | 0.92 | 66.7 | 66.0 | 0.99 |

Table 5 Response Results (X-Direction)

# Seismic Behavior of Joint Panels in Mixed Systems

Comportement sismique des noeuds dans les systèmes de structure mixtes

Verhalten von Rahmenknoten eines Mischbausystems unter Erdbebenbelastung

**Hiroyuki YAMANOUCHI**
Dr.-Eng.
Building Res. Inst.
Tsukuba, Japan

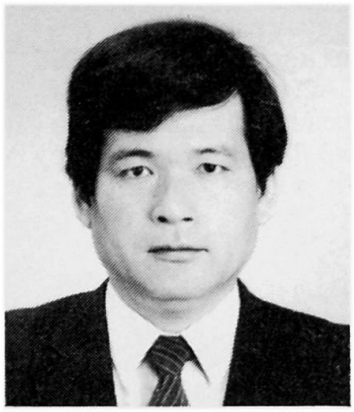

Hiroyuki Yamanouchi, born in 1944, received his engi. degree and his doctrate from the University of Tokyo. Since 1972, he has been working in the Building Res. Inst., currently the Head of the Structural Dynamics Division. His major field is in earthquake engineering of building structures.

**Yukio IZAKI**
Structural Engineer
Sato Kogyo Co., LTD.
Atsugi, Japan

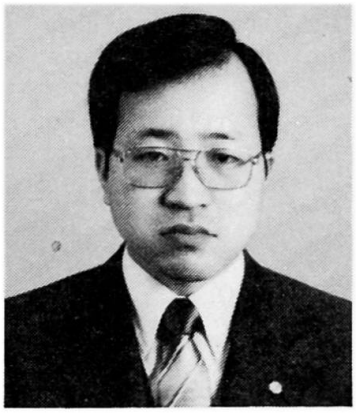

Yukio Izaki, born in 1951, received his masters degree of engineering from Nagoya Institute of Technology. Since 1976, he has been working at the Engineering Research Institute of Sato Kogyo Co., LTD. He, currently Chief, has involved mainly in seismic research on reinforced concrete structures.

**Isao NISHIYAMA**
Dr.-Eng.
Building Res. Inst.
Tsukuba, Japan

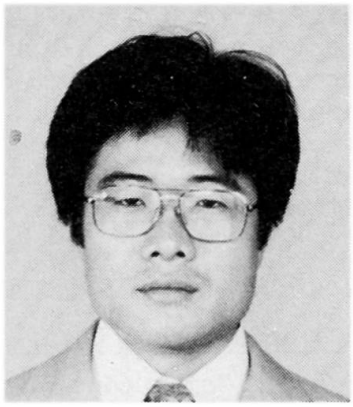

Isao Nishiyama, born in 1953, received his engineering degree and his doctorate from the University of Tokyo. Since 1981, he has been working in the Building Res. Inst. Currently, he is Senior Research Engineer. His major field is in earthquake engineering of steel building structures.

**SUMMARY**
A new mixed structural system comprised of reinforced concrete columns and structural steel girders is proposed. In order to apply this mixed system to actual structures, a structural evaluation of "joint panels in mixed system" and a quantitative assessment compared to other structural systems were carried out. The investigation results show the advantages of the proposed mixed system for practical application.

**RÉSUMÉ**
Un nouveau système structural mixte avec des poteaux en béton armé et des poutres en acier est proposé. Une évaluation structurale ainsi qu'une estimation quantitative de l'ensemble ont été déterminées. Les résultats obtenus reflètent le bon comportement du système et font ressortir certains avantages par rapport aux autres systèmes.

**ZUSAMMENFASSUNG**
Ein neues Mischbausystem aus Stahlbetonstützen und Stahlträgern wird vorgestellt. Zur Abschätzung der Anwendungsvorteile dieses Mischbausystems in Prototyp-Bauwerken wurden konstruktive Untersuchungen und quantitative Auswertungen zum Vergleich mit anderen Bausystemen durchgeführt. Die Untersuchungsergebnisse zeigen die Vorteile des vorgestellten Systems für praktische Anwendungen.

## 1. INTRODUCTION

Although steel structures have their own advantages in weight, ductility, span length, term of the construction contract etc., compared with reinforced concrete structures, they are not always more competitive in the total construction cost, since the material of reinforced concrete is significantly cheaper than steel. Introduced in this paper is a challenging mixed structural system comprised of reinforced concrete columns and structural steel girders which utilizes both, the advantages of steel and reinforced concrete. In order to apply this mixed system to actual structures, a structural performance evaluation and a quantitative assessment compared to other structural systems are discussed in the following.

The first item discussed in this paper is the structural performance evaluation of the steel girder to reinforced concrete column joint panels. Results from half scale tests on perpendicular girder + column joint sub-assemblages are presented and discussed. The second one is to assess the advantages of the mixed structural system quantitatively and to find out the most effective practical applications, such as the optimal span length. For this purpose, design simulations and comparisons were carried out on a prototype 3x3 bay, three story build-ing, designed in steel, reinforced concrete and as a mixed structural system.

## 2. CYCLIC LOADING TESTS ON GIRDER-TO-COLUMN SUB-ASSEMBLAGES

### 2.1 Joint Panel Details

Typical joint panel details are shown in Fig. 1. Depicted are the details of the full-flange-type panel, in which two perpendicular structural steel I-girders penetrate the reinforced concrete column, see Fig. 1(a), with the main reinforcing bars (rebars) in the column corners passing through the panel zone, while center line rebars are welded to the top and bottom of the steel girders. Fig. 1(b) shows the details of the tapered-flange-type panels, in which girder flanges are tapered by cutting. The taper angle measures 45 degrees. These cut girder flanges assure reliable concrete casting in the panel zone.

### 2.2 Test Specimens And Loading

Five test specimens of one half scale girder-to-column sub-assemblages with short transverse girders were investigated. The ratio of the strength of columns to that of girders and the amount of the flange cutting of the steel girder in the panel zone were selected as test parameters. The shape of the specimens is shown in Fig. 2. The mechanical properties of steel, rebar and concrete are shown in Table 1. The specimens, whose columns are weaker than girders, are denoted by "A" and the specimens with strong column and weak girders are affixed with "B". The specimens with full-flange-type panels are denoted by "1", those with tapered-flange-type panels whose taper started from the rebar location are denoted by "2" and the specimen with the taper starting at the column face is denoted by "3". (see Fig. 2)

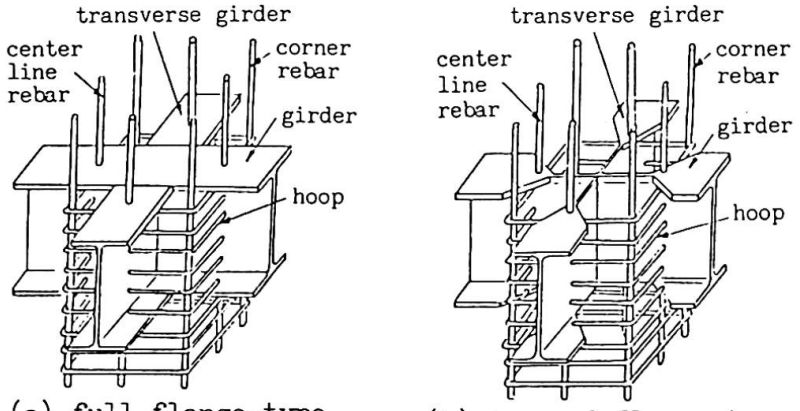


(a) full-flange-type (b) tapered-flange-type

Fig. 1 Details of joint panels

The both ends of the girder were loaded inversely by two actuators simulating seismic forces with a constant axial column load of 620kN, as shown in Fig. 3.

Table 1 Mechanical properties

| Specimen | Steel | | | Reinforcing bar | | | concrete |
|---|---|---|---|---|---|---|---|
| | | $\sigma y$ | $\sigma t$ | size | $\sigma y$ | $\sigma t$ | $\sigma c$ |
| A-1 | flange | 31.0 | 45.8 | D16 | 35.6 | 51.8 | 2.12 |
| | web | 33.6 | 47.1 | D13 | 37.7 | 55.4 | |
| A-2 | flange | 30.1 | 43.6 | D16 | 35.0 | 52.2 | 2.17 |
| | web | 33.8 | 45.2 | D13 | 35.9 | 50.6 | |
| B-1 | flange | 34.7 | 50.3 | D16 | 35.6 | 51.8 | 2.10 |
| | web | 37.5 | 51.5 | D13 | 37.7 | 55.4 | |
| B-2 | flange | 33.1 | 44.8 | D16 | 35.0 | 52.2 | 2.19 |
| | web | 38.6 | 47.2 | D13 | 35.9 | 50.6 | |
| B-3 | flange | 33.1 | 44.8 | D16 | 35.0 | 52.2 | 2.15 |
| | web | 38.6 | 47.2 | D13 | 35.9 | 50.6 | |

(unit:MPa)

## 2.3 Test Results

General Behavior:- First, flexural cracks were observed in the columns followed by subsequent diagonal cracking in the panel zone. Then, the shear yielding of the web plate of the steel girder in the panel zone occurred. Finally, in case of the specimens with full-flange-type panels ("1"), the center line rebars fractured close to the weld point on the top of the girder flange because of poor workmanship of the weld execution. This fracture brought about the spalling of the cover concrete in the panel zone. On the other hand, in case of the specimens with tapered-flange-type panels, the center line rebars did not fracture, forces were transmitted properly from steel girder to reinforced concrete column and the yielding of the tensile reinforcement occurred. Only minor spalling of the concrete cover was observed.

Hysteresis Behavior:- The hysteresis curves of the column shear force (Qc) vs. story drift angle (R) relationships are shown in Fig. 3. Each specimen showed quite stable loops. The maximum strength has the tendency to reduce as the amount of the flange cutting of the steel girder in the panel zone increases. Severe deterioration of load carrying capacity was observed in specimens with full-flange-type panels (A-1 & B-1) at the drift angle of 0.05 radian, where the severe spalling of cover concrete was observed in the panel zone because of the fracture of center line rebars fractured.

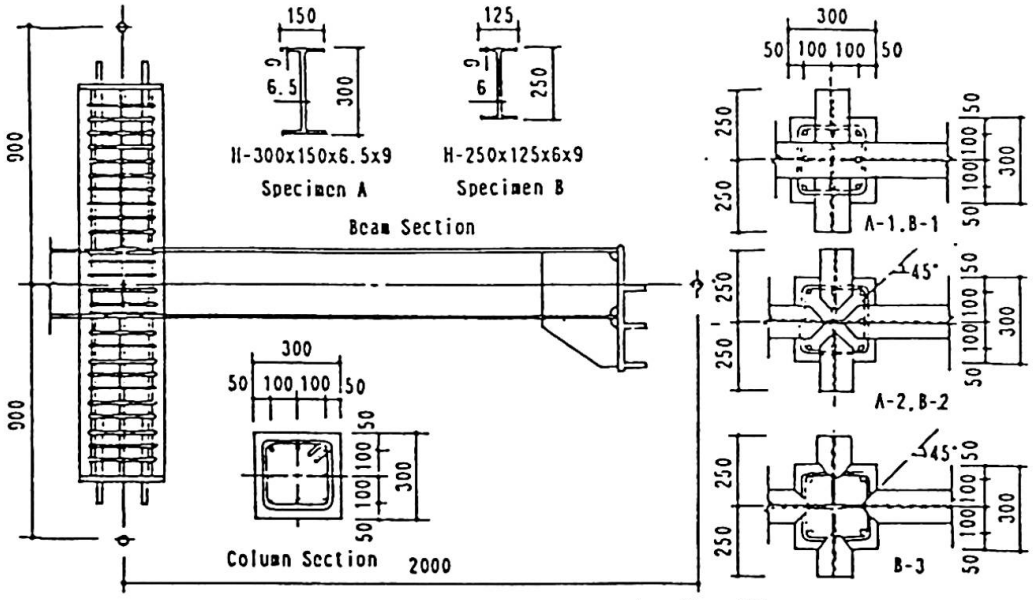


Fig. 2 Shape of specimens

Maximum Strength and Crack Initiation Strength:- The experimental and the calculated strengths of each specimen are summarized in Table 2. The experimental maximum strength to the calculated strength ratios are all larger than

unity. This means that even tapered-flange-type joints well satisfy the required maximum strength criteria (eq.(1)) recommended by SRC Standard of AIJ [1],

$$jMu = cVe\ (\ jFs \cdot j^{\delta} + rPw \cdot w\sigma y\ ) + 1.2\ sV \cdot sw\sigma y\ /\ \sqrt{3} \qquad (1)$$

where, cVe=(b/2)·dc·db=effective panel concrete volume(mm3), b=width of column(mm), dc(db)=distance from centroid of compression steel to that of tension in column (girder)(mm), jFs=concrete shear strength which is smaller value of 0.12Fc or 1.76+(3.6Fc/100) (MPa), Fc=nominal design strength of concrete(MPa), $j^{\delta}$=coefficient dependent on the joint shape (cross-shaped=3), rPw=aw/(b·x) =reinforcement ratio of hoops < 0.6%, aw=2 times area of the hoop rebar(mm2), x=spacing between hoops(mm), $w\sigma y$=tensile yield strength of hoops(MPa),

Table 2 Experimental and calculated strengths

| Specimen | Maximum strength (kN) | | | Diagonal crack strength in panel zone (kN) | | |
|---|---|---|---|---|---|---|
| | Exp | Cal | Exp/Cal | Exp | Cal | Exp/Cal |
| A-1 | 125.0 | 96.9 | 1.29 | 87.3 | 32.6 | 2.68 |
| A-2 | 105.6 | 97.5 | 1.08 | 66.6 | 33.4 | 1.99 |
| B-1 | 130.1 | 81.2 | 1.60 | 75.3 | 25.5 | 2.95 |
| B-2 | 92.3 | 83.2 | 1.11 | 65.8 | 26.5 | 2.49 |
| B-3 | 85.4 | 82.6 | 1.03 | 51.4 | 26.1 | 1.97 |

*1 Strengths in the above table are shown as column shear force.
*2 Maximum strength is calculated from eq.(1).
*3 Panel shear crack strength is estimated as Qcra=τ·(b·dc+15tw·dc), τ=0.1Fc.

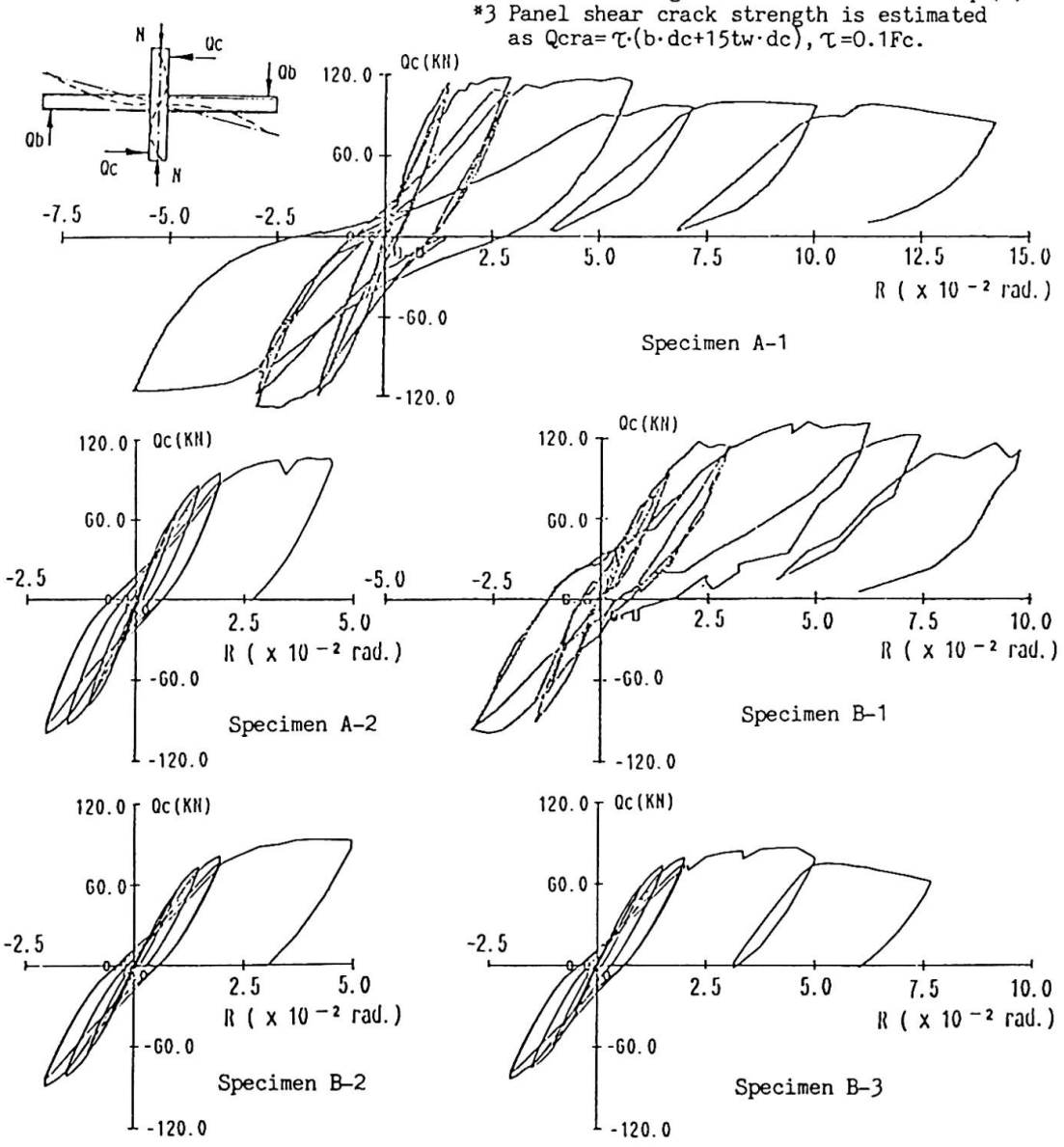


Fig. 3 Hysteresis curves (Qc-R relationships)

sV=db·dc·tw=effective panel steel volume(mm3), tw=thickness of steel web panel(mm) and sw$\sigma$y=tensile yield strength of the structural steel(MPa).

As for the crack initiation strength of the joint panels, the test results are two or three times higher than the calculated ones. The shear stress ($\tau$) at the onset of diagonal cracking is taken as 0.1Fc in Ref.[1]. (see Table 2) Therefore, the experiments show that the crack initiation shear stress might be considered to be 0.3Fc in the case of full-flange-type panels and 0.2Fc in the case of tapered-flange-type panels.

Table 3 Design conditions

| | |
|---|---|
| System | moment resisting frame<br>(mixed, steel, reinforced concrete) |
| Dimen-sions | 3x3 bay, 3 stories<br>clear story height: 2.9m<br>longitudinal span: 8,10,12,14m<br>transverse span: 6m |
| Dead Load | floor<br>mixed,steel metal deck + RC slab t=107.5mm<br>reinforced concrete RC slab t=150mm<br>miscellaneous<br>interior/exterior wall, stairs, pent house and parapet are not considered |
| Live Load | roof floor 0.59kN/m2<br>2,3 floor 1.27kN/m2<br>(for seismic design) |
| Mate-rials | steel SS41(Japan Industrial Standard)<br>rebar SD30(JIS) for slab<br>SD35(JIS) for column<br>concrete Fc=2.06MPa |

## 3. DESIGN SIMULATION

### 3.1 Designed Buildings

Design simulations were conducted on a prototype 3x3 bay, three story building. This structure, shown in Fig. 4, was designed with mixed, steel and reinforced concrete structural systems. The span length in the longitudinal direction of the prototype, 8m, was changed to 10m, 12m and 14m. For these three additional model struc-tures, the same design simulations as that done for the prototype model were carried out to examine the effect of span length. The height of the story was set at 2.90m as the clear story height, i.e. the distance from the top of the floor slab to the bottom of the upper floor girder. All assumed design conditions are summarized in Table 3.

### 3.2 Results Of Simulation

Table 4 summarizes the various characteristics of the designed structures; the story height, the story drift, the total weight and the construction cost. The ratios of the calculated panel strengths by eq.(1) to the required panel moments are listed in Table 5.

Girder Height and Story Height:- The depth of the girders and the story height are almost the same in buildings designed with mixed and steel systems. The depth of the girders designed for the reinforced concrete system is not so different from those designed with mixed and steel systems in the case of 10m or less span length. However, as the span length becomes larger than 12m, the required girder depth significantly increases in the reinforced concrete system.

Story Stiffness:- The story drift angles of designed buildings subjected to seismic force of 20% of the building weight are summarized in Table 4. The inverse of the story drift angle of the mixed system is 70% of that of the reinforced concrete system and about 200% of that of the steel system.

Weight of Designed Buildings:- The weight per unit floor area is listed in Table 4, where the weight of interior and exterior walls, stairs etc. are not considered. The unit weight of the mixed system, 9.64-10.04kN/m2, is rather light compared to that of the reinforced concrete system, 13.02-16.95kN/m2, and is nearly equal to the unit weight of the steel system, 8.89-9.07kN/m2.

Construction Cost:- The construction cost per unit floor area are summarized in Table 4, where the following unit costs are used: concrete=12,300yen/m3, formwork=3,600yen/m2, rebar=8.57yen/N, structural steel=18.9yen/N, metal deck=17.3yen/N and fire protective covers=2,600yen/m2. The unit cost of the

Table 4 Summarized characteristics of designed buildings

| System | | Mixed | | | | Steel | | | | Reinforced concrete | | | |
|---|---|---|---|---|---|---|---|---|---|---|---|---|---|
| Item \ Span length (m) | | 8 | 10 | 12 | 14 | 8 | 10 | 12 | 14 | 8 | 10 | 12 | 14 |
| Story Height (Girder Depth) (m) | 3rd | 3.50 (0.40) | 3.70 (0.60) | 3.70 (0.58) | 3.70 (0.59) | 3.60 (0.50) | 3.70 (0.60) | 3.70 (0.58) | 3.80 (0.69) | 3.60 (0.70) | 3.75 (0.85) | 4.00 (1.10) | 4.40 (1.50) |
| | 2nd | 3.55 (0.45) | 3.70 (0.60) | 3.70 (0.58) | 3.70 (0.59) | 3.60 (0.50) | 3.70 (0.60) | 3.70 (0.58) | 3.80 (0.69) | 3.65 (0.75) | 3.75 (0.85) | 4.00 (1.10) | 4.40 (1.50) |
| | 1st | 3.55 (0.45) | 3.70 (0.60) | 3.70 (0.58) | 3.70 (0.59) | 3.60 (0.50) | 3.70 (0.60) | 3.70 (0.58) | 3.80 (0.69) | 3.70 (0.80) | 3.75 (0.85) | 4.00 (1.10) | 4.40 (1.50) |
| Story Drift Angle (radian) | 3rd | 1/447 | 1/596 | 1/633 | 1/602 | 1/324 | 1/376 | 1/411 | 1/474 | 1/829 | 1/791 | 1/1031 | 1/1406 |
| | 2nd | 1/375 | 1/438 | 1/467 | 1/480 | 1/214 | 1/282 | 1/307 | 1/340 | 1/645 | 1/577 | 1/741 | 1/864 |
| | 1st | 1/543 | 1/527 | 1/541 | 1/582 | 1/307 | 1/306 | 1/301 | 1/328 | 1/705 | 1/594 | 1/722 | 1/809 |
| Weight(kN/m2) | | 9.83 | 9.66 | 9.64 | 10.04 | 8.89 | 9.04 | 8.91 | 9.07 | 13.05 | 13.02 | 14.10 | 16.95 |
| Cost(x10⁻yen/m2) | | 1.93 | 2.03 | 2.07 | 2.21 | 2.22 | 2.25 | 2.24 | 2.45 | 1.64 | 1.64 | 1.76 | 2.15 |

building designed as reinforced concrete system is the cheapest among three systems in all span length simulations. However the unit cost of the mixed system becomes close to that of the reinforced concrete system for buildings with longer span length.

Recommended Strength and Required Strength for Joint Panels:- The ratios of the calculated strength by eq.(1) to the required strength estimated from the ultimate strengths of adjacent members for the joint panels are summarized in Table 5. The ratios are all larger than unity. This means that the joint panels are not needed to be strengthened for practical use if eq.(1) is satisfied.

Table 5
Ratios of calculated strengths to required strength of joint panels in design simulations for the mixed system

| Location \ Span length (m) | | 8 | 10 | 12 | 14 |
|---|---|---|---|---|---|
| Roof Floor | y1x1 | 1.52 | 1.68 | 2.24 | 2.12 |
| | y1x2 | 1.65 | 2.03 | 2.51 | 1.49 |
| | y2x1 | 1.14 | 2.81 | 1.57 | 1.56 |
| | y2x2 | 1.87 | 3.01 | 3.09 | 1.73 |
| 3rd Floor | y1x1 | 2.45 | 2.01 | 2.24 | 2.72 |
| | y1x2 | 1.56 | 1.42 | 1.43 | 1.67 |
| | y2x1 | 1.67 | 1.74 | 1.49 | 1.76 |
| | y2x2 | 1.33 | 1.63 | 1.62 | 1.14 |
| 2nd Floor | y1x1 | 2.86 | 2.11 | 2.34 | 2.72 |
| | y1x2 | 1.84 | 1.33 | 1.46 | 1.67 |
| | y2x1 | 1.94 | 1.81 | 1.54 | 1.76 |
| | y2x2 | 1.20 | 1.25 | 1.22 | 1.18 |

*1 The locations of joint panels are expressed by frame numbers in both x and y directions. Frame "1" means exterior frame and "2" means interior frame, where y direction is the longitudinal direction.

## 4. CONCLUSIONS

The strength of the joint panel decreases as the girder flange is cut in the panel zone. However, the strength satisfies the value recommended by SRC Standard of AIJ. Therefore the strength of the joint panel is not so critical for design applications. The ductility is quite large and it does not deteriorate at least up to a story drift of 1/20 radians.

The mixed system showed that it has both, the advantages of reinforced concrete and steel systems, in story height, story stiffness and total weight. It is somewhat inferior to the reinforced concrete system in construction cost, but there are many factors which can not be considered in the cost estimates, such as the terms of the construction contract.

The above mentioned conclusions show the high capability of the advanced mixed system proposed in this paper.

## REFERENCE

[1] SRC Design Standard, Architectural Institute of Japan, 1987 (in Japanese).

Leere Seite
Blank page
Page vide

Leere Seite
Blank page
Page vide